



Optimization of post-harvest processing of dried cannabis (*Cannabis sativa*) inflorescences,  
including particle size reduction, extraction, decarboxylation, and molecular distillation

Sai Uday Kumar Reddy Sagili  
Department of Bioresource Engineering  
McGill University, Montreal, Qc, Canada

A thesis submitted to McGill University in partial fulfillment of the requirements of the degree  
of Master of Science  
June 2023

© Sai Uday Kumar Reddy Sagili, 2023

## Abstract

*Cannabis* (*Cannabis sativa*) belongs to the family Cannabaceae and has been cultivated for food, fibre, oil, medicine, recreational, and religious purposes. The female inflorescence of the cannabis plant forms glandular trichomes, which serve as the primary site for the production and storage of valuable secondary metabolites, including cannabinoids and terpenes, which exhibit medicinal properties. Preserving and recovering the secondary metabolites, while minimizing losses, is important to obtain food- and pharmaceutical-grade products and can be achieved by optimizing their post-harvest techniques. This thesis focused on optimizing particle size reduction, extraction, decarboxylation, and molecular distillation techniques for upscaling in the cannabis industry.

A research study was conducted to investigate the effects of the dried cannabis biomass particle size [coarse (2-4 mm), medium (0.5-2 mm), fine (0.25-0.5 mm)], solvents (ethanol, butanol, hexane), and extraction temperature (-20 °C, 4 °C, room temperature) on extracted crude cannabis oil yield and cannabinoid/terpene concentrations using a full factorial design. Results showed that ethanol extraction with fine-sized cannabis particles at 4 °C obtained the highest crude oil yield of 28 % and had improved recovery rates of 41 % for tetrahydrocannabinolic acid (THCA), 36 % for cannabigerolic acid (CBGA), along with higher total terpenes concentration (1550 mg 100g dry matter<sup>-1</sup>) in the extracts.

Efficient production and development of cannabis products comprising neutral cannabinoids (i.e., tetrahydrocannabinol (THC), cannabigerol (CBG), and cannabidiol (CBD)) are essential for assuring quality and safety for consumers. When subjected to heat, acidic cannabinoids present in the crude cannabis oil, including THCA, CBGA, and cannabidiolic acid (CBDA), undergo decarboxylation and convert to neutral cannabinoids such as THC, CBG, and CBD, respectively. Thermal decarboxylation of crude cannabis oil was conducted using a rotary evaporator to find the optimal conditions of temperature (95 °C to 155 °C) and time (0 to 180 min with 30 min interval) required for the efficient conversion of CBDA to CBD. Results indicate that a shorter time is optimal at high temperatures and vice versa. Complete CBDA decarboxylation was observed in 30 min at high temperatures from 135 °C to 155 °C compared to 60 min at 115 °C. Although CBGA was initially present in minimal amounts in the crude cannabis oil sample (<LOD), CBGA production was surprisingly observed after 60 min at 115 °C and 30 min at 135 °C and 155 °C.

Few studies have explored the molecular distillation techniques that can improve the recovery of cannabinoids from crude cannabis oil with scale-up potential. Wiped-film short path (WFSP) molecular distillation is a two-cut process, where the distillation of terpenes and cannabinoids occurs at the first and second cuts, respectively. In this experiment, the effects of the distillation parameters in the second cut, including feed flow rate (FFR) (35–55 Hz) (41.6–71.3 mL min<sup>-1</sup>) and internal condensation temperature (ICT) (60–90 °C), were examined and optimized using a central composite rotatable design towards maximizing cannabinoid mass and recovery efficiency in the distillate and minimizing cannabinoid mass in the residue. Results show that irrespective of ICT, reducing FFR increased the cannabinoid's yield and recovery. The recovery efficiency of THC was 93.4 % in the distillate at the predicted optimal conditions; FFR of 35 Hz (41.6 mL min<sup>-1</sup>) and an ICT of 75 °C. The findings presented in this thesis have the potential to enhance the efficiencies of the extraction, decarboxylation, and molecular distillation processes while ensuring the preservation of the secondary metabolite's quality from the cannabis plant.

## Résumé

Cannabis (*Cannabis sativa*), appartenant à la famille des Cannabaceae, est cultivé pour l'alimentation, les fibres, l'huile, la médecine, et pour fins de loisirs et d'activités religieuses. L'inflorescence femelle de la plante de cannabis forme des trichomes glandulaires, qui servent de site principal pour la production et le stockage de précieux métabolites secondaires, notamment les cannabinoïdes et les terpènes, qui présentent des propriétés médicinales. La conservation et la récupération des métabolites secondaires, tout en minimisant les pertes, sont importantes pour obtenir des produits de qualité alimentaire et pharmaceutique, et cela peut être réalisé en optimisant les techniques post-récoltes. Cette thèse s'est concentrée sur l'optimisation de la réduction de la taille des particules, de l'extraction, de la décarboxylation et des techniques de distillation moléculaire pour une mise à l'échelle dans l'industrie du cannabis.

Des recherches ont été menées pour étudier les effets de la taille des particules de biomasse de cannabis séché [grossière (2-4 mm), moyenne (0,5-2 mm), fine (0,25-0,5 mm)], des solvants (éthanol, butanol, hexane) et de la température d'extraction (-20 °C, 4 °C, température ambiante) sur le rendement en huile brute extraite du cannabis et les concentrations de cannabinoïdes/terpènes en utilisant une conception factorielle complète. Les résultats ont montré que l'extraction à l'éthanol avec des particules de cannabis de petite taille à 4 °C obtenait le rendement en huile brute le plus élevé, soit 28 %, et présentait des taux de récupération améliorés de 41 % pour l'acide tétrahydrocannabinolique (THCA), 36 % pour l'acide cannabigérolique (CBGA), ainsi qu'une concentration totale de terpènes plus élevée (1550 mg/100g de matière sèche) dans les extraits.

La production et le développement efficaces de produits à base de cannabis comprenant des cannabinoïdes neutres (c'est-à-dire le tétrahydrocannabinol (THC), le cannabigérol (CBG) et le cannabidiol (CBD)) sont essentiels pour garantir la qualité et la sécurité des consommateurs. Lorsqu'ils sont soumis à la chaleur, les cannabinoïdes acides présents dans l'huile brute de cannabis, notamment le THCA, le CBGA et l'acide cannabidiolique (CBDA), subissent une décarboxylation et se convertissent en cannabinoïdes neutres tels que le THC, le CBG et le CBD, respectivement. La décarboxylation thermique de l'huile brute de cannabis a été réalisée à l'aide d'un évaporateur rotatif pour trouver les conditions optimales de température (95 °C à 155 °C) et de temps (0 à 180 min avec un intervalle de 30 min) nécessaires pour la conversion efficace du CBDA en CBD. Les résultats indiquent qu'un temps plus court est optimal à des températures



élevées et vice versa. Une décarboxylation complète du CBDA a été observée en 30 min à des températures élevées de 135 °C et 155 °C, par rapport à 60 min à 115 °C. Bien que le CBGA soit initialement présent en quantités minimales dans l'échantillon d'huile de cannabis brute (<LOD), la production de CBGA a été observée de manière surprenante après 60 minutes à 115 °C et 30 minutes à 135 °C et 155 °C.

Peu d'études ont exploré les techniques de distillation moléculaire qui peuvent améliorer la récupération des cannabinoïdes à partir de l'huile brute de cannabis avec un potentiel de mise à l'échelle. La distillation moléculaire à court trajet avec film raclé (WFSP) est un processus en deux étapes, où la distillation des terpènes et des cannabinoïdes se produit lors des première et deuxième coupes, respectivement. Dans cette expérience, les effets des paramètres de distillation de la deuxième coupe, notamment le débit d'alimentation (FFR) (35-55 Hz) (41,6-71,3 mL/min) et la température interne de condensation (ICT) (60-90 °C), ont été examinés et optimisés à l'aide d'une conception composite rotative centrale afin de maximiser la masse et le rendement des cannabinoïdes dans le distillat et de minimiser la masse de cannabinoïdes dans le résidu. Les résultats montrent que, quel que soit l'ICT, la réduction du FFR a augmenté le rendement et la récupération des cannabinoïdes. L'efficacité de récupération du THC était de 93,4 % dans le distillat dans les conditions optimales prévues : FFR de 35 Hz (41,6 ml min<sup>-1</sup>) et ICT de 75 °C. Les résultats présentés dans cette thèse ont le potentiel d'améliorer l'efficacité des processus d'extraction, de décarboxylation et de distillation moléculaire tout en assurant la préservation de la qualité des métabolites secondaires de la plante de cannabis.

## Acknowledgements

Firstly, I am sincerely thankful to my uncle, Mr. Ashok Kumar Reddy Sagili, and aunty, Mrs. Lakshmi Devi Sagili, for their unconditional love, support, financial assistance, and immense belief in my abilities. Their encouragement and confidence played a pivotal role in making my dreams of studying abroad a reality and have been instrumental in my journey toward success. I would like to thank my mother, Late Sujatha Sagili, father, Mr. Venkata Subbareddy Sagili, and sister, Mrs. Saisree Sagili, for the hardships they faced and the sacrifices they made to foster my academic pursuits. I am extremely grateful to Late Chinnanagireddypalle Srinivasula Reddy for providing financial support to support my education. I express my gratitude to my grandmother, Mrs. Laxumma K, and aunt, Mrs. Parvathi Kadapalayagari, for their care and support during times of need since my childhood.

I would like to express my heartfelt gratitude to my supervisors, Dr. Valérie Orsat and Dr. Mark Lefsrud. I am immensely thankful for the opportunity they gave me to demonstrate my abilities and for their unwavering financial, moral, and scholastic support. Their support and guidance throughout my Master's journey have been truly invaluable. I will forever be grateful for their belief in me and their contributions to my academic success. Their expertise, guidance, and willingness to invest time and resources in my growth have made a significant impact on my journey. I would like to thank Dr. Vijaya Raghavan for being a committee member and granting me access to his lab for my experiments.

I am forever grateful to Dr. Philip Wiredu Addo for his invaluable teachings, guidance, moral and academic support, and the opportunities he provided me to contribute to his research projects. His exceptional mentorship has been invaluable in making my experiments more manageable, as he guided and provided solutions to challenges, actively participated in the brainstorming of my ideas, and taught me proactive problem-solving strategies. I am equally thankful to Dr. Sarah MacPherson for her constant encouragement, academic and emotional support, and steadfast presence throughout my Master's journey. I am deeply appreciative of her exceptional support, especially during my health challenges, which I value tremendously.

I sincerely appreciate Mr. Yvan Gariépy for his invaluable help and assistance during the experiments. I would like to express my gratitude to Dr. Michael Ngadi and Dr. Christopher Kucha for providing rotary evaporator equipment for my experiment. I extend my thanks to Jérôme Trudel-Brais for his support and assistance during my industrial internship. I am deeply

grateful to Eugene Roy Antony Samy for his unwavering presence, continuous moral support, and invaluable encouragement and help during my challenging times. I would like to acknowledge the support provided by EXKA, C-medical, and Bloom Labs, which was instrumental in the completion of my experiments.

I would like to extend my heartfelt appreciation to Dr. A. Shanthi, Dr. Shamaroa Jahagirdar, and Dr. V. Ramesh for their invaluable encouragement and the commendable recommendation letters they provided. I am sincerely grateful to my best friends, Usha Palukuru, Venkata Saiteja Reddy Kolakalapudi, Harikrishnan Poiyamozi, Sai Prasad Ayyappa Tummalapalli, Raghu Narayana Nakkireddy, Sabarigrish Pandian, Lakshmi Devi Ramakichenen, Kiran Kumar Reddy Mallam, Mahaboob Basha Shaik Hakim, Sudhakar Reddy Kadapalayagari, Sindhuja Pabba, Lakshmi Devi Balijapalli, Venkata Ramana Bharatakavi, and Mustafa Shaik, for their unconditional support throughout my life, from childhood till now. They have been a constant source of strength and comfort, standing by me through both the highs and lows, including my emotional breakdowns.

Last but not least, I express my gratitude to John Spurgeon Battu for his guidance and valuable information that paved the way for my Master's journey and to Manoj Krishna Guttula, Venkata Manikanta Bellam, and Tejasvita Awale for facilitating a seamless transition to Canada and showing the right path in difficult times. Special acknowledgements go to my graduate best friends, particularly Farhan Ahmad for taking care of me as your own brother, Sushree Sangeetha Dash for always lending your shoulders to rely on during difficult times, Farzin Eslami, and Vidya Sagar Kuncham, for their unwavering support and for keeping me motivated and spirited throughout this journey.

## **Contribution of authors**

In adherence with the McGill Guidelines for a Manuscript-Based Thesis, this section outlines the contributions made by the candidate and co-authors in completing this work. Sai Uday Kumar Reddy Sagili is the principal author of all the chapters in this thesis, supervised by Dr. Valérie Orsat from the Department of Bioresource Engineering, McGill University, Sainte-Anne-de-Bellevue, Quebec, Canada.

Dr. Valérie Orsat and Dr. Mark Lefsrud, the supervisor and co-supervisor, co-authored all manuscripts and offered scientific guidance throughout the research process, including designing and implementing of the research work, co-editing, and reviewing the manuscripts.

Dr. Philip Wiredu Addo aided in the experiments, helped in the preparation of original drafts, and reviewed and co-authored all manuscripts.

Dr. Sarah MacPherson reviewed and improved all the manuscripts and co-authored all manuscripts.

Ms. Michelle Shearer and Mrs. Nicole Taylor assisted with and jointly co-supervised the analytical analyses of cannabinoids and terpenes and co-authored chapters 3 and 4.

Dr. Maxime Paris provided funding assistance and necessary resources and supervised experiments conducted at EXKA Inc. He reviewed and co-authored all manuscripts.

Mr. Frederick-Alexandre Gladu-Gallant and Mr. Samuel Eichhorn Bilodeau provided assistance and reviewed and co-authored chapters 4 and 5.

## Table of Contents

<i>Abstract</i> .....	2
<i>Résumé</i> .....	4
<i>Acknowledgements</i> .....	6
<i>Contribution of authors</i> .....	8
<i>List of figures</i> .....	11
<i>List of tables</i> .....	13
<i>List of acronyms</i> .....	14
<i>Chapter 1: General Introduction</i> .....	16
1.1 Thesis motivation .....	16
1.2 Research problem .....	17
1.3 Objectives .....	17
<i>Chapter 2: Literature review</i> .....	19
2.1 Cannabis plant .....	19
2.2 Cannabinoid biosynthesis .....	20
2.3 The pharmacological activity of cannabinoids and terpenes .....	21
2.4 Cannabis cultivation .....	23
2.5 Post-harvest handling .....	23
2.6 Post-harvest operations .....	24
2.6.1 Drying .....	24
2.6.2 Grinding or particle size reduction .....	25
2.6.3 Extraction .....	28
2.6.4 Decarboxylation .....	30
2.6.5 Distillation .....	31
2.6.5.1 Molecular distillation .....	31
2.6.6 Distillation techniques in the cannabis industry .....	36
<i>Chapter 3: Effects of particle size, solvent type, and extraction temperature on the extraction of crude cannabis oil, cannabinoids, and terpenes</i> .....	40
Abstract .....	40
3.1 Introduction .....	41
3.2 Materials and methods .....	43
3.3 Results .....	48
3.4 Discussion .....	60

3.5	Conclusion .....	65
3.6	References .....	67
<i>Chapter 4: Cannabinoid decarboxylation in crude cannabis oil: a kinetic study .....</i>		<i>75</i>
	Abstract .....	75
4.1	Introduction .....	76
4.2	Materials and methods .....	78
4.3	Results and discussion .....	81
4.4	Conclusion .....	89
4.5	References .....	90
<i>Chapter 5: Optimization of wiped-film short path molecular distillation for recovery of cannabinoids from cannabis oil using response surface methodology .....</i>		<i>93</i>
	Abstract .....	93
5.1	Introduction .....	94
5.2	Materials and methods .....	95
5.3	Results .....	101
5.4	Discussion .....	114
5.5	Conclusion .....	116
5.6	References .....	117
<i>Chapter 6: General discussion .....</i>		<i>121</i>
<i>Chapter 7: Conclusion and future studies .....</i>		<i>123</i>
7.1	General conclusion .....	123
7.2	Future suggested studies .....	124
<i>8. Master Reference List .....</i>		<i>125</i>
<i>Appendix .....</i>		<i>149</i>

## List of figures

Figure 2.1. Biosynthetic pathway of cannabinoids .....	21
Figure 2.2. Evaporation and condensation in the molecular distillation process.....	32
Figure 2.3. Rotary evaporator .....	36
Figure 2.4. Wiped-film short path molecular distillation equipment.....	37
Figure 3.1. Methodology followed for this study .....	44
Figure 3.2. Effect of particle size reduction (grinding) on the initial concentrations (mg 100 g dry matter <sup>-1</sup> ) of THCA (A), CBGA (B), and CBG (C) before extraction. ....	49
Figure 3.3. Effect of particle size, solvent, and extraction temperature on the recovery rates of acidic cannabinoids, THCA (A-C) and CBGA (D-F). ....	50
Figure 3.4. Representative images of different colors observed in crude cannabis oil extracted using different solvents; (A) ethanol, (B) butanol, and (C) hexane.....	51
Figure 3.5. Effect of particle size, solvent type, and extraction temperature on the cannabis oil yield (%); (A) ethanol, (B) butanol, (C) hexane. ....	53
Figure 3.6. Effect of particle size, solvent, and extraction temperature on the concentration (mg 100 g dry matter <sup>-1</sup> ) of THCA (A-C), CBGA (D-F), CBG (G-I), and THC (J-L). ....	56
Figure 3.7. Effect of particle size, solvent type, and extraction temperature on major monoterpene concentrations (mg 100 g dry matter <sup>-1</sup> ), including limonene (A-C) and fenchol (D-F). ....	58
Figure 3.8. Effect of particle size, solvent type, and extraction temperature on concentration (mg 100 g dry matter <sup>-1</sup> ) of sesquiterpenes, including caryophyllene (A-C), caryophyllene oxide (D-F), humulene (G-I), and total terpenes (J-L). ....	59
Figure 4.1. Molecular structure of major cannabinoids and their simplified biosynthetic, decarboxylation, and oxidation pathways.....	77
Figure 4.2. Left: Sample preparation flowchart; Right: rotary evaporator setup used for the decarboxylation study. ....	79
Figure 4.3. Concentrations (mg 100 g dry matter <sup>-1</sup> ) of Total CBD, CBD, CBDA (A, B, C, D), and CBGA (E) as a function of time (min) during the decarboxylation process. ....	85

Figure 4.4. Decarboxylation kinetics of CBDA in crude cannabis oil at 95 °C and 115 °C.....	88
Figure 5.1. Sample preparation flowchart used for optimizing wiped-film short path (WFSP) molecular distillation in this study.....	96
Figure 5.2. Wiped-film short path (WFSP) molecular distillation equipment used for this study. .....	98
Figure 5.3. 3D response surface plots demonstrating the combined effects of FFR (Hz) and ICT (°C) on the mass (g) of THC (A), Total THC (B), Total CBD (C), CBG (D), CBC (E), CBN (F) in the distillate of the second cut.....	107
Figure 5.4. 3D response surface plots demonstrating the combined effects of FFR (Hz) and ICT (°C) on the mass (g) of THC (A), Total THC (B), Total CBD (C), CBG (D), CBC (E), CBN (F) in the residue of the second cut.....	108
Figure A.1. Plots comparing the actual and predicted RSM values for the mass (g) of (A) THC, (B) Total THC, (C) Total CBD, (D) CBG, (E) CBC, and (F) CBN in the distillate. ....	149
Figure A.2. Plots comparing the actual and predicted RSM values from RSM for the mass (g) of (A) THC, (B) Total THC, (C) Total CBD, (D) CBG, (E) CBC, (F) CBN in the residue.....	150
Figure A.3. Plots comparing the actual and predicted RSM values for recovery efficiency (%) of (A) THC, (B) Total THC, (C) Total CBD, (D) CBD, (E) CBG, (F) CBC, (G) CBN in the distillate.....	151



## List of tables

Table 3.1. Coded levels of the independent variables for solvent extraction of cannabis. ....	48
Table 3.2. Variability sources and significance levels on the responses.....	52
Table 4.1. Range of temperatures (°C) and time (min) used for thermal decarboxylation in this experiment.....	81
Table 4.2. Cannabinoid concentrations (mg 100 g dry matter <sup>-1</sup> ) with different experimental conditions for decarboxylation of crude cannabis oil.....	83
Table 4.3. Kinetic rate constants (k) and Activation energies (E <sub>A</sub> ) for the CBDA decarboxylation. ....	89
Table 5.1. Uncoded levels of the independent variables with WFSP molecular distillation of cannabis oil.....	100
Table 5.2. Cannabinoid analysis of decarboxylated cannabis oil and distillate, residue, and cold trap collections from the terpene distillation (first cut).....	102
Table 5.3. Matrix of the CCRD and observed responses (Y <sub>j</sub> ) for different experimental conditions for WFSP molecular distillation of cannabis oil. ....	103
Table 5.4. Optimal experimental conditions for WFSP molecular distillation of cannabis oil and the predicted response values. ....	110
Table 5.5. ANOVA for responses at different experimental conditions.....	112
Table A.1. Regression equation coefficients for different experimental conditions. ....	152

## List of acronyms

Activation energy	$E_A$
Analysis of variance	ANOVA
Cannabichromene	CBC
Cannabichromenenic acid	CBCA
Cannabidiol	CBD
Cannabidiolic acid	CBDA
Cannabigerol	CBG
Cannabigerolic acid	CBGA
Cannabinol	CBN
Carbon dioxide	$CO_2$
Central composite rotatable statistical design	CCRD
Collaborative Research and Training Experience	CREATE
Complete composite design	CCD
Feed flow rate	FFR
Flame ionization detector	FID
Food and Drug Administration	FDA
Full factorial design	FFD
Gas chromatography	GC
Generally recognised as safe	GRAS
High performance liquid chromatography	HPLC
Internal condensation temperature	ICT
Kinetic rate constant	$k$
Limit of detection	LOD
Microwave-assisted hot-air drying	MAHD
Natural Sciences and Engineering Research Council	NSERC
Quality Assurance and Quality Control for Cannabis	QAQCC
Response surface methodology	RSM
Room temperature	RT
Short path distillation	SPD
Tetrahydrocannabinol	THC

Tetrahydrocannabinolic acid	THCA
Tetrahydrocannabivarin	THCV
Tunable ultraviolet	TUV
Ultra high-performance liquid chromatography	UPLC
Wiped-film short path	WFSP

## **Chapter 1: General Introduction**

This chapter presents the background and rationale for the development of the research project, along with a statement of the research problems and objectives of this study.

### **1.1 Thesis motivation**

Cannabis is widely recognized for its medicinal properties attributable to the availability of bioactive secondary metabolites. Canada was the first of the G7 countries to legalize cannabis production and sale on a federal level in 2013 with the Marijuana for Medical Purposes Regulations, and recreational use was legalized in 2018 with The Cannabis Act (Blake and Nahtigal, 2019). The increase in the legalization of cannabis in various countries has reduced the negative stigma associated with cannabis consumption and is recognized for its potential health benefits (Addo et al., 2021). Cannabinoids and terpenes are valuable secondary metabolites responsible for the therapeutic bioactivity of the cannabis plant.

Post-harvest operations encompass all processing activities conducted after the harvesting of the plant. Optimizing post-harvest technologies, particularly grinding, extraction, decarboxylation, and molecular distillation are essential in maximizing crude cannabis oil yield, having the highest concentrations of cannabinoids and terpenes, while simultaneously minimizing losses, reducing operational expenses, and thereby making a significant contribution to the overall economy. Although optimization of cannabis postharvest activities is discussed in the literature, it is essential to understand the effects of postharvest factors for maximizing extraction yield and ensuring high-quality medical-grade products (Al Ubeed et al., 2022).

Various processes are crucial in obtaining a substantial amount of valued neutral cannabinoids (THC, CBD, CBC, and CBG) in a high-quality distillate, which is imperative for their subsequent applications in the medicinal and recreational cannabis markets. Particle size reduction (grinding) of the biomass increases the surface contact area between the biomass and the solvent, and the yield of extracted oil (Nieh and Snyder, 1991; Russin et al., 2007) could be enhanced by employing proper extraction conditions. Decarboxylation has emerged as a critical stage in the cannabis supply chain (Moreno et al., 2020b), as the desired neutral cannabinoids having therapeutic properties occur as carboxylic acids (THCA, CBDA, CBCA, CBGA) in the cannabis plant. After decarboxylation, the separation and recovery of the pure and neutral cannabinoids from undesirable compounds (terpenes, waxes, and heavy compounds) present in

the decarboxylated crude cannabis oil by molecular distillation determine the quality and quantity of the final distillate.

## **1.2 Research problem**

Optimized medicinal plant processing and extraction can improve extraction yield and efficiency for valued secondary metabolites, while reducing operating costs.

1. Investigated the ideal particle size of dried cannabis for maximizing extraction yield while simultaneously comparing various solvents at different temperatures for industrial extraction.
2. Determining the optimal temperature and time required for the decarboxylation of acidic to neutral cannabinoids in crude cannabis oil is necessary to ensure product safety and prevent thermal degradation by prolonged exposure to higher temperatures.
3. Developing an optimized process using a scientific approach to recovery of all neutral cannabinoids from the decarboxylated crude cannabis oil into the distillate is essential. Only one study has explored the effects of wiped-film short path molecular distillation parameters on CBD recovery and concentration of CBD.

## **1.3 Objectives**

1. To investigate the effects of the particle size of dried cannabis biomass [coarse (2-4 mm), medium (0.5-2 mm), fine (0.25–0.5 mm)], solvents type (ethanol, butanol, hexane), and extraction temperature (–20 °C, 4 °C, room temperature) on the extracted yield and recovery of crude cannabis oil and cannabinoid/terpene concentrations using a full factorial design.
2. To perform a kinetic and impact analysis and determine the optimal temperature (95 °C to 155 °C) and time (0 to 180 min) required for the decarboxylation of CBDA to CBD in crude cannabis oil using a rotary evaporator.
3. To optimize the operating parameters of wiped-film short path molecular distillation, including feed flow rate (35 to 55 Hz) (41.6 to 71.3 mL min<sup>-1</sup>) and internal condensation temperature (60 to 90 °C) on maximizing cannabinoid mass and recovery efficiency in the distillate and minimizing the cannabinoid mass in the extraction residue using response surface methodology.

**Connecting text**

This following chapter provides a summary of the cannabis plant, highlighting the biosynthesis and significance of cannabinoids and terpenes. It also discusses important operating parameters in the cannabis post-harvest supply chain, with particular focus on grinding methods, decarboxylation, and molecular distillation techniques applicable to the cannabis industry.

## Chapter 2: Literature review

### 2.1 Cannabis plant

Cannabis belongs to the Cannabaceae family and it is an ancient crop cultivated in East Asia for various purposes such as food and fibre production, as well as recreational, medical, and ritual uses (Merlin, 2003; Ren et al., 2019). Schultes et al. (1975) categorized the genus Cannabis into three distinct species: *Cannabis sativa*, *Cannabis indica*, and *Cannabis ruderalis*.

The *sativa* and *indica* varieties are more commonly grown and have greater economic importance than the *ruderalis* variety. *Ruderalis* is typically found in the northern Himalayas and southern states of the former Soviet Union and is known for its hardiness and sparse, weed-like growth. It is not commonly cultivated for its psychoactive properties. In contrast to the *sativa* variety of Cannabis, which can grow between 2.5 and 3.5 meters tall, the *indica* variety is typically shorter, with an average height of around 1.8 meters. The plants of the *indica* variety tends to be bushier and have broader, darker green leaves that mature earlier when grown outdoors (ElSohly and Slade, 2005).

Cannabis produces many valued secondary metabolites including cannabinoids, terpenes, and flavonoids, which are involved in the plant's defence against pathogens, pests, and herbivores, while they regulate the plant's response to environmental stresses, act as antimicrobial and antioxidants and exhibit medicinal properties. The concentration and chemical profile of cannabis inflorescences and products are influenced by various environmental and processing factors such as genetics, growing conditions, drying, storage, curing, and packaging (Potter, 2014). Cannabis secondary metabolites are mainly produced and stored in the glandular trichomes in large numbers on the female inflorescences (Andre et al., 2016b; Chandra et al., 2017; Hammond and Mahlberg, 1977; Raman et al., 2017). Jin et al. (2020) reported that the concentration of cannabinoids and terpenes varies depending on the part of the cannabis plant, with the highest levels found in inflorescences, followed in decreasing order by leaves, stem, seeds, and roots.

Phytochemically, *C. sativa* can be differentiated from *C. indica* by the presence of a higher  $\Delta^9$ -tetrahydrocannabinol (THC) to cannabidiol (CBD) ratio compared to a higher CBD to THC ratio of *C. indica* (McPartland, 2018). Depending on the cannabis accession, the THC: CBD ratio remains consistent regardless of the gender of the plant (De Meijer, 2014; Fetterman et al., 1971), during both vegetative and flowering growth stages (Aizpurua-Olaizola et al., 2016;

De Backer et al., 2012; Pacifico et al., 2008). The THC to CBD ratio is considered a qualitative trait, while the qualitative character is the total yields of THC and CBD (Jin et al., 2019).

## **2.2 Cannabinoid biosynthesis**

Cannabinoids are a class of secondary metabolites with a terpenophenolic C<sub>21</sub> backbone, synthesized through biosynthetic pathways (Chasiotis et al., 2022; Radwan et al., 2021). The three prominent naturally occurring acidic cannabinoids are tetrahydrocannabinolic acid (THCA), cannabidiolic acid (CBDA), and cannabigerolic acid (CBGA) and undergo decarboxylation in the presence of light and heat to produce their neutral analogues, THC, CBD, and cannabigerol (CBG), respectively (Ternelli et al., 2020; Thomas and Elsohly, 2015). Minor cannabinoids include cannabichromene (CBC), tetrahydrocannabivarin (THCV), cannabidivarin (CBDV), and cannabinol (CBN). CBN is produced by the degradation of THC degradation.

THCA, CBDA, and CBCA (cannabichromenic acid) are synthesized from CBGA using specific oxidoreductases, THCA synthase, CBDA synthase, and CBCA synthase, respectively (Figure 2.1) (Morimoto et al., 1998; Sirikantaramas and Taura, 2017a; Taura et al., 1996; Taura et al., 1995). In the cannabis plant, olivetolic acid and geranyl pyrophosphate are synthesized to form CBGA catalyzed by geranyl pyrophosphate:olivetolate geranyl transferase (Fellermeier and Zenk, 1998). The formation of olivetolic acid involves a cyclization reaction of the tetraketide-CoA intermediate in the presence of olivetolic acid cyclase, a polyketide cyclase enzyme found in plants (Gagne et al., 2012; Sirikantaramas and Taura, 2017a; Taura et al., 2009).



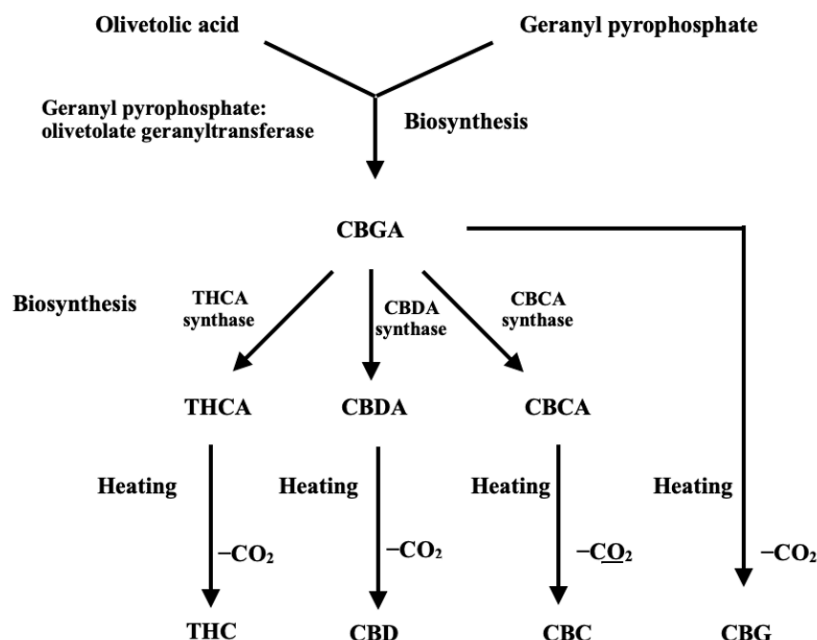


Figure 2.1. Biosynthetic pathway of cannabinoids

### 2.3 The pharmacological activity of cannabinoids and terpenes

The pharmacological activity of phytocannabinoids can interfere with various parts of the endocannabinoid system or other cellular pathways, which can impact the advancement or progression of various diseases, such as cancer (Dariš et al., 2019). THC and CBD are responsible for psychoactive and therapeutic effects, respectively; THC interacts with cannabinoid receptors, i.e., CB<sub>1</sub> and CB<sub>2</sub> of the endocannabinoid system in the body (Russo, 2011), whereas, CBD exhibits a minimal affinity for these receptors (Elsaid et al., 2019; Forester et al., 2022). Various pharmacokinetic studies have reported the potential pharmacological activities of THC in bronchodilation, pain modulation, sedation, appetite stimulation, and control of spasticity or mood, as well as exhibiting anti-oxidant, anti-inflammatory, and neuroprotective antioxidant properties (Addo et al., 2023b; Evans, 1991; Hampson et al., 1998; Russo and Marcu, 2017; Williams et al., 1976). In recent years, CBD has gained interest as a pharmacologically broad-spectrum medication for various neuropsychiatric disorders and exhibits potent anti-fungal and anti-bacterial properties (Alexandri et al., 2023; Appendino et al., 2011; Blessing et al., 2015; Boggs et al., 2018; Khan et al., 2018). CBG, a non-psychoactive phytocannabinoid, is demonstrating antiproliferative, analgesic, and antibacterial properties and

is growing in popularity as a potential therapeutic agent for colon cancer, glaucoma, and inflammatory bowel disease (Hartsel et al., 2016; Russo and Marcu, 2017).

Terpenes, as aromatic hydrocarbon compounds, constitute the major composition of essential oil and are responsible for the distinct aroma found in the cannabis plant (Andre et al., 2016b; Sommano et al., 2020). There are over 150 different terpenes that have been identified in the resin of various cannabis varieties (Hanuš et al., 2016). Terpenes are synthesized via the isoprenoid biosynthetic system, which begins in the cytosol with the mevalonic acid pathway and in plastids with the methylerythritol phosphate pathway (Booth and Bohlmann, 2019). These pathways involve two stages: the production of isopentenyl pyrophosphate and dimethylallyl pyrophosphate molecules, and the subsequent condensation of these compounds to produce different terpenes (Hunter, 2007).

Based on the number of isoprene (5-carbon building block) units in the chemical structure, terpenes can be classified as monoterpenes (10 carbons), sesquiterpenes (15 carbons), and triterpenes (obtained from a 30-carbon framework) based on the number of carbon units in the chemical structure (Andre et al., 2016a; Ashour et al., 2018; Sommano et al., 2020). Major monoterpenes are myrcene,  $\beta$ -ocimene, terpinolene  $\alpha$ -pinene,  $\beta$ -pinene, and limonene (Booth and Bohlmann, 2019), sesquiterpenes consists of  $\alpha$ -humulene,  $\beta$ -caryophyllene, farnesene, and bergamotene (Booth et al., 2017), and triterpenes include  $\beta$ -amyrin, friedelin, cycloartenol, epifriedelanol, and dammaradienol (Montserrat-de la Paz et al., 2014; Slatkin et al., 1971).

Kogan and Mechoulam (2022) reviewed that cannabinoids and cannabis-derived terpenes are potent therapeutic agents for treating neurological disorders, including anxiety, depression, epilepsy, insomnia, seizures, and many ailments, such as cancer, Alzheimer's, and Parkinson's diseases. The use of extracts that contain a complex mixture of cannabinoids and terpenes may result in a more comprehensive therapeutic effect through the entourage effect, as compared to pure synthetic cannabinoids (Russo, 2011). The entourage effects of terpenes with specific cannabinoids can make them more efficient for treating anxiety and mood disorders (Ferber et al., 2020). Preserving and recovering the valued secondary metabolites in the cannabis plant while minimizing losses are important and can be achieved by optimizing post-harvest techniques (Addo et al., 2021).

## **2.4 Cannabis cultivation**

Cannabis which is grown hydroponically i.e., on substrates like rock wool, coco fibre, perlite, and vermiculite instead of soil, is gaining popularity among cannabis producers and has become the dominant method for indoor cultivation (Vanhove et al., 2011). Chemotype, planting densities, day lengths, growth medium ingredients, growing temperature, irradiance levels, and harvesting time are crucial factors to consider for indoor cultivation of cannabis (Chandra et al., 2017). Cannabis plants can be grown either by using seeds or by using cuttings from the healthy mother plant. The cuttings are inserted into moist rooting coir plugs after the application of a small quantity of rooting hormone. The cuttings establish a robust root system after a 14-day period of being maintained in humid environment and exposed to continuous light (Potter, 2004; Vanhove et al., 2011).

Afterward, the cuttings are transplanted into pots containing peat-based growth medium for subsequent vegetative (3 weeks) and flowering stages (10 weeks, including flower formation and maturation). Ensuring the correct structure, pH level, nutrient content, and absence of pesticides and heavy metal residues is crucial when selecting a growth medium. Pruning, de-leafing, and pinching should be performed at regular intervals. Potable water should be utilized for irrigating the plants consistently during their growth cycle. If needed, fertilizers can be employed to supply additional nutrients. To prevent pests and diseases, it is important to employ predatory beneficial insects and avoid creating favorable conditions for disease-causing pathogens, respectively. The plants should be harvested by cutting them at the base of the stem, after the completion of the growth cycle (Vanhove et al., 2011).

## **2.5 Post-harvest handling**

The leaves and flowers remain attached to the freshly harvested cannabis stem for subsequent hang/air-drying in a warm, dark, and dehumidified environment for 1 week at 25 °C (Vanhove et al., 2011). During the hang drying process, branches are cut off or entire plants are suspended upside down to facilitate the drying procedure. Afterward, the flowers and leaves should be stripped off from the stem for further processing operations (Vanhove et al., 2011).

## 2.6 Post-harvest operations

Post-harvest operations refer to all the processes a plant undergoes after harvest. This may include drying, curing, grinding, extraction, decarboxylation, molecular distillation, chromatographic analysis, formulation, and packaging. Although optimization of cannabis postharvest activities is discussed in the literature, it is essential to understand the effects of postharvest factors for maximizing yield and ensuring high-quality medical-grade products (Al Ubeed et al., 2022).

### 2.6.1 Drying

Drying is a unit operation in which liquid, solid, or semi-solid materials are converted into solid products by removing water through evaporation with a significant influence of temperature gradient in the transformation (Addo et al., 2023a; Kwaśnica et al., 2020). It is an important postharvest process step along the cannabis supply chain. Cannabis inflorescence has a moisture content of approximately 76-80 %, offering a favourable environment for microbial activity. Moisture content denotes the quantity of water, including free and bound forms, contained within a substance (Pou and Raghavan, 2020). Drying offers several advantages, such as regulating microbial growth, prolonging storage, and preserving the therapeutic benefits of medicinal plants (Al Ubeed et al., 2022; Hawes and Cohen, 2015). Various drying techniques have been utilized to preserve cannabis plant material, while oven drying can increase plant shelf life, its limited application and the high risk of quality changes have prompted the development of alternative drying technologies such as vacuum freeze-drying, atmospheric freeze-drying, and microwave-assisted hot-air drying (MAHD) (Addo et al., 2021; Prakash and Kumar, 2014; VijayaVenkataRaman et al., 2012).

Terpenes and cannabinoids can be preserved using MAHD (Chandrasekaran et al., 2013; Chasiotis et al., 2022). Another study reported that vacuum-microwave drying with 240 W effectively preserved the chemical profile of fresh cannabis, including 93 volatile compounds such as  $\beta$ -myrcene, limonene, and  $\beta$ -(E)-caryophyllene, as well as  $\alpha$ -humulene. The dried samples maintained high quality, exhibiting similar chemical profiles to the fresh cannabis biomass (Kwaśnica et al., 2020). In a recent study on hops (*Humulus lupulus*), a close relative of cannabis in the Cannabaceae family, Addo et al. (2022c) examined the effects of microwaves on drying behaviour and terpene concentrations and observed that as the moisture content

decreased, the drying rate decreased, whereas an increase in microwave power led to an increase in drying rate. Additionally, the MAHD and freeze-drying process reduced the terpene concentrations compared to a reference, undried hops samples due to pre-freezing and drying temperature.

Choosing the appropriate drying technique is of vital concern to improve and maintain the quality of cannabis for large-scale operations. In the cannabis industry, hang drying is mostly used due to the low capital and operational costs. However, this technique requires ample space to prevent overcrowding, which can cause ineffective drying and microbial growth (Das et al., 2022). Improving the drying rate and moisture diffusion is paramount in optimizing drying systems. In contrast to conventional hot-air drying methods, freeze-drying produces superior dried products that preserve nutritional value and colour (Cao et al., 2018; Ratti, 2001). It is a three-step technology that removes water molecules through sublimation and surface desorption (Tsinontides et al., 2004). This method maintains the chemical profile (Ratti, 2001). Addo et al. (2023a) reported that freeze-drying increased the cannabinoid (CBDA, CBGA, CBG) concentrations in dried cannabis by 6.9 % - 87.7 % compared to fresh, undried cannabis. Unlike other drying methods, freeze drying decreases the loss of phytochemicals, but the high cost and limited-size batch drying are significant drawbacks (Addo et al., 2021; Bantle et al., 2011; Rahman and Mujumdar, 2008).

### **2.6.2 Grinding or particle size reduction**

Particle size reduction or grinding is a mechanical process that reduces biomass to a desired particle size. It enables the transformation of its components into various materials for use in different sectors such as food, chemical, biofuels, and fodder industries. Grinding is essential for the efficient extraction of secondary metabolites from cannabis, as it enhances the contact surface area between the biomass and extraction solvents (Patel et al., 2017). The particle size of the biomass sample affects and regulates the mass transfer kinetics and solvent availability in the extractable components (Yunus et al., 2013). Particle size reduction by grinding breaks the cell walls and release more of the oil content, and increases the specific area (surface area-to-volume ratio), and the surface of smaller particles with larger specific areas contain more oil (del Valle and Uquiche, 2002). Efficiency is influenced by various variables, including mode of grinding, grinding speed, filling rate, feed size distribution, and hardness of

the material (Bu et al., 2020). Common methods used for particle size reduction of biomass include grinding (wet or dry), impact, cutting, chopping, attrition or shear, and crushing using a compressor (Barbosa-Cánovas et al., 2005; Moiceanu et al., 2019). However, grinding biomass is energy-intensive, and it is essential to use the proper equipment and optimal process parameters to achieve high efficiency in the transformation of biomass into valuable components, or else, the process would be inefficient and yield poor grinding efficiencies (Mayer-Laigle et al., 2018a; Mayer-Laigle et al., 2018b).

#### **2.6.2.1 Wet and dry grinding**

Wet grinding involves five consecutive steps: soaking, grinding with excess water, filtering, drying, and sieving. Sieving is used to achieve the desired distribution of different particle sizes. This process requires the utilization of multiple machines and a significant amount of manpower. Dry grinding does not involve water use and thus produces no wastewater (Ngamnikom and Songsermpong, 2011). Choosing between dry and wet grinding is a significant factor to consider in the grinding process, as it affects the efficiency and effectiveness of the process, and dry grinding is generally more energy-intensive and time-consuming than wet grinding (Addo et al., 2021; Mani et al., 2004; Moiceanu et al., 2019). Generally, dry grinding can prevent the creation of a solid suspension and result in greater oil production than wet grinding (Li et al., 2016). Apart from dry and wet grinding, mechanical grinding is the application of external or specialized forces to a material, resulting in its breakdown into smaller particles. Chemical grinding, a kind of wet grinding, removes some portion of particles by dissolving, digesting, or transforming a substance into a different substance (Ogonowski et al., 2018). Ngamnikom and Songsermpong (2011) observed higher grinding yields with dry grinding than with wet grinding. This was attributed to the particle loss during the five processing steps involved in the wet grinding of rice flour.

#### **2.6.2.2 Micronization**

Micronization is the process of reducing the size of biomass particles to below ten microns (Joshi, 2011). It is a useful approach to grinding biomaterials into superfine particles, resulting in the efficient extraction of bioactive compounds (Chen et al., 2018). It involves the use of hydrodynamic and mechanical methods to break the material and hasten particles,

resulting in grinding by the impact of particle-to-particle or against a solid surface (Dhiman and Prabhakar, 2021; Karam et al., 2016). This method enables the release of compounds that are tightly bound to the food matrix (Zhu et al., 2014). The process changes the material's structural, physicochemical, and functional properties as the particle size is reduced to the micron-level (Dhiman and Prabhakar, 2021). Fluidized-bed, fluid-energy, ball, and spiral jet mills are commonly used for micronization (Bender et al., 2020; Karam et al., 2016). At the micron scale, increased surface area improves properties such as solubility, reaction rate, absorption, and flavour release (Chen et al., 2018). However, the amount of energy needed for particle size reduction is directly related to the particle's fineness or the surface area created during the reduction process (Karam et al., 2016; Murthy et al., 1999). Grinding into the finest possible powder increases sample uniformity and enhances the efficiency of the extraction (Xu et al., 2010).

Various studies demonstrated the effects of micronization in increasing extraction yields (Aguilar et al., 2018; Espínola et al., 2009; Hu et al., 2012; Speroni et al., 2019; Wang et al., 2016a; Zhu et al., 2014). In a study, Espínola et al. (2009) found that using micronized calcium carbonate as a coadjuvant led to higher extraction yields of virgin olive oil compared to controlled extractions. Micronization resulted in a higher extractable polyphenols yield and increased the antioxidant activity of olive pomace. This can be associated with modifying the sample's structure and liberating polyphenols associated with the fibre matrix (Speroni et al., 2019; Zhu et al., 2014). Hu et al. (2012) reported the increased extraction of tea polysaccharides, which exhibit the more potent scavenging capacity of green tea powder extracts on  $\cdot\text{OH}$ . Micronization has demonstrated efficacy in enhancing the extraction of polyphenols and improving DPPH radical scavenging in mushrooms and isolated compounds like trans-resveratrol (Aguilar et al., 2018; Wang et al., 2016a).

### **2.6.2.3 Cryogenic grinding**

Excessive heating during grinding and contamination of the initial biomass are factors that can have a negative impact on a ground material's properties (Moiceanu et al., 2019). Cryogenic grinding involves cooling the biomass beyond its glass state using liquid nitrogen, dry ice or pre-freezing before grinding to protect and preserve secondary metabolites (Atkins, 2019; Balasubramanian et al., 2012). The low temperatures used in cryogenic grinding enhance the

brittleness of the material, resulting in increased production of fine particles while reducing the energy consumption required for the grinding (Goswami and Singh, 2003; Manohar and Sridhar, 2001; Singh and Goswami, 2000). The contraction caused by the cooling of materials allows imperfections or flaws in molecular bonds to expand and induce the formation of cracks (Balasubramanian et al., 2012).

Liquid nitrogen is used to achieve low temperatures and acts as the required refrigerant to precool the material and maintain the intended cool temperature by efficiently absorbing the heat generated during the grinding (Hemery et al., 2011; Singh and Goswami, 1999a). Liquid nitrogen offers clear advantages such as easy handling, minimal additional equipment requirements, and the ability to render the grinding plant inert, thus preventing dust explosions without the need for extra security measures. However, these advantages must be balanced against the disadvantage of high operational costs associated with using liquid nitrogen (Wilczek et al., 2004). Cryogenic grinding has been developed to improve extraction efficiency and maintain the integrity of volatile and heat-sensitive components in the materials (Hemery et al., 2011).

Ngamnikom and Songsermpong (2011) reported that cryo-grinding consumed less energy than wet grinding, and a higher yield after sieving was obtained than after dry grinding due to the formation of smaller particles. According to Saxena et al. (2015), cryo-ground coriander (*Coriandrum sativum*) samples exhibited higher levels of volatile oil, oleoresin, total phenols, flavonoids, and crude seed extract compared to non-cryogenic ground samples. Singh and Goswami (1999b) noted a 31 % increase in preserving volatile oil from cumin (*Cuminum cyminum*) when grinding was conducted at cryogenic temperatures compared to ambient temperatures. Also, cryogenic grinding increased the yield of *Cymbopogon schoenanthus* essential oil by 41 % obtained from microwave-assisted hydrodistillation compared to standard grinding (Bellik et al., 2019).

### **2.6.3 Extraction**

Extraction is the first step in analyzing the chemical components of a plant. A proper extraction procedure must be followed to avoid damaging the plant's chemical constituents throughout the process (Sasidharan et al., 2011). Efficient extraction of essential oils that contain pharmacologically significant bioactive substances is vital (Addo et al., 2021). The differences in



the quality and quantity of essential oils can be attributed to various factors such as geographic region, growth stages of the plants, environmental conditions, and extraction techniques (Badi et al., 2004; Heikal, 2017). Extraction is considered effective when the bioactive substances are soluble in the appropriate solvent. For this purpose, plant cell structures should be broken down to expose the active compounds and interact with the solvent (Ramirez et al., 2019).

Conventional solvent-based extraction methods, including maceration, Soxhlet extraction, and hydro-distillation, suffer from high solvent requirements and longer extraction times (Agarwal et al., 2018). To overcome these constraints, attention has recently been given to a range of modern or unconventional extraction methods facilitated by microwave, ultrasound, enzymes, pulsed electric field, supercritical fluid, and pressured liquid extraction (Azmir et al., 2013). A number of solvents such as ethanol, propane, butane, hexane, diethyl ether, petroleum ether, methyl tertbutyl ether, supercritical carbon dioxide (CO<sub>2</sub>), and olive oil can be employed (Dussy et al., 2005; Lazarjani et al., 2021; Lehmann and Brenneisen, 1992; Romano and Hazekamp, 2013; Rovetto and Aieta, 2017). Solubility, co-solvent, molecular affinity, toxicity, mass transfer, and environmental safety are essential factors to consider when selecting a solvent (Azmir et al., 2013).

Maceration refers to all extraction methods conventionally used today, where biomass is submerged in a solvent for a specific time to ensure efficient mass transfer. It includes using machines in batch, semi-batch, or continuous forms to ensure proper contact between the solvent and solute at any scale. In contrast to Soxhlet extraction, organic solvent extraction methods are referred to as immersion or dipping extraction methods. These methods are often named after the solvent used, such as ethanol extraction, which involves immersing the biomass in ethanol (Valizadehderakhshan et al., 2021). Soxhlet extraction is typically conducted at the solvent's boiling point for a prolonged period, which may result in the thermal degradation of the metabolites (Addo et al., 2022a). Although modern extraction methods can enhance the efficiency and quality of extracts, they are often burdened by high initial investment costs and limitations regarding the amount of material that can be used in each batch (Addo et al., 2021; Addo et al., 2022a; Addo et al., 2022b; Al Ubeed et al., 2022; Valizadehderakhshan et al., 2021).

#### 2.6.4 Decarboxylation

Effective production of neutral cannabinoids, including THC, CBD, and CBG, is crucial for effective dose formulations for the appropriate medicinal use of cannabis. These neutral cannabinoids are not found in high amounts in plants, which instead primarily synthesize their carboxylic acid forms, including THCA, CBDA, and CBGA (Wang et al., 2016b). Acidic cannabinoids vary from neutral cannabinoids by the presence of additional carboxylic acid (COOH) in their chemical structure. The pharmacological activity of acidic cannabinoids is less than neutral cannabinoids and is scarcely reported in the literature. Due to the occurrence of neutral cannabinoids as carboxylic acids in the cannabis plant, decarboxylation is now an important stage in the cannabis supply chain (Moreno et al., 2020b). The decarboxylation process occurs gradually within plants over time, but it can be expedited by exposing the plant to oxygen, light, or heat (Citti et al., 2018; Moreno et al., 2020b; Perrotin-Brunel et al., 2011; Veress et al., 1990a; Wang et al., 2016b). The decarboxylation of acidic cannabinoids follows a first-order or pseudo-first-order reaction (Wang et al., 2016b). Various factors influence the rate of this process. However, temperature and time are the primary factors, with higher temperatures and shorter time resulting in faster decarboxylation, but care has to be taken to avoid degradation. Unlike enzymatic reactions, decarboxylation is a simple chemical reaction catalyzed by heat, and it can occur even at room temperature, albeit at a slower rate (Citti et al., 2018).

Recreational cannabis users usually accomplish decarboxylation through smoking, vaping, or baking. A more controlled and precise process is needed for regulated medicinal products (Reason et al., 2022b). Depending on the end product, this process can be done either before or after the extraction of crude cannabis oil. The presence of oxygen and a decrease in plant mass causes an increase in decarboxylation rates (Moreno et al., 2020b). Wang et al. (2016b) conducted a decarboxylation study on cannabis extracts using a vacuum oven to determine the corresponding first-order rate constants. Veress et al. (1990a) were the first to publish on a kinetic decarboxylation study of THCA and CBDA using various sorbent surfaces and a glass surface in an open oven and described decarboxylation as a first-order reaction. Using a vacuum oven, Perrotin-Brunel et al. (2011) investigated the decarboxylation of THCA in cannabis plant material and defined it as a pseudo-first-order process catalyzed by the short-chain organic acids present in the flowers. Citti et al. (2018) reported that the ratio of CBDA to CBD concentrations in hemp seed oil serves as an important indicator for both the production process

and storage conditions. The decarboxylation of THCA to THC was investigated in various cannabis to assess stability under two different storage conditions. Results concluded that storing the in the dark at a temperature of 4 °C resulted in less decarboxylation of THCA, CBDA, and CBGA than storing in the light at 15-25 °C (Milay et al., 2020; Peschel, 2016).

### **2.6.5 Distillation**

Distillation is a unit operation consisting of physically separating components in a liquid mixture by partial evaporation based on their respective boiling points (Ketenoglu and Tekin, 2015; Shi et al., 2007). When heated, the mixture divides into two phases, gas and liquid. Highly volatile compounds enter the gaseous phase, where they can be separated and condensed to produce the distillate (Sharma, 2021).

#### **2.6.5.1 Molecular distillation**

Molecular distillation is a distillation technology used to separate and purify thermally unstable compounds in addition to liquids with high molecular weight and low vapour pressure. (Fregolente et al., 2007a; Micov et al., 1997). Molecular distillation is a kind of evaporative distillation wherein liquid evaporates without boiling, and vapours reach the surface of the condenser without being impeded (Hollo et al., 1971; Manohar and Udaya Sankar, 2009). It takes place at lower temperatures, which minimizes the risks of thermal decomposition, and additionally, a high vacuum prevents oxidation from occurring in the presence of air (Figure 2.2). This process has the unique characteristic of being completed without using solvents and instead relies solely on heat energy. This feature eliminates the need for additional solvent costs and helps reduce overall expenses (Meyer et al., 2011).

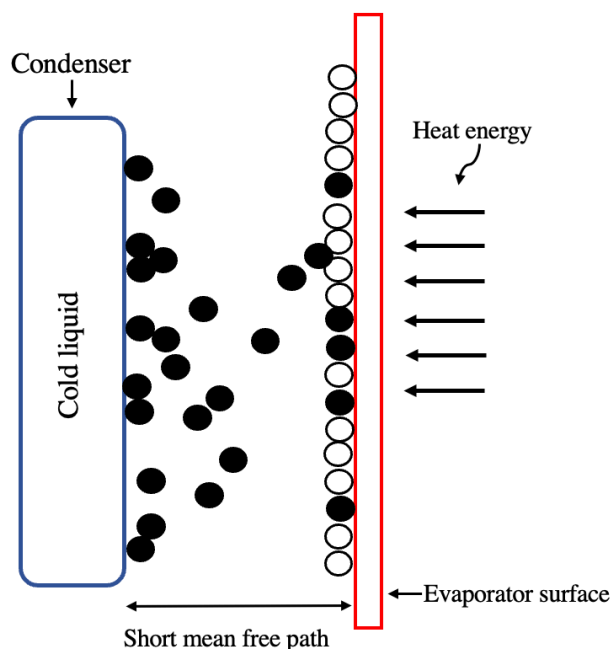


Figure 2.2. Evaporation and condensation in the molecular distillation process.

The vapour pressure values of pure substances depend on their boiling point or vaporization temperature, and the boiling point decreases when the pressure is lowered (Ketenoglu and Tekin, 2015). During heating, the vapour pressure increases for each component in the multi-component liquid, causing bubbling and evaporation (Valizadehderakhshan, 2022). So, the vapour contains a higher proportion of the more volatile component with the highest vapour pressure (Shi et al., 2007). In this process, the more volatile constituent moves from the liquid to the vapour phase, whereas the less volatile component moves from the vapour to the liquid phase, and evaporation and condensation are continuous at the interface due to the phase transition (Bandini et al., 1992; Battisti et al., 2020; Kienle et al., 1995; Liang et al., 2017). Evaporation of components at near boiling points occurs simultaneously, leading to the condensation of vapours and re-evaporation of the volatile components for purer separation (Treybal, 1980; Valizadehderakhshan, 2022).

Due to heat sensitivity, bioactive compounds in the cannabis essential oil degrade or lose their potency at high temperatures. Vacuum pumps, developed in the last century, have expanded the use of distillation to a broader range of applications, including refining and extracting heat-sensitive compounds, by allowing distilling under reduced pressure, which lowers the boiling point of the compounds being distilled by approximately 25 °C for every tenfold reduction in

pressure (Bethge, 2014; Mahrous and Farag, 2022). Vacuum distillation helps in the distillation of these compounds, of which there are two types depending on the application of vacuum levels; simple vacuum distillation (e.g., rotary evaporators) and high vacuum distillation (e.g., thin-film evaporators and short-path distillation systems) which require the application of lower and higher vacuum levels, respectively (Ketenoglu and Tekin, 2015). As a result, high boiling point substances susceptible to thermal degradation can be obtained as a distillate through a high vacuum distillation process (Mahrous and Farag, 2022).

Evaporation is a process of separating a liquid mixture into its components depending on boiling temperature differences (Valizadehderakhshan et al., 2022b). The evaporation rate in molecular distillation is influenced by the rate at which molecules move from the liquid's free surface and condense on the condenser, and this transfer distance is compared to the mean free path of vapour molecules (Shi et al., 2007). The mean free path is the average distance a molecule travels in the vapour phase without colliding with other vapour molecules. The lack of intermolecular collisions of vapour molecules entering the condenser prevents the dynamic equilibrium between the vapour and liquid (Eckles et al., 1991; Shi et al., 2007).

#### **2.6.5.2 Centrifugal molecular still**

The centrifugal molecular distiller consists of two main components: a heated evaporator and a cooling condenser surface. It is equipped with an electrical heating system and control units for temperature, pressure, and flow rate (Tovar et al., 2012). The feed/liquid that needs distillation is heated until the feed temperature has a significant temperature difference with the heater (Batistella and Maciel, 1998). The fluid is pumped into the centre of the apparatus, where a rotating plate/disk at high speed uses centrifugal force to spread the mixture throughout the heating surface (Batistella et al., 2002). Centrifugal force enables the creation of a thin liquid film that flows over the heated disk and contacts the condenser surface. The central rotational heated disk is a mechanical method of producing a uniform thin liquid film across the evaporator surface (Tovar et al., 2012). Centrifugal force facilitates evaporation without the risk of losing samples due to bumping or foaming (Liu and Seo, 2010). Condensation of most volatile components occurs in the condenser and is collected as a distilled fraction, while the heavier compounds are collected as residue (Tang et al., 2011). The high speed of the liquid film flow results in a very short residence time within the device, providing certain benefits in terms of

minimizing the chemical degradation of the products (Cvengroš et al., 2000; Cvengroš et al., 2001; Fregolente et al., 2007a; Xubin et al., 2005).

### **2.6.5.3 Falling film evaporator**

A falling film evaporator works like a shell and tube heat exchanger (Prost et al., 2006). The feed or fluid is introduced into the evaporator from the top of the tank, and it is evenly distributed across the heated cylindrical walls by the distributors (Batistella et al., 2002; Valizadehderakhshan, 2022). The shell side is where steam condenses and provides latent heat, which evaporates the feed flowing through the tube side (Prost et al., 2006). The fluid then flows downward by gravity, forming a thin film that is heated and evaporated in the process (Batistella et al., 2002; Valizadehderakhshan, 2022). Separation depends on the thermodynamic equilibrium between the compounds in the feed. The vapour produced by evaporation is condensed using a separate condenser, whereas the concentrate gets removed/collected from the unit for additional processing (Prost et al., 2006). It is beneficial because of the downward pull of gravity, which creates a fast-moving and thin liquid film with high heat transfer and short heating periods. This is particularly useful for heat-sensitive substances, requiring shorter residence times and minimal temperature variation between the heating medium and the liquid ( $<15\text{ }^{\circ}\text{F}$ ). It is commonly employed in concentrating various substances, including dairy products such as milk protein, cream, whey, skim milk, hydrolyzed milk, sugar solutions, phosphoric acid, urea, and black liquor (Valizadehderakhshan, 2022).

Querino et al. (2019) conducted a study on separation, energy and exergetic evaluation of multicomponent petrochemical naphtha, demonstrating that the use of a falling film evaporator resulted in a 12 % reduction in total energy consumption compared to a conventional system. Batistella and Maciel (1998) reported that the performance of centrifugal and falling film distillators was negatively affected by factors such as prolonged exposure and residence times, as well as high distillation temperatures resulting in thermal decomposition. Regarding distillation time, the centrifugal distillator would require a shorter duration than the falling film distillator. This is because the centrifugal force increases the velocity of the distilling liquid, facilitating faster separation. For obtaining the same quantity of distillate, the falling film distillator operates at relatively lower temperatures than the centrifugal distillator. Overall, the centrifugal distillator is preferable since the equipment is more compact and allows for uniform liquid distribution on

the rotor, facilitating effective mass and energy transfers, thereby enhancing efficiency (Batistella and Maciel, 1998).

#### **2.6.5.4 Wiped-film short path (WFSP) evaporator/molecular still**

The wiped film evaporator with an integrated condenser is currently the most commonly used equipment in the large cannabis processing facilities. The feed is distributed evenly at the top of a heated cylindrical container equipped with a heating jacket, flows down due to gravity as a thin film, and is continuously wiped (Bethge, 2014). This includes a basket with three-stranded wipers that aid in evenly distributing feed across the surface of the evaporator (Sagili et al., 2023). The speed of the wipers determines the thickness of the film. As a result of heating, the volatile components evaporate and condense in the internal condenser. The resulting distilled liquid is collected at the lower end of the condenser. The remaining non-volatile part, known as the residue, flows along the evaporator and collects in the residue section through the residue nozzle (Bethge, 2014). A cold trap is connected to the distillation unit to prevent vapours from escaping and damaging the vacuum pump. The cold trap captures these vapours and ensures the vacuum pump remains protected (Sagili et al., 2023).

#### **2.6.5.5 Rotary Evaporator**

Although it is not a molecular distillation technique, the rotary evaporator is a popular method used in many commercial applications to remove or evaporate solvents from feed or reaction mixtures. The apparatus comprises various components, including a condenser connected to a vacuum, receiving and evaporating flasks, a heating water bath, a vapour duct, an action jack lift for manually elevating the evaporating flask, and a manually adjustable rotation speed (rpm) for rotating the evaporating flask while boiling the reaction mixture (Figure 2.3). The rotation increases the effective surface area of the sample during boiling, which facilitates faster evaporation. To prevent damage to the vacuum unit, a condenser with a cold trap is connected to the sample flask to trap metabolites escaping from the system. The evaporation rates can be enhanced by reducing the pressure, which further lowers the boiling point of the solvent and promotes faster evaporation. Overall, the rotary evaporator is a versatile and efficient tool used in various industries, including pharmaceuticals, chemical and food processing.

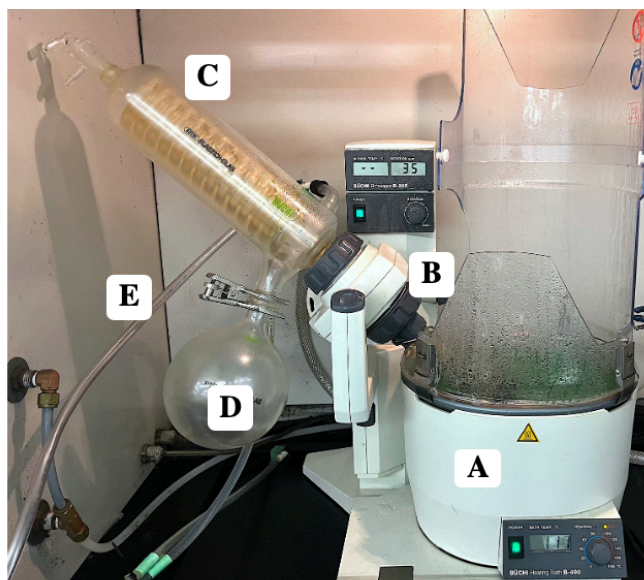


Figure 2.3. Rotary evaporator; (A) Water bath with heating element, (B) Motor connected with evaporator flask, (C) Condenser, (D) Condenser flask, (E) Vacuum pump.

## 2.6.6 Distillation techniques in the cannabis industry

Commonly used distillation techniques in the cannabis industry are short-path distillation (SPD) and WFSP molecular distillation. These processes usually occur at reduced pressures and temperatures and in two stages, i.e., terpenes which are the most volatile substances having lower boiling points, will be separated and collected from the cannabinoids with the heavy compounds (chlorophyll, waxes, etc.) in the first stage and while the cannabinoids will be separated from the heavy compounds in the second stage.

### 2.6.6.1 Short-path distillation (SPD)

SPD is commonly used in the small-scale cannabis industry to purify crude cannabis oil in two stages, where terpenes and cannabinoids are removed in the first and second stages, respectively. The crude cannabis oil (feed) is heated in a flask insulated with a heating jacket. An electric heating mantle provides the required temperature for the oil evaporation. The application of temperature depends on the type of metabolite that needs separation. The vapours produced during evaporation travel a short distance to reach the condenser, where they are condensed and collected in a receiver flask. A cold trap is used to prevent vapours from escaping the system and causing damage to the vacuum pump. Although cost-effective, SPD systems suffer from lower



refinement and product recovery than WFSP molecular distillation (Valizadehderakhshan et al., 2022b).

#### 2.6.6.2 Wiped-film short path (WFSP) molecular distillation

WFSP molecular distillation is one of the efficient molecular distillation techniques because it is a rapid process that results in higher recovery and concentration, and it can be used for large-scale operations as shown in Figure 2.4 (Valizadehderakhshan et al., 2022b). The formation of thin film, which exposes a greater surface area by rotating wipers, is the key specialty of this system. Several parameters play an important role in determining the distillation efficiency, including the feed flow rate, evaporative and internal condensation temperature, pressure, feed temperature, and the speed of the wiper blades. The system is equipped with a heating jacket to ensure optimal performance to prevent heat loss during molecular distillation. In addition, using Marlotherm SH thermic oil allows proper control over temperature and maintains constant feed temperature throughout the distillation process.

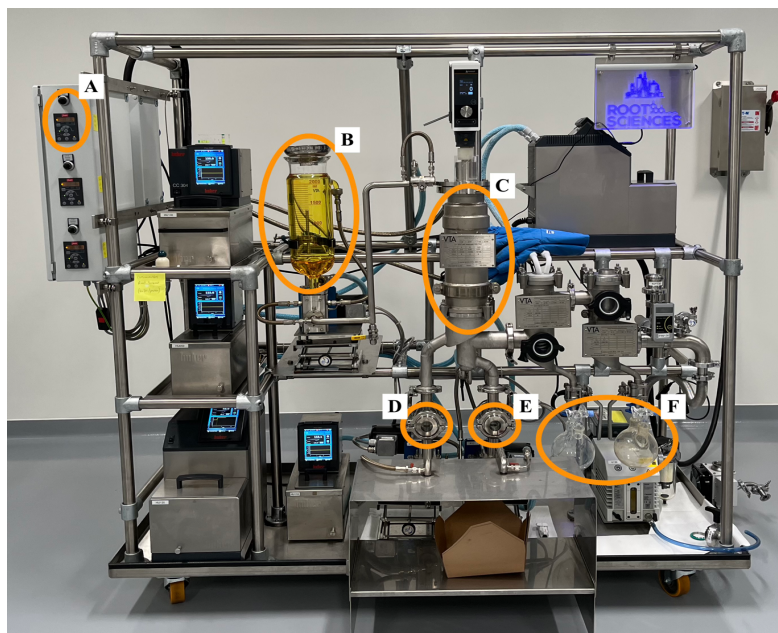


Figure 2.4. Wiped-film short path molecular distillation equipment; (A) Feed flow rate regulator, (B) Feed tank, (C) Combined evaporator internal condenser section, (D) Distillate discharge unit, and (E) Residue discharge unit, and (F) Cold traps.

Sagili et al. (2023) reported that a wiped-film short path molecular distillation system achieved a THC recovery efficiency of 93.4 % for cannabis biomass, while Valizadehderakhshan et al. (2022b) refined CBD with the highest recovery and concentration of 92.7 % and 80.2 %, respectively, with wiped-film molecular distillation. Comparable findings have been reported for other plants; the WFSP molecular distillator prevented the thermal degradation of bioactive compounds and pigments during the separation of D-limonene and other oxygenated compounds from the orange essential oil (García-Fajardo et al., 2023). With the use of WFSP molecular still, Martins et al. (2012) observed an increased concentration of methyl chavicol up to 90 % from basil essential oil.

### **Connecting text**

Chapter 2 reviewed the importance of preserving and obtaining secondary metabolites, specifically cannabinoids and terpenes, through the optimization of post-harvest technologies. It provided a description of potential particle size reduction or grinding techniques. However, limited literature exists regarding the determination of optimal particle size with suitable extraction conditions to enhance the extraction yield and concentration of cannabinoids and terpenes. In Chapter 3, the effects of particle size, solvent type, and extraction temperature on the extraction of crude cannabis oil, cannabinoids, and terpenes are examined.

Chapter 3 has been submitted for publication and is cited as the following:

**Sagili, S.U.K.R.,** Addo, P.W., MacPherson, S., Shearer, M., Taylor, N., Paris, M., Lefsrud, M., Orsat, V., 2023. Effects of particle size, solvent type, and extraction temperature on the extraction of crude cannabis oil, cannabinoids, and terpenes. ACS Food Science & Technology. <https://doi.org/10.1021/acsfoodscitech.3c00129>

### **Chapter 3: Effects of particle size, solvent type, and extraction temperature on the extraction of crude cannabis oil, cannabinoids, and terpenes**

#### **Abstract**

Optimized medicinal plant processing and extraction can improve extract yield and efficiency for valued secondary metabolites while reducing operation costs. This study investigated the effects of the particle size [coarse (2-4 mm), medium (0.5-2 mm), fine (0.25–0.5 mm)], solvents (ethanol, butanol, hexane), and extraction temperature (–20 °C, 4 °C, room temperature) on extracted crude cannabis oil yield and cannabinoid/terpene concentrations using a full factorial design. Results indicate finer particle size significantly increased the cannabinoid concentrations in the extracts. Ethanol extraction with fine-sized cannabis particles at 4 °C obtained the highest crude oil yield of 28 % and had improved recovery rates: 41 % for THCA, 36 % for CBGA, along with higher total terpenes concentration (1550 mg 100 g dry matter<sup>-1</sup>) in the extracts. Irrespective of temperature and particle size, the solvents produced extracts with different colors: ethanol (dark green), butanol (green), and hexane (yellow). This research provides grinding and extraction conditions with scale-up potential by the cannabis industry to achieve higher crude cannabis oil yield with significant cannabinoids and terpene concentrations.

**Keywords:** Cannabis industry, *Cannabis sativa*, chlorophyll, cryo-grinding, full factorial design, organic solvents

### 3.1 Introduction

*Cannabis sativa*, a dioecious, annual, and short-day plant in the Cannabaceae family, is growing extensively around the world and is renowned for its medical, historical, and social implications (Brighenti et al., 2017; Challa et al., 2021; Hartsel et al., 2016). The production of cannabis has evolved into one of the fastest-developing markets because of the global trend toward legalization (Bahji and Stephenson, 2019; Eichhorn Bilodeau et al., 2019). The female inflorescence of the cannabis plant forms glandular trichomes, which serve as the primary site for the production and storage of valued cannabinoids and terpenoids (Appendino et al., 2011; Livingston et al., 2020). Flavonoids represent a third major group of secondary metabolite categories with added value potential; these are found in the highest abundance in leaves, followed by the inflorescence (Jin et al., 2020).

Cannabis accessions, environmental conditions during cultivation, harvesting techniques, and post-harvest processing are four critical parameters that affect secondary metabolite profiles, in addition to the quality of the cannabis plant biomass or cannabis derived products; as such, post-harvest activities are considered by some as crucial to the entire economy, requiring technological evaluation and innovation (Addo et al., 2021; Morello et al., 2022; Pusiak et al., 2021; Valizadehderakhshan et al., 2021). Cannabis post-harvest technologies have been developed to reduce operational costs and maximize solvent recovery and oil yields while maintaining secondary metabolite quality. Extraction is an essential process in cannabis to free the bioactive compounds from the plant matrix and to broaden the range of utilization of these compounds in the medicinal and food industry (Al Ubeed et al., 2022). Several factors influence extraction yield and efficiency of cannabis essential oil containing bioactive compounds. These include drying methods, biomass particle size, the method and frequency of extraction, solvent type, biomass-to-solvent ratio, extraction temperature and time.

Particle size reduction of the biomass material improves the extracted oil yield by increasing the surface contact area between the biomass and the solvent (Nieh and Snyder, 1991; Russin et al., 2007). Grinding damages plant cell walls, improving the permeability of the solvent into the cells; grinding further increases the temperature which can lead to biochemical changes and alter the physicochemical properties of the material. These changes may result in a loss of bioactivity in the material (Maaroufi et al., 2000; Pesek et al., 1985; Zaiter et al., 2016). Cryo-grinding involves using liquid nitrogen (LN<sub>2</sub>) to cool the plant material beyond the glass

state before grinding. This method maintains the quality of plant material by preserving the secondary metabolites and preventing the degradation of the cannabinoids (Addo et al., 2021; Atkins, 2019; Balasubramanian et al., 2012). The particle size of the biomass sample affects and regulates the mass transfer kinetics and solvent availability in the extractable components (Yunus et al., 2013).

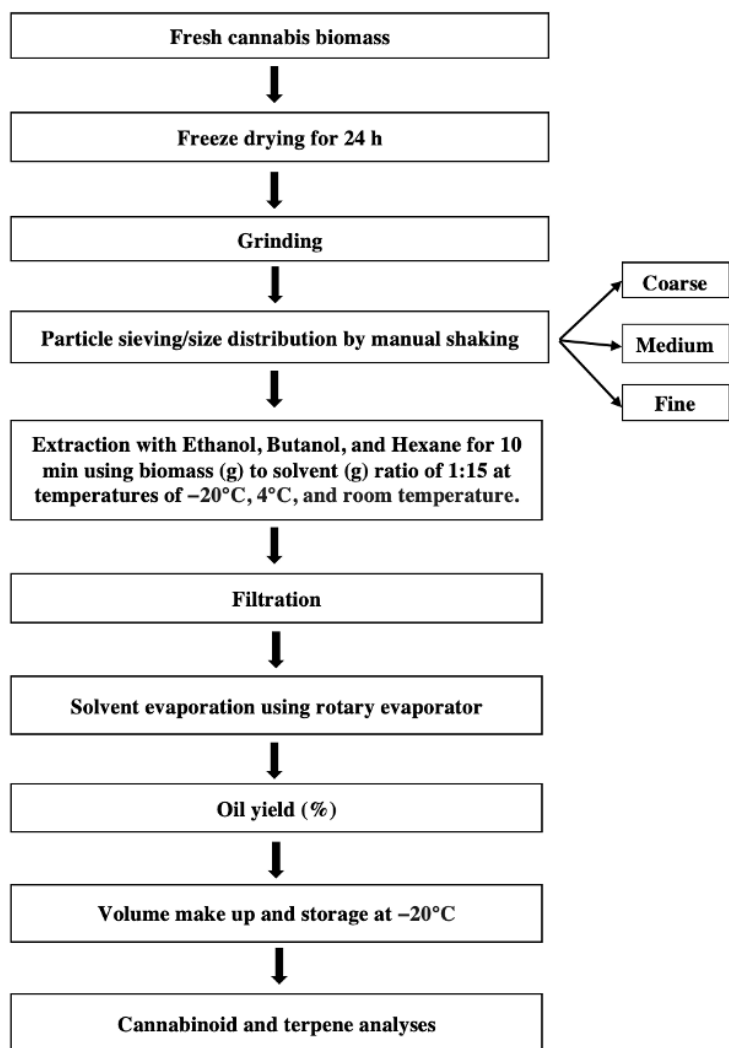
Extraction solvent selection plays a crucial role in influencing and maximizing the extraction process and yield (Chang et al., 2017; Nahar et al., 2021). The extraction of secondary metabolites depends on the solvation power and affinity of the solvent used (Li et al., 2014). The extraction process for producing different types of concentrates depends on the ability of cannabinoids and other molecules of interest to dissolve in the organic solvents, including hydrocarbons and alcohols (Rovetto and Aieta, 2017). Organic solvents are generally used for cannabis extraction due to the lipophilic nature of the majority of cannabinoids (Nahar et al., 2021). While solvents such as methanol, ethanol, chloroform, butane, and hexane are commonly used, safety is a concern due to the possibility of toxicity and flammability (Romano and Hazekamp, 2013; Rovetto and Aieta, 2017). Green solvents, including deep eutectic solvents, gas-expanded liquids, and supercritical carbon dioxide pose low toxicity and less environmental impact than organic solvents, but extraction efficiency, preparation, and economic considerations should be taken into account (Hashemi et al., 2022).

Extraction temperature additionally influences extraction yield and cannabinoid and terpenes concentrations (Addo et al., 2022a). Currently, limited studies have explored ideal particle size for dried cannabis biomass while simultaneously comparing various solvents at different temperatures for industrial extraction. The main objective of this experiment was to optimize particle size (coarse, medium, and fine) of cannabis biomass and explore the impact of different extraction conditions, including solvent type (ethanol, butanol, and hexane) and temperature ( $-20\text{ }^{\circ}\text{C}$ ,  $4\text{ }^{\circ}\text{C}$ , or room temperature) on crude cannabis oil yield and concentration of cannabinoids and terpenes using a full factorial design. Data reported here may prove useful for feasibly evaluation in an industrial setting, to improve extraction and achieve the highest yield of crude cannabis oil containing significant concentrations of cannabinoids and terpenes.

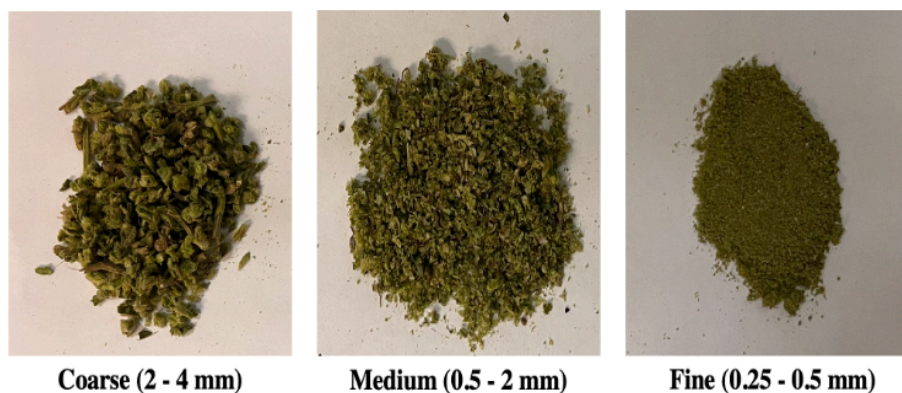
## **3.2 Materials and methods**

### **3.2.1 Sample Preparation**

Freshly harvested cannabis inflorescence (accession ‘Black Dog’) was obtained from an outdoor licensed producer, Les Entreprises C-Medical Inc. (Mirabel, Qc, Canada). The process flowchart for sample preparation is illustrated in Figure 3.1. Cannabis inflorescence was pre-frozen at  $-20\text{ }^{\circ}\text{C}$  for 24 h before subjecting to a laboratory-scale vacuum freeze dryer (Martin Christ Gefriertrocknungsanlagen GmbH Gamma 1–16 LSCplus, Osterode, Lower Saxony, Germany). A total of 1 kg fresh biomass was freeze-dried for 24 h at condenser and plate temperatures of  $-55\text{ }^{\circ}\text{C}$  and  $10\text{ }^{\circ}\text{C}$ , respectively, under 0.85 mbar pressure, resulting in 274 g of dry mass. The moisture content of the cannabis inflorescence was measured initially by using a hot air oven (Fisher Scientific 6903 Isotemp, Waltham, MA, US). The samples were subjected to a drying process at  $50\text{ }^{\circ}\text{C}$  for 24 h. The initial moisture content was 72.6 % (wb).



(a)



(b)

Figure 3.1. Methodology followed for this study; (a) Process flowchart; (b) Different particle sizes.



### **3.2.2 Grinding and Sieving**

Freeze-dried inflorescence was divided into three groups, and each group was cryo-ground using liquid nitrogen. Cryo-grinding was performed using two grinders: a laboratory-scale food processor and a Black and Decker coffee grinder (CBG100S, Richmond Hill, Ontario, Canada). The food processor was used to obtain coarse and medium-sized particles, while the coffee grinder was used to obtain fine-sized particle samples. After cryo-grinding, the ground cannabis biomass was exposed to room temperature to allow the LN<sub>2</sub> to evaporate. Subsequently, manual sieve separation was performed on the dry and ground biomass to determine the particle size ranges. A manual sieve separation system was used to determine the particle size ranges. The sieve sizes used in this study were 4, 2, 0.5, and 0.25 mm, which correspond to ASTM sieve numbers (#) of 5, 10, 35, and 60, respectively. The particle sizes were determined based on the retention of ground cannabis on particular sieve openings. Three particle sizes were obtained, namely coarse (2-4 mm), medium (0.5-2 mm), and fine (0.25-0.5 mm). The ground biomass was placed in different clean zip-lock plastic bags for the different particle sizes and kept at -20 °C, 4 °C, or room temperature for 24 h prior to extraction.

### **3.2.3 Extraction procedure**

The organic solvent extraction procedure outlined by Addo et al. (2022a) was used for this study. Three organic solvents, including ethanol, butanol, and hexane, were obtained from Thermo Fisher Scientific (Waltham, Massachusetts, US). Solvent extraction at different temperatures (-20 °C, 4 °C, and room temperature) was used for the extraction of crude cannabis oil. A sample (g) to solvent (g) ratio of 1:15 and an extraction time of 10 min was used based on optimal conditions obtained from our previously reported findings (Addo et al., 2022a). Before extraction, the predetermined quantity of ground cannabis samples and each extraction solvent were separately taken into 50-mL Falcon tubes and kept at -20 °C or 4 °C for 24 h to achieve the desired temperatures for extraction. Ground cannabis samples for cold solvent extraction (-20 °C and 4 °C) were placed at the appropriate temperature for 24 h before extraction. The ground cannabis was mixed with the solvent and mounted onto a Corning LSE variable speed vortex mixer (Corning, Glendale, AZ, USA) for 10 min. Extraction at -20 °C and 4 °C was performed by keeping the vortex mixer in the freezer together with the sample soaked in the respective solvent at the desired temperature. This was to mimic the cold solvent extraction used in the

cannabis industry. Full factorial design (FFD) was employed to evaluate the impact of the biomass particle size, solvent type, and extraction temperature on cannabis oil yield and the concentration of cannabinoids and terpenes. Each experimental condition was carried out in triplicate, with three various cannabis biomass samples.

### 3.2.4 Calculation of oil yield

After extraction, residual biomass from each extract was removed by manual filtration using Whatman No.4 filter paper (Sigma Aldrich, St. Louis, MO, USA). Extracts were stored at  $-20\text{ }^{\circ}\text{C}$  before the oil yield calculation. A rotary evaporator (HNZXIB, Henan Zhuoxian Import & Export Trading Co., Ltd., China) was operated at 35 rpm while under a vacuum (50 mbar) to evaporate the solvent contained in the extracts to determine the mass of cannabis oil. Solvent evaporation temperatures of  $50\text{ }^{\circ}\text{C}$  were used for ethanol and hexane, and evaporation temperature of  $85\text{ }^{\circ}\text{C}$  for butanol. Equation (3.1) was used to calculate the crude cannabis oil yield. The recovery rate was calculated using Equation (3.2), and the initial cannabinoid concentration of the coarse (reference) sample was utilized to evaluate the influence of particle size, solvent type, and extraction temperature on the recovery rate (%) of acidic cannabinoids.

$$\text{Oil Yield (\%)} = \frac{\text{mass of crude cannabis oil (g)}}{\text{mass of dried cannabis sample (g)}} \times 100 \quad (3.1)$$

$$\begin{aligned} \text{Recovery rate (\%)} = \\ \frac{\text{THCA or CBGA content in extract (mg 100 g dry matter}^{-1})}{\text{THCA or CBGA content in reference coarse sample (mg 100 g dry matter}^{-1})} \times 100 \end{aligned} \quad (3.2)$$

### 3.2.5 Cannabinoid analyses

The cannabinoids were analyzed using a Waters Acquity ultra high-performance liquid chromatography (UPLC) with a tunable ultraviolet (TUV) detector (Waters<sup>TM</sup>, Mississauga, Ontario, Canada). Extracts were diluted 50x with high performance liquid chromatography (HPLC) grade methanol (Thermo Fisher Scientific, Waltham, Massachusetts, US) for major cannabinoids and 4x for minor cannabinoids, followed by pipetting and transferring 1 mL of each extract to HPLC vials for analysis. The Waters cortex column with an isocratic gradient pump was employed to isolate the cannabinoids while maintaining a column temperature of  $35\text{ }^{\circ}\text{C}$ .

°C and a sample injection volume of 2 µL for the analysis. A total of 41 % reverse osmosis (RO) water and 0.1 % formic acid (Sigma-Aldrich, St. Louis, Missouri, US) was utilized for mobile phase A, while mobile phase B was composed of 78 % HPLC-grade acetonitrile (Thermo Fisher Scientific, Waltham, Massachusetts, US). A wavelength of 280 nm was used for detection, and the run time was 10 minutes. Calibration curves were established using 8 standard cannabinoids, of which acidic cannabinoids, tetrahydrocannabinolic acid (THCA), cannabidiolic acid (CBDA), and cannabigerolic acid (CBGA) were supplied in acetonitrile at a concentration of 1 mg mL<sup>-1</sup>, while the neutral cannabinoids, including tetrahydrocannabinol (THC), cannabidiol (CBD), cannabigerol (CBG), cannabichromene (CBC), and cannabinol (CBN), were supplied in methanol at 1 mg mL<sup>-1</sup>. (LGC standards, Manchester, New Hampshire, US and Sigma Aldrich, St. Louis, Missouri, US).

### 3.2.6 Terpene Analyses

Terpenes were analyzed using a gas chromatography-tandem mass spectrometer. The terpenes were examined by transferring 1 mL of each sample extract using a pipette into gas chromatograph (GC) vials. Terpenes were separated using Agilent 7820A GC connected to an Agilent 7693 autosampler and a flame ionization detector (FID) (Agilent Technologies, Mississauga, Ontario, Canada). The configuration consisted of an injector equipped with a capillary column (30 m x 250 µm x 0.25 µm nominal Agilent Technologies DB-5 Model). Split injection with a ratio of 50:1 was used, and the system utilized a hydrogen carrier gas with a flow rate of 40 mL per minute. Also, a syringe size of 10-µL was used to inject 5 µL of each sample into the system. Initially, the temperature of the oven in the mass spectrometer was set to 35 °C and maintained constant for 4 minutes. Subsequently, it was raised at a speed of 10 °C per minute until it attained 105 °C, where it was maintained for 0 min. It was then raised to 205 °C at a rate of 15 °C per min and maintained for 0 min, followed by an ultimate rise to 270 °C at a speed of 35 °C per min and maintained for 5 min. The FID detector's inlet temperature was fixed to 340 °C. Three scans were performed to record spectra ranging from 50 m z<sup>-1</sup> to 400 m z<sup>-1</sup>. An electronic impact at 70 eV was utilized in the ionization mode. For terpenes quantification, an external calibration was performed using 37 typically found terpenes (LGC standards, Manchester, New Hampshire, US and Sigma Aldrich, St. Louis, Missouri, US) in the cannabis.

### 3.2.7 Statistical analysis

JMP software (JMP 4.3 SAS Institute Inc.) was used to design the experiment. A three-level-by-three-variables randomized FFD was used for this experimental study to evaluate the effect of independent variables/factors on the responses (Table 3.1). A total of 81 experimental runs were generated with all possible combinations of variables at all levels. The order of experimental runs was randomized to minimize the possibility of experimental errors. Data collected were statistically analyzed using JMP software (JMP 4.3 SAS Institute Inc.), and the significance of the developed models was determined. The differences at a probability level of  $p < 0.05$  were deemed significant.

Table 3.1. Coded levels of the independent variables for solvent extraction of cannabis.

Independent variables	Symbol	Levels
Particle size	$X_1$	Coarse Medium Fine
Solvent type	$X_2$	Ethanol Butanol Hexane
Extraction temperature ( $^{\circ}\text{C}$ )	$X_3$	$-20\text{ }^{\circ}\text{C}$ $4\text{ }^{\circ}\text{C}$ Room temperature (RT) ( $22\text{ }^{\circ}\text{C} \pm 2\text{ }^{\circ}\text{C}$ )

## 3.3 Results

### 3.3.1 Effect of particle size on cannabinoid concentrations of dried cannabis biomass before extraction

The effects of dried biomass particle size on concentrations of THCA, CBGA, THC, and CBG, were examined prior to extraction. The initial cannabinoid concentration (mg 100 g dry matter<sup>-1</sup>) of cannabinoids in the ground cannabis biomass for each studied particle sizes are shown in Figure 3.2. Concentrations of THCA obtained from coarse, medium, and fine are statistically ( $p < 0.05$ ) different from each other (Figure 3.2 (A)). Statistical parameter effect analyses demonstrated the significant effect ( $p < 0.05$ ) of particle size on the concentrations of THCA, CBGA, and CBG, with a high  $R^2$  and adjusted  $R^2$  value of 0.99. Smaller (fine) particle size of the ground cannabis biomass increased the concentration of cannabinoids. Specifically, THCA, CBGA, and CBG concentrations were higher, by 30.9 %, 24.6 %, and 27.3 %, respectively, when the size of biomass particles was decreased from coarse to medium. A similar observation was made by decreasing the particle size from coarse to fine [THCA (53 %), CBGA (40.2 %), and CBG (45.4 %)]. However, an unexplained trend was observed with the THC,

where medium-sized particles obtained higher concentrations compared to coarse and fine particle sizes. CBDA and CBD were below the limit of detection (LOD) of the instruments and are not presented.

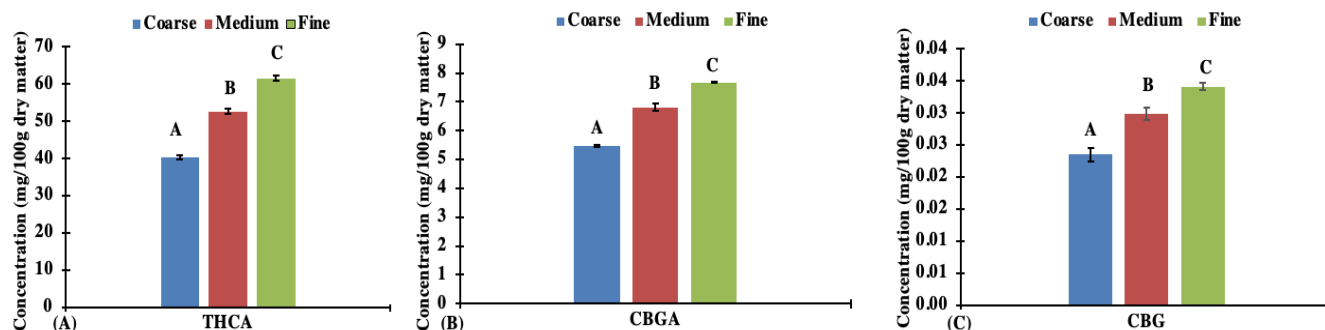


Figure 3.2. Effect of particle size reduction (grinding) on the initial concentrations (mg 100 g dry matter<sup>-1</sup>) of THCA (A), CBGA (B), and CBG (C) before extraction. Bars with the same letter are not significantly ( $p > 0.05$ ) different.

The recovery rates for acidic cannabinoids (THCA and CBGA) were calculated using Equation 3.2 and are presented in Figure 3.3. Statistical analyses showed that particle type ( $X_1$ ) and solvent type ( $X_2$ ) played a significant ( $p < 0.05$ ) role, whereas extraction temperature ( $X_3$ ), and the interactive effects of the three parameters were non-significant ( $p > 0.05$ ) on the recovery rates of acidic cannabinoids (THCA and CBGA). In Figure 3 (A), the recovery rates (%) of THCA for ethanol at  $-20\text{ }^{\circ}\text{C}$  show that coarse (A), medium (B), and fine (C) particles are statistically ( $p < 0.05$ ) different from each other, as indicated by distinct first connecting letters. However, coarse at  $4\text{ }^{\circ}\text{C}$  (A) is significantly ( $p < 0.05$ ) different from  $-20\text{ }^{\circ}\text{C}$  (B) and RT (B), but, coarse at  $-20\text{ }^{\circ}\text{C}$  (B) and RT (B) are not significantly ( $p > 0.05$ ) different from each other, as indicated by second connecting letters. Data analyses showed that the highest recovery rates of 41 % (THCA) and 36.1 % (CBGA) were obtained with ethanol extraction of fine particles at  $4\text{ }^{\circ}\text{C}$ . When using ethanol at  $-20\text{ }^{\circ}\text{C}$ ,  $4\text{ }^{\circ}\text{C}$ , and RT, reducing the particle size from coarse to fine resulted in an increase in the recovery rates of THCA from 26.7 % to 40.7 %, 26.9 % to 41 %, and 28.4 % to 40.9 %, respectively. Similarly, the recovery rates for CBGA increased from 25.8 % to 35.6 % ( $-20\text{ }^{\circ}\text{C}$ ), 25.3 % to 36.1 % ( $4\text{ }^{\circ}\text{C}$ ), and 27.1 % to 35.7 % (RT). At a temperature of  $-20\text{ }^{\circ}\text{C}$ , the recovery of THCA decreased when particle size was increased from medium to coarse, specifically from 32.3 % to 26.7 % (ethanol) and 27.3 % to 23.4 % (hexane). Similar

observations were made for CBGA; the recovery rates decreased from 29.7 % to 25.8 % (ethanol) and 24.2 % to 21.8 % (hexane).

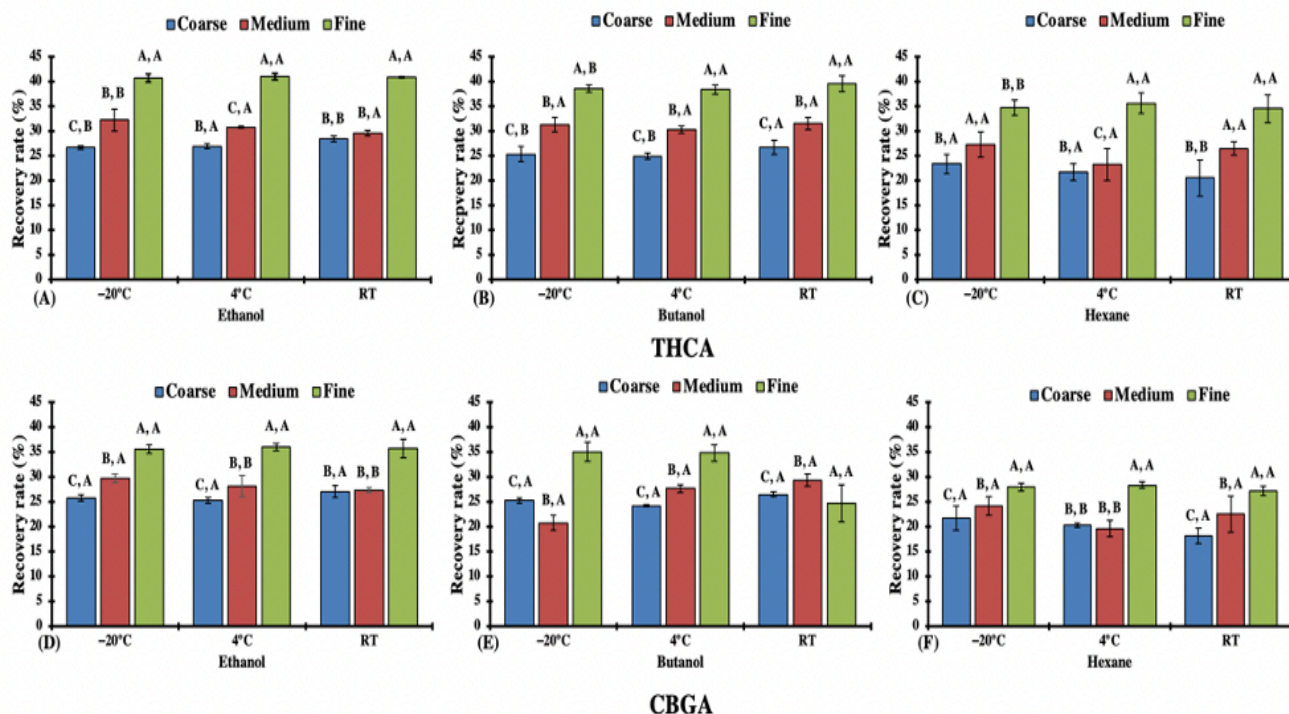


Figure 3.3. Effect of particle size, solvent, and extraction temperature on the recovery rates of acidic cannabinoids, THCA (A-C) and CBGA (D-F). Bars with the same first letter are not significantly ( $p > 0.05$ ) different between the particle sizes for the same extraction temperature and solvent type. Bars with the same second letter are not significantly ( $p > 0.05$ ) different between the extraction temperature for the same particle size and solvent type.

When using finer particles at 4 °C, replacing ethanol with hexane led to a decrease in recovery rates for THCA, from 41.0 % to 35.6 % and for CBGA from 36.1 % to 28.4 %. However, with coarse particles at RT, substituting hexane with butanol resulted in an increase in the recovery rates for THCA increased from 20.6 % to 26.7 %, while for CBGA, the recovery rates increased from 18.2 % to 26.5 %. When medium-sized particles were extracted with ethanol and the temperature was raised from –20 °C to RT, an increase in THCA recovery rates from 26.7 % to 28.4 % and CBGA from 25.8 % to 27.1 % was observed. Similarly, for the butanol extraction of fine particles and lowering the temperature from 4 °C to –20 °C, the recovery rates of THCA and CBGA increased from 38.4 % to 38.6 % and 34.9 % to 35.1 %,

respectively. At all tested conditions, the recovery rates for CBG and THC were greater than 100 %.

The dried cannabis biomass was extracted using various solvents at different temperatures. Following extraction, marked differences in color between extracts obtained with each solvent were observed. Extracts had a dark green, green, and yellow color for ethanol, butanol, and hexane extraction solvents, respectively (Figure 3.4).

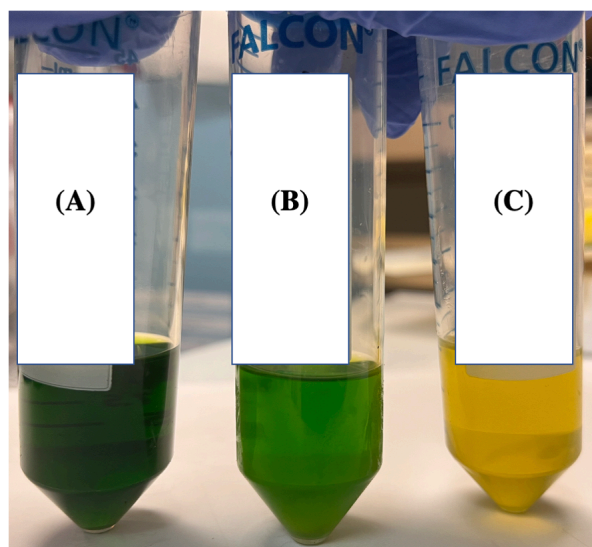


Figure 3.4. Representative images of different colors observed in crude cannabis oil extracted using different solvents; (A) ethanol, (B) butanol, and (C) hexane.

### 3.3.2 Effect of particle size, solvent type, and extraction temperature on oil yield (%)

Statistical analyses performed for this study show that extracted cannabis oil yield was significantly ( $p < 0.05$ ) influenced by the linear effects of particle size ( $X_1$ ), solvent type ( $X_2$ ), and as well as the interactive effects of particle size and solvent type ( $X_1X_2$ ), solvent type and temperature ( $X_2X_3$ ), and particle size and temperature ( $X_1X_3$ ) (Table 3.2). Extraction temperature ( $X_3$ ) did not have a significant effect ( $p < 0.05$ ) on cannabis oil yield. Data presented are mean values with corresponding standard deviations.

Table 3.2. Variability sources and significance levels on the responses.

Response	Variability ( <i>P</i> )						
	Particle size ( $X_1$ )	Solvent type ( $X_2$ )	Extraction Temperature ( $X_3$ )	Particle size*Solvent type ( $X_1X_2$ )	Solvent type*Extraction temperature ( $X_2X_3$ )	Particle size*Extraction Temperature ( $X_1X_3$ )	Particle size*Solvent type*Temperature ( $X_1X_2X_3$ )
<b>Recovery rate (%)</b>							
THCA	<0.0001*	<0.0001*	0.34	0.51	0.54	0.49	0.33
CBGA	0.0024*	0.0081*	0.86	0.92	0.89	0.62	0.29
<b>Oil yield (%)</b>	<0.0001*	<0.0001*	0.19	0.0171*	<0.0001*	0.0056*	0.26
<b>Cannabinoid concentration ( mg 100 g dry matter<sup>-1</sup>)</b>							
THCA	<0.0001*	<0.0001*	0.49	0.74	0.78	0.73	0.81
CBGA	<0.0001*	<0.0001*	0.81	0.87	0.82	0.45	0.23
CBG	0.09	0.81	0.42	0.48	0.45	0.42	0.48
THC	<0.0001*	<0.0001*	0.86	<0.0001*	0.71	0.61	0.77
<b>Terpenes concentration ( mg 100 g dry matter<sup>-1</sup>)</b>							
Limonene	0.37	<0.0001*	<0.0001*	0.39	<0.0001*	0.52	0.72
Fenchol	<0.0001*	<0.0001*	0.27	0.0033*	0.0014*	0.72	0.90
Caryophyllene	<0.0001*	<0.0001*	0.0007*	<0.0001*	<0.0001*	0.0031*	0.0019*
Caryophyllene Oxide	<0.0001*	<0.0001*	0.61	<0.0001*	0.0115*	0.15	0.25
Humulene	<0.0001*	<0.0001*	0.09	<0.0001*	<0.0001*	0.0063*	0.17
Total terpenes	<0.0001*	<0.0001*	<0.0001*	<0.0001*	<0.0001*	0.013*	0.2

\*Effects are statistically significant



Oil yields ranging from 12 % – 28 % for the different experimental conditions are presented in Figure 3.5. The oil yield (%) for ethanol at  $-20^{\circ}\text{C}$  (Figure 3.5 (A)), shows that coarse (A), medium (B), and fine (C) particles are statistically different ( $p < 0.05$ ) from each other, as indicated by distinct first connecting letters. However, coarse at  $4^{\circ}\text{C}$  (A) is significantly ( $p < 0.05$ ) different from  $-20^{\circ}\text{C}$  (B) and RT (B), but, coarse at  $-20^{\circ}\text{C}$  (B) and RT (B) are not significantly ( $p > 0.05$ ) different from each other, as indicated by second connecting letters. Oil yield with ethanol extraction using finely ground biomass at  $4^{\circ}\text{C}$  and room temperature (RT) presented the highest oil yield with 28 % and 25.7 % extracted oil, respectively. Butanol and hexane extraction had reduced oil yield by 14.3 % and 23.8 %, respectively, compared to ethanol extraction using finely ground biomass at  $4^{\circ}\text{C}$ . Results indicate that ethanol and butanol are highly effective in promoting a substantial oil yield from fine-sized particles compared to hexane, a non-polar solvent.

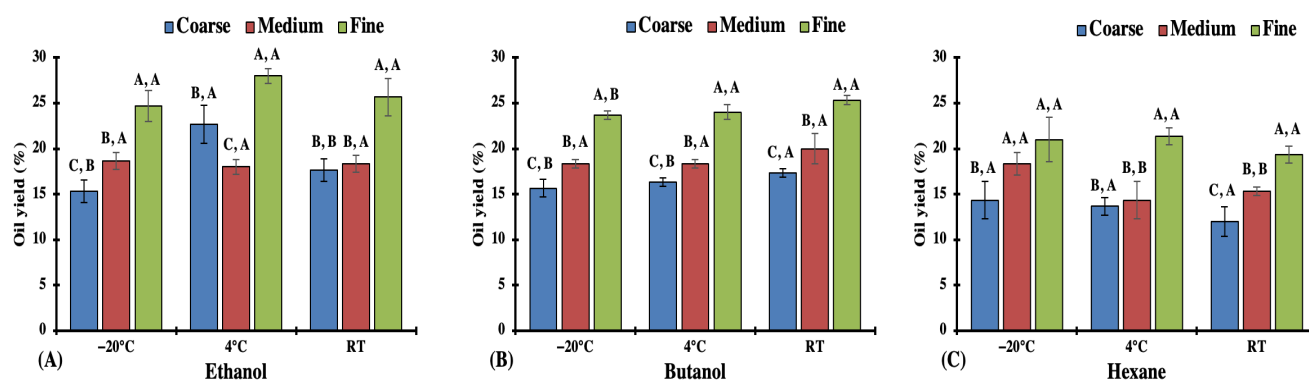


Figure 3.5. Effect of particle size, solvent type, and extraction temperature on the cannabis oil yield (%); (A) ethanol, (B) butanol, (C) hexane. Bars with the same first letter are not significantly ( $p > 0.05$ ) different between the particle sizes for the same extraction temperature and solvent type. Bars with the same second letter are not significantly ( $p > 0.05$ ) different between the extraction temperature for the same particle size and solvent type.

When using the same extraction temperature and solvent type, fine particle size produces the highest oil yield (%) compared to coarse- and medium-sized particles. Decreasing the particle size of cannabis from coarse to fine using ethanol as the solvent significantly ( $p < 0.05$ ) increased oil yield (%) from 15.3 % to 24.7 % and 22.7 % to 28 % at  $-20^{\circ}\text{C}$  and  $4^{\circ}\text{C}$ , respectively. A similar observation was made for butanol and hexane extraction solvents. Reduced particle size (coarse to fine) increased oil yield (%) by 51 % and 47 % at  $-20^{\circ}\text{C}$  and  $4^{\circ}\text{C}$ , respectively, for

butanol and by 46.5 % and 56.0 % at  $-20\text{ }^{\circ}\text{C}$  and  $4\text{ }^{\circ}\text{C}$ , respectively for hexane. ANOVA analyses showed that when using an extraction temperature of  $-20\text{ }^{\circ}\text{C}$ , an increase in the particle size from medium to coarse significantly ( $p < 0.05$ ) reduced the oil yield (%) by 17.9 %, 14.5 %, and 21.8 % for ethanol, butanol, and hexane, respectively due to the reduced exposed extraction surface area.

### **3.3.3 Effects of particle size, solvent type, and extraction temperature on cannabinoid concentration**

Statistical analyses revealed that the concentrations of THCA, CBGA, and THC are significantly influenced ( $p < 0.05$ ) by the linear effects of particle size ( $X_1$ ) and solvent type ( $X_2$ ), while their interactive effects with particle size and solvent type ( $X_1X_2$ ), solvent type and temperature ( $X_2X_3$ ), and particle size and temperature ( $X_1X_3$ ), are not significant ( $p > 0.05$ ), except for the interaction effect of particle size and solvent type ( $X_1X_2$ ), which significantly ( $p < 0.05$ ) impacts THC concentration. Furthermore, the temperature parameter ( $X_3$ ) had no significant effect on cannabinoid concentrations. In contrast, the concentration of CBG was not significantly affected ( $p > 0.05$ ) by any of the linear or interactive effects of the three parameters.

In Figure 3.6 (A), the concentration of THCA for ethanol at  $-20\text{ }^{\circ}\text{C}$  shows that coarse (A), medium (B), and fine (C) particles are statistically ( $p < 0.05$ ) different from each other, as indicated by distinct first connecting letters. However, coarse at RT (A) is significantly ( $p < 0.05$ ) different from  $-20\text{ }^{\circ}\text{C}$  (B) and  $4\text{ }^{\circ}\text{C}$  (B), but, coarse at  $-20\text{ }^{\circ}\text{C}$  (B) and  $4\text{ }^{\circ}\text{C}$  (B) are not significantly ( $p > 0.05$ ) different from each other, as indicated by second connecting letters. At  $-20\text{ }^{\circ}\text{C}$  and  $4\text{ }^{\circ}\text{C}$ , with either of the three investigated particle sizes, ethanol extracted the highest concentrations of THCA and CBGA, compared to butanol and hexane (Figure 3.6). Extraction with butanol yielded a higher concentration of THC than other solvents, and that with the three particle sizes at the three temperatures tested. For instance, at  $4\text{ }^{\circ}\text{C}$  with medium particle size, butanol obtained a THC concentration ( $\text{mg } 100\text{ g dry matter}^{-1}$ ) of 0.25 compared to ethanol (0.1) and hexane (0.02). For each solvent type, fine particles resulted in higher concentrations of THCA, CBGA, and THC (Figure 3.6). Even though the extraction temperature did not have a significant effect on cannabinoid concentrations ( $p > 0.05$ ), when the temperature was increased from  $-20\text{ }^{\circ}\text{C}$  to RT, THCA and CBGA concentrations increased by 5.88 % and 5.07 % with butanol and by 5.24 % and 4.96 % with ethanol when using coarse-sized particles. When fine

particles were extracted at 4 °C, and hexane and butanol were replaced with ethanol, the concentration (mg 100 g dry matter<sup>-1</sup>) of THCA increased from 14.3 and 15.5 to 16.45, respectively, corresponding to 15.0 % and 6.1 % increases, respectively. Although the interaction effect ( $X_1X_2$ ) is significant, the influence of ethanol interacting with medium-sized particles on THC concentration is not significant ( $p > 0.05$ ). By using ethanol at different temperatures (−20 °C, 4 °C, and RT) and replacing coarse with fine particles, there was an observed increase in THCA concentration. Specifically, there was a 52.7 % increase at −20 °C, a 51.7 % increase at 4 °C, and a 44.2 % increase at RT.

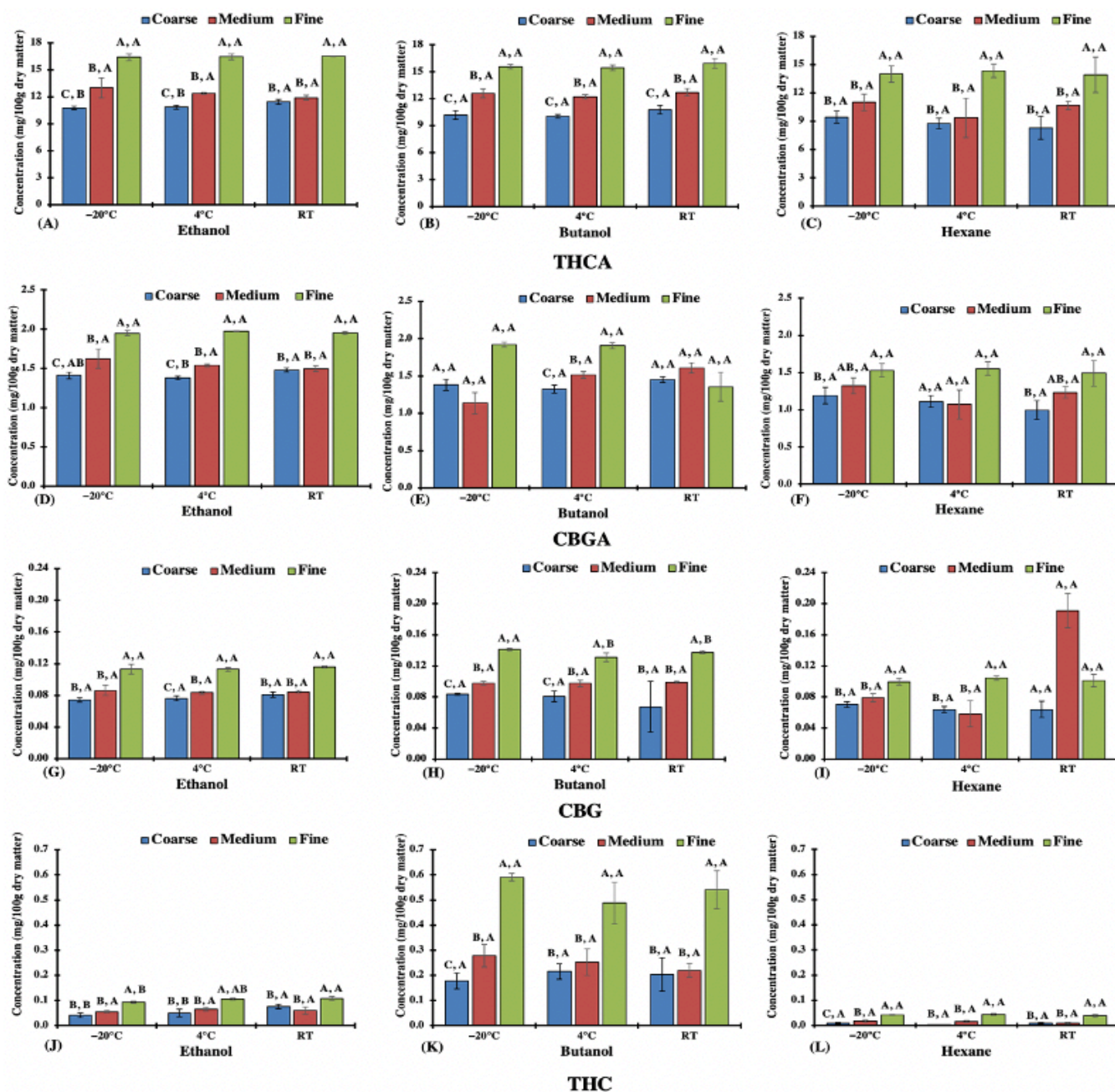


Figure 3.6. Effect of particle size, solvent, and extraction temperature on the concentration (mg 100 g dry matter<sup>-1</sup>) of THCA (A-C), CBGA (D-F), CBG (G-I), and THC (J-L). Bars with the same first letter are not significantly ( $p > 0.05$ ) different between the particle sizes for the same extraction temperature and solvent type. Bars with the same second letter are not significantly ( $p > 0.05$ ) different between the extraction temperature for the same particle size and solvent type.

### 3.3.4 Effects of particle size, solvent type, and extraction temperature on total terpene concentrations

The main terpenes detected and identified in this study were limonene, fenchol, humulene, caryophyllene, and caryophyllene oxide. Other terpenes such as myrcene,  $\alpha$ -pinene,  $\beta$ -pinene, camphene, and camphor could not be detected by the employed analytical method ( $< \text{LOD}$ ). Total terpenes refer to the sum of the identified and detected terpenes. Data show that the linear and interactive effects of each variable (particle size, solvent type, and extraction temperature) play a different role in each type of identified terpene, and they significantly ( $p < 0.05$ ) influenced total terpene concentrations, monoterpene and sesquiterpene concentrations (Figures 3.7 and 3.8). The highest concentration of total terpenes was obtained with the combination of finely ground cannabis biomass particles and ethanol extracted at 4 °C (Figure 3.8).

In Figure 3.7 (D), the concentration of fenchol for ethanol at  $-20$  °C shows that coarse (A), medium (B), and fine (C) particles are statistically ( $p < 0.05$ ) different from each other, as indicated by distinct first connecting letters. However, coarse at  $-20$  °C (A), 4 °C (A), and RT (A) are not significantly ( $p > 0.05$ ) different from each other, as indicated by the same second connecting letters. When comparing different solvents at the same temperature and particle size, ethanol extracted a higher concentration of total terpenes. However, butanol was less effective in obtaining total terpenes compared to ethanol and hexane. When using the same solvent and operating at the same temperature, extraction of fine-sized particles yielded a higher amount of total terpenes compared to coarse- and medium-sized particles. A total of 69.8 % and 4.4 % increases in total terpenes were observed when the temperature was increased from  $-20$  °C to 4 °C and  $-20$  °C to RT, respectively, but a decrease of 38.5 % was observed when the temperature was increased from 4 °C to RT, during extraction of fine-sized particles using ethanol as a solvent.

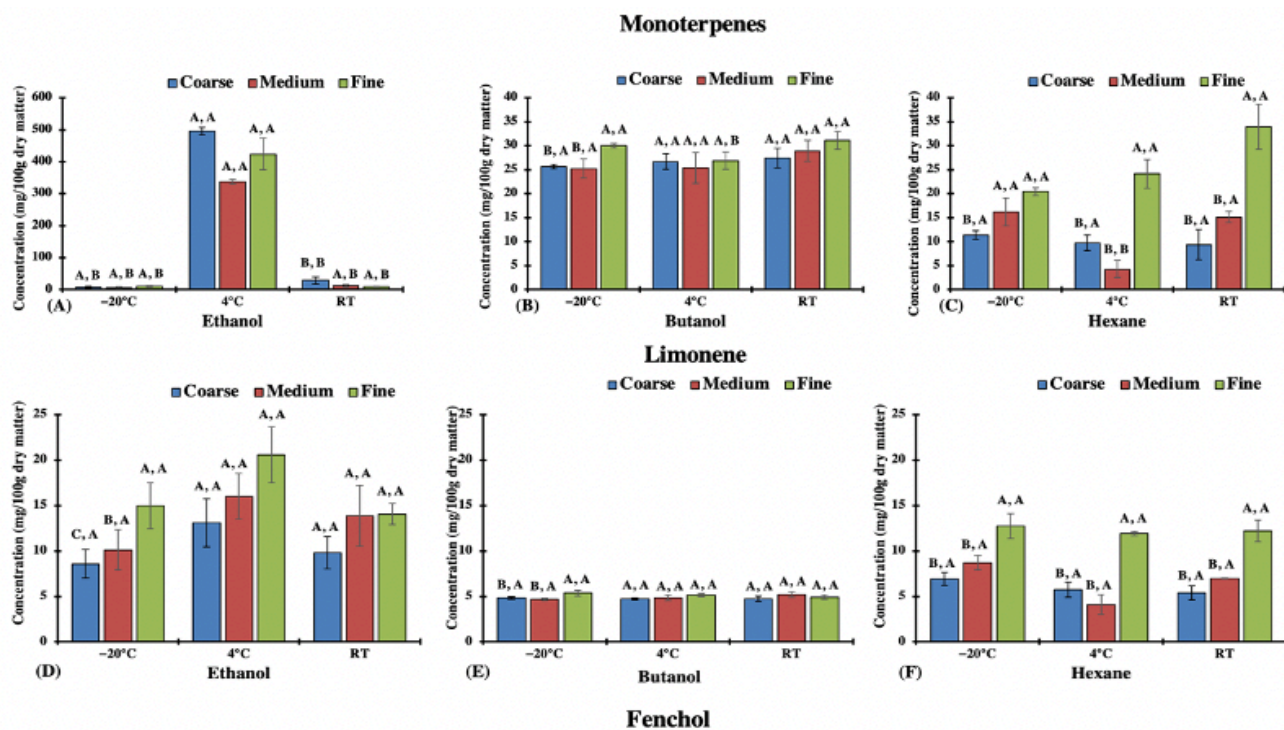


Figure 3.7. Effect of particle size, solvent type, and extraction temperature on major monoterpene concentrations (mg 100 g dry matter<sup>-1</sup>), including limonene (A-C) and fenchol (D-F). Bars with the same first letter are not significantly ( $p > 0.05$ ) different between the particle sizes for the same extraction temperature and solvent type. Bars with the same second letter are not significantly ( $p > 0.05$ ) different between the extraction temperature for the same particle size and solvent type.



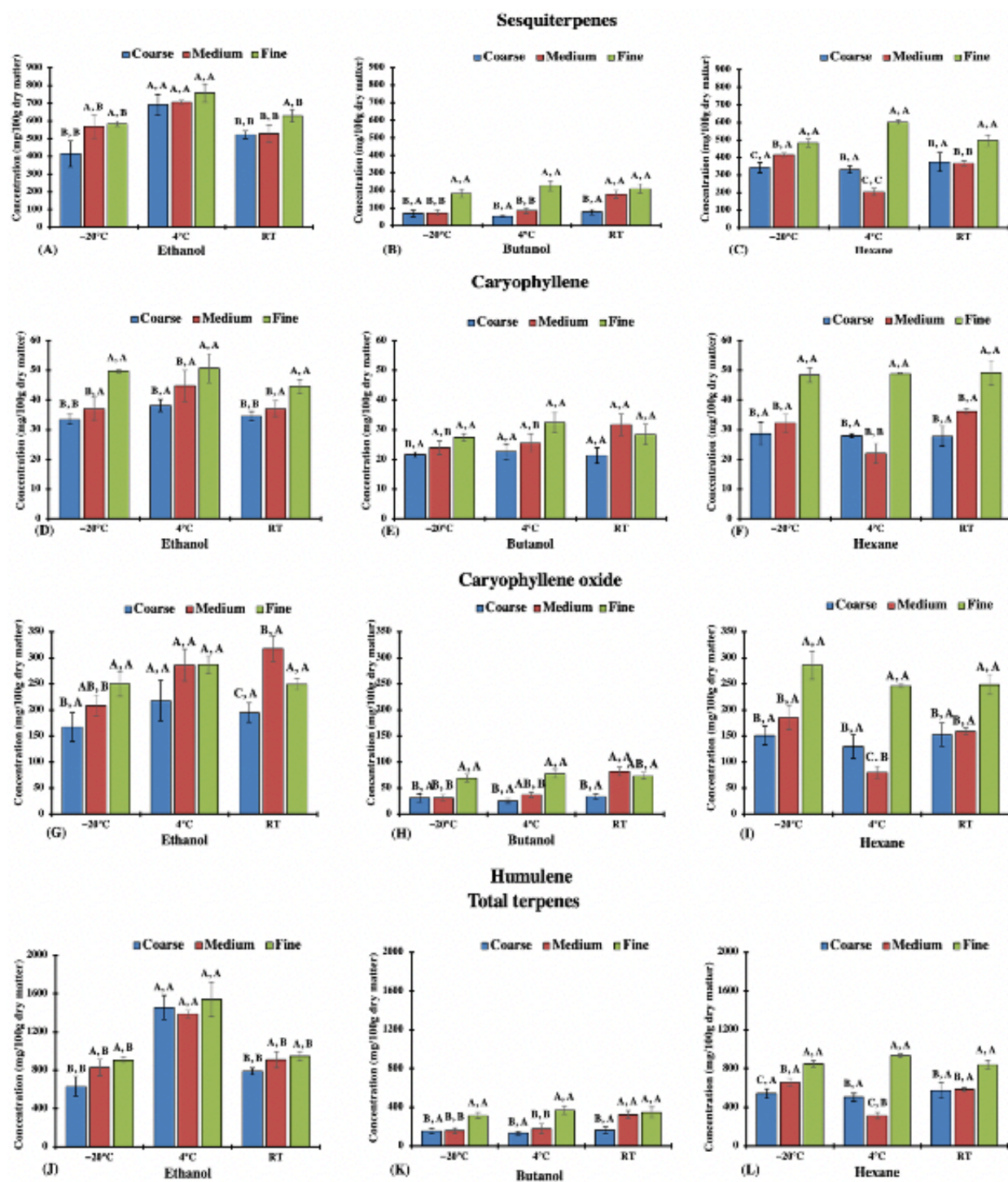


Figure 3.8. Effect of particle size, solvent type, and extraction temperature on concentration (mg 100 g dry matter<sup>-1</sup>) of sesquiterpenes, including caryophyllene (A-C), caryophyllene oxide (D-F), humulene (G-I), and total terpenes (J-L). Bars with the same first letter are not significantly ( $p > 0.05$ ) different between the particle sizes for the same extraction temperature and solvent type.

Bars with the same second letter are not significantly ( $p > 0.05$ ) different between the extraction temperature for the same particle size and solvent type.

### 3.4 Discussion

FFD was used for the determination of optimal particle size, type of solvent, and extraction temperature for cannabis biomass. Even though FFD requires a greater number of experimental runs compared to central composite design, FFD encompasses all possible interactions between the factors/variables, whereas some interactions may not be explicitly examined in the latter design (Panneton et al., 1999). Factorial design is an efficient method for characterizing processes with multiple variables and allows for the separation of significant components from those that are not, as well as the identification of any potential interactions between them (Paterakis et al., 2002). However, the feasibility of using FFD becomes prohibitive as the number of variables or levels to be considered increases. Analyses show that the concentration of THC is  $> 0.3 \%$ , while CBD is  $< 0.3 \%$  mass mass<sup>-1</sup> and can be considered as a drug-type chemovar (Schilling et al., 2020).

This research determined that grinding the dried cannabis biomass into different particle sizes was not detrimental to preserving its contained cannabinoids and increased the final concentrations in extracts as the particle size decreased. Grinding cannabis biomass to a finer size is not a widely adopted practice in the cannabis industry for several reasons. In many facilities, 2-mm particle sized biomass, referred to as coarse in this study, is used for extraction purposes. Addo et al. (2021) reviewed that an increase in the temperature of biomass during grinding or particle size reduction can change the chemical profile of the biomass. LN<sub>2</sub> maintains the cold temperature during cryo-grinding. This prevents the degradation and loss of secondary metabolites in the biomass (Singh and Goswami, 1999a). The undeniable advantage of LN<sub>2</sub> is its ability to render the grinding material inert (Wilczek et al., 2004), thereby eliminating the considerable risk of undesired chemical reactions resulting from high nitrogen levels. LN<sub>2</sub>, when vaporized under normal ambient conditions with proper ventilation, produces chemically stable and inert diatomic nitrogen gas that does not readily react with other substances (Shi et al., 2015).

Pre-freezing dried cannabis biomass at temperatures of to  $-20\text{ }^{\circ}\text{C}$ ,  $-40\text{ }^{\circ}\text{C}$  or  $-80\text{ }^{\circ}\text{C}$  for 24 h before grinding is a potential alternative to using LN<sub>2</sub> in industrial settings to avoid the



elevated levels of LN<sub>2</sub>. Challenges with LN<sub>2</sub> in the work environment include higher operational costs (Wilczek et al., 2004), and frostbite caused by mishandling of the LN<sub>2</sub> (Gupta et al., 2021). Even though atmospheric air contains 78 % nitrogen, the faster expansion of nitrogen can rapidly displace oxygen in a confined space with inadequate ventilation, leading to oxygen deprivation and asphyxiation (Morales et al., 2017).

Finer particles (0.25 – 0.5 mm) can be trapped in the crevices of machines causing operational difficulties or serve as a conducive environment for microbial growth (Friesen, 2020), often resulting in costly downtime. Cleaning the grinding equipment and reducing contamination are clearly difficult and pose challenges in industrial settings (Nakach et al., 2004). Grinding of dried cannabis has further undergone scrutiny due to health hazard and safety concerns from exposure to allergens, endotoxins, and volatile organic compounds (Couch et al., 2020). Standards are currently under development to establish effective measures for air filtration, air quality, and personal protective equipment to ensure workspaces and employees' safety against the inhalation of toxic levels of ground cannabis dust during processing (ASTM-WK84667, 2023).

The higher recovery rates of CBG and THC, which exceeded 100 % at all tested conditions, was due to their increased concentrations in the resulting extracts compared to the initial ground biomass, as well as the potential conversion or biosynthesis of CBG and THC from other unknown cannabinoids during the extraction process. This observation is consistent with the data reported by Addo et al. (2022b) during microwave and ultrasound-assisted extraction of cannabis biomass. To improve recovery rates for THCA and CBGA, by performing a second extraction can be effective using the residual biomass obtained after the initial extraction.

The difference in the color of extracts obtained with different solvents can be attributed to the affinity of the solvents for chlorophyll and its derivatives. Esmaeilzadeh Kenari and Dehghan (2020) showed a decrease in the oil color index from dark green to yellow when the polar solvent (isopropanol) was changed to a non-polar solvent (hexane) during the extraction of hemp (*Cannabis sativa*) seed using an ultrasound-assisted system. Chlorophyll, a photosensitive pigment, is a prooxidant in oils and increases the susceptibility of cannabis oil to the oxidation of fatty acids, and phenolic compounds (terpenes), and accelerates rancidity (Liang et al., 2018). Dechlorophyllization or 'degreening' improves cell-based biological assessments, thus facilitating the easier evaluation of the pharmacological properties of plant extracts (Kim et al.,

2020). The amount of chlorophyll can be significantly reduced to low levels by employing conventional methods of bleaching and refining (Liang et al., 2018). Some of the chlorophyll removal methods include activated charcoal bleaching, ultrasound bleaching, polymeric ChloroFiltr® sorbent, and by the molecular distillation (Liang et al., 2018; Sagili et al., 2023; Tzima et al., 2020). Bleaching of cannabis oil is often performed in the cannabis industry to reduce the concentration of extracted chlorophyll. The distinctive green color of extracts obtained using polar solvents like ethanol and butanol, as opposed to non-polar hexane, is due to the polar nature of chlorophyll molecules, which makes them more soluble in polar solvents. Further studies could be conducted to quantify the effects of various solvents on extracted chlorophyll concentrations.

### 3.4.1 Oil yield (%)

Various factors such as type of extraction system, sample-to-solvent ratio, solvent, and extraction temperature affect the mass of extracted cannabis essential oil (Addo et al., 2022a; Addo et al., 2022b; Brighenti et al., 2017; Chang et al., 2017; Esmaeilzadeh Kenari and Dehghan, 2020). Previous studies have demonstrated that the optimal settings for ultrasound-assisted and microwave-assisted cannabis extraction had sample-to-solvent ratios of 1:15 and 1:14.4, respectively, for 30 min at 60 °C (Addo et al., 2022b). Optimal conditions for cold ethanol extraction were cannabis-to-ethanol ratio of 1:15 and 10 min extraction time (Addo et al., 2022a).

Several studies have investigated the impact of biomass particle size and solvents on extraction yield. Particle size reduction by grinding breaks the cell walls and increases the specific area (surface area-to-volume ratio) and the surface of smaller particles exposes larger specific areas to release more oil (del Valle and Uquiche, 2002). Meziane et al. (2006) showed that reducing the particle size of olive cake biomass from 1.69 to 0.69 mm caused a significant increase in the oil yield from 25 % to 51 % using 96 % ethyl alcohol. A similar observation was made by Yunus et al. (2013) where reducing the particle size of dried *Areca catechu* seeds from 500  $\mu\text{m}$  to 125  $\mu\text{m}$  increased the extracted oil yield (%) by 21.2 %. Vega and Dávila (2022) reported that reducing the particle size of non-psychoactive residual cannabis biomass (stems and leaves) from 428  $\mu\text{m}$  to 109  $\mu\text{m}$  at a constant extraction time of 8 h and the solid-to-solvent ratio of 6.18 g mL<sup>-1</sup>, increased the total phenolic content from 308 to 903 mg GAE g<sup>-1</sup> DW and total

antioxidant capacity (mM Trolox) by 25 %. Makanjuola (2017) observed an increase in total phenolic content (mg GAE L<sup>-1</sup>) of aqueous ethanolic tea powdered extracts by 50.5 % when the particle size of tea was reduced from 1.18 mm to 0.71 mm.

Uoonlue and Muangrat (2019) conducted a study where they tested the effectiveness of three different organic solvents (subcritical hexane, petroleum ether, and isopropanol) on extracting oil from Assam tea seeds (*Camellia sinensis* var. *assamica*) and found that all three solvents were successful in recovering the oil, with recovery rates ranging from 92.9 % to 98.1 %. Hidalgo et al. (2016) reported that a solvent mixture (addition of non-polar solvent to polar solvent) such as chloroform-methanol mixture (25:75 % v v<sup>-1</sup>) can increase the extraction efficiency of esterifiable lipids from the microalgae *Botryococcus braunii* to 98.9% mass compared to 57.4 % mass when ethanol (100 % v v<sup>-1</sup>) was used. Li et al. (2004) showed that using hexane and isopropanol (60:40 % v v<sup>-1</sup>) as an extraction solvent for soybeans resulted in a stronger affinity between the solvent and lipophilic compounds than using either of the solvents alone. Lipids such as phospholipids and glycolipids are strongly bonded to proteins through hydrogen or electrostatic bonds within the cell membrane; although a non-polar solvent has high solvation power, adding a polar solvent such as an alcohol causes the denaturation of proteins and the breaking of bonds between lipids and proteins (Halim et al., 2011). This increases the solvation power of the solvents.

The extracts contained a significant amount of wax and it is considered as a heavier compound that can degrade the quality of cannabis oil. Its presence increases the thickness and opacity of the extract, and therefore, it is usually eliminated to enhance the quality of the final product. Winterization using ethanol is commonly employed in the cannabis industry for the removal of waxes (Blake and Nahtigal, 2019). However, further studies require to be conducted on the effect of temperature on the extraction of unwanted heavier compounds such as waxes.

### **3.4.2 Cannabinoid concentration**

Data collected in this study are consistent with the results reported by Brighenti et al. (2017), in that the polar solvent ethanol is a preferred extraction solvent compared to the non-polar solvent hexane. In supercritical fluid extraction, the low polarity of supercritical CO<sub>2</sub> requires a co-solvent, such that adding ethanol achieved the highest extraction yields compared to pure supercritical CO<sub>2</sub> (Grijó et al., 2018). According to Grijo et al. (2019), increasing the

polarity of the solvent in supercritical CO<sub>2</sub> extraction i.e., the use of 5 % ethanol as a co-solvent or modifier for the un-decarboxylated samples, could significantly increase the extraction yields. Rovetto and Aieta (2017) conducted a study to analyze THC extraction using a combination of supercritical CO<sub>2</sub> with ethanol and noticed a higher concentration of THC in the extracts compared to using supercritical CO<sub>2</sub> alone, without any additional quantity of solvents. The majority of industrial cannabis processing operations prefer ethanol as an extraction solvent because it is considered a GRAS (Generally Recognized As Safe) solvent by the FDA (Chen and Pan, 2021). The low toxicity and easy recovery of ethanol make it a preferred choice, as it reduces risks to human health and can minimize operational costs. A significant increase of THC with butanol was explained by the application of higher temperatures during the solvent evaporation step which caused the decarboxylation of THCA, thereby increasing the THC concentration. The reason for the elevated concentrations of THCA, CBGA, and CBG with a fine particle size using any of the three solvents can be described by the rupturing of the plant cell wall, a greater surface area-to-volume ratio for fine particles and these surfaces tend to have more oil, which later comes in contact with the solvent during extraction. Raising the temperature likely enhances the solvent's capacity to dissolve the target compound and lowers the solvent's viscosity, facilitating its penetration into the substance (Péres et al., 2006).

### **3.4.3 Total terpene concentration:**

Major monoterpenes present in *C. sativa* include  $\alpha$ -pinene,  $\beta$ -pinene, myrcene, limonene, fenchol, camphor,  $\beta$ -ocimene, camphene, terpinolene and sesquiterpenes which include,  $\alpha$ -humulene,  $\beta$ -caryophyllene, caryophyllene oxide, farnesene, and bergamotene (Booth and Bohlmann, 2019; Desaulniers Brousseau et al., 2021). Terpene profiles in cannabis are accession-specific and appear partially dependent on the expression of several terpene synthase genes (Booth and Bohlmann, 2019; Fischedick, 2017). Further terpene metabolomic research may elucidate how accessions differentially synthesize these compounds. The main terpenes present in this accession are limonene, fenchol, humulene, caryophyllene, and caryophyllene oxide, all have boiling points >100 °C. The higher total terpenes concentrations observed with ethanol extraction are likely due to that the terpenes are predominantly polar in nature, making them more easily extractable by a polar solvent such as ethanol. The efficacy of butanol in obtaining total terpenes was comparatively lower because terpenes are highly volatile

compounds that tend to evaporate quickly especially at elevated temperature. This is a possible consequence of the boiling temperatures employed for evaporating the butanol under a vacuum which caused terpenes to evaporate and escape from the system. The higher extraction temperature causes an initial increase, and then a distinct decrease in the estimated total terpenes content. This is different from the observed behaviour of a previous study (Addo et al. (2022a), where increasing extraction temperature decreased the concentration of total terpenes. Specifically, the extracted total terpenes concentration decreased by 32.2 % and 54.1 % at  $-20^{\circ}\text{C}$  and RT, respectively, compared to extraction at  $-40^{\circ}\text{C}$ . Further study will be conducted on investigating the effects of extraction parameters on the cannabinoid and terpenes concentrations in the solvent recovered through evaporation.

#### **5.2.4 Applicability at industrial scale:**

Scaling up cryo-grinding by installing a readily available cryo-grinder in the cannabis industry, despite the higher costs involved in equipment and operations, has the potential to preserve the secondary metabolites present in the biomass. Additionally, preserving these metabolites in the extracts through optimal extraction conditions can ultimately increase income over the course of time. Conventional hang air drying is time-consuming (10-14 days) and susceptible to microbial contamination, jeopardizing product quality, safety, and financial outcomes. However, despite equipment costs, freeze-drying improves scalability and economic feasibility by greatly reducing drying times, preventing contamination, and producing high-quality dried biomass. Industrial freeze dryers have been evaluated using sensors to determine the end of the drying process in real-time (Addo et al., 2023a). This preservation enables valuable end products, boosting market value and customer satisfaction.

### **3.5 Conclusion**

This study aimed to evaluate the effects of particle size (coarse, medium, and fine), solvent type (ethanol, butanol, and hexane) and extraction temperature ( $-20^{\circ}\text{C}$ ,  $4^{\circ}\text{C}$ , and room temperature), on extracted crude cannabis oil yield and concentrations of valued secondary metabolites. In this study, the results demonstrate that particle size and solvent type play a significant role on the crude cannabis oil and cannabinoid concentration. In addition to these factors, extraction temperature, also notably influences the total terpenes concentrations. From

this research, particle size reduction of dried cannabis biomass preserved and increased cannabinoid concentration during extraction. Optimal conditions for extracting the highest yield of crude cannabis oil with significant concentrations of THCA, CBGA, and total terpenes involve using finely ground biomass in ethanol, at a temperature of 4 °C. Extraction yield is positively correlated with a reduction in particle size. The color of extracted cannabis oil varied depending on the solvent used during extraction. This study may be useful for the industry for maximizing extract yield while ensuring desired secondary metabolite profiles.

### 3.6 References

- Addo, P.W., Brousseau, V.D., Morello, V., MacPherson, S., Paris, M., Lefsrud, M., 2021. Cannabis chemistry, post-harvest processing methods and secondary metabolite profiling: A review. *Ind. Crops Prod.* 170, 113743. <https://doi.org/10.1016/j.indcrop.2021.113743>.
- Addo, P.W., Chauvin-Bossé, T., Taylor, N., MacPherson, S., Paris, M., Lefsrud, M., 2023a. Freeze-drying *Cannabis sativa* L. using real-time relative humidity monitoring and mathematical modeling for the cannabis industry. *Ind. Crops Prod.* 199, 116754. <https://doi.org/10.1016/j.indcrop.2023.116754>.
- Addo, P. W., Sagili, S. U. K. R., Bilodeau, S. E., Gladu-Gallant, F.-A., MacKenzie, D. A., Bates, J., McRae, G., MacPherson, S., Paris, M., Raghavan, V., Orsat, V., Lefsrud, M. 2022. Cold Ethanol Extraction of Cannabinoids and Terpenes from Cannabis Using Response Surface Methodology: Optimization and Comparative Study. *Molecules*. 27 (24), 8780. <https://doi.org/10.3390/molecules27248780>.
- Addo, P.W., Sagili, S.U.K.R., Bilodeau, S.E., Gladu-Gallant, F.-A., MacKenzie, D.A., Bates, J., McRae, G., MacPherson, S., Paris, M., Raghavan, V., Orsat, V., Lefsrud, M., 2022b. Microwave-and ultrasound-assisted extraction of cannabinoids and terpenes from cannabis using response surface methodology. *Molecules* 27, 8803. <https://doi.org/10.3390/molecules27248803>.
- Al Ubeed, H.M.S., Bhuyan, D.J., Alsherbiny, M.A., Basu, A., Vuong, Q.V., 2022. A comprehensive review on the techniques for extraction of bioactive compounds from medicinal cannabis. *Molecules* 27, 604. <https://doi.org/10.3390/molecules27030604>.
- Appendino, G., Chianese, G., Tagliatalata-Scafati, O., 2011. Cannabinoids: occurrence and medicinal chemistry. *Curr. Med. Chem.* 18, 1085-1099. <https://doi.org/10.2174/092986711794940888>.
- ASTM-WK84667. 2023. New Guide for Working with Ground Cannabis and Kief. [accessed 16 March 2023; Available from: <https://www.astm.org/workitem-wk84667>].
- Atkins, P.L., 2019. Sample processing and preparation considerations for solid cannabis products. *J. AOAC Int.* 102, 427-433. <https://doi.org/10.5740/jaoacint.18-0203>.
- Bahji, A., Stephenson, C., 2019. International perspectives on the implications of cannabis legalization: a systematic review & thematic analysis. *Int. J. Environ. Res. Public Health*. 16, 3095. <https://doi.org/10.3390/ijerph16173095>.

Balasubramanian, S., Gupta, M.K., Singh, K., 2012. Cryogenics and its application with reference to spice grinding: a review. *Crit. Rev. Food Sci. Nutr.* 52, 781-794. <https://doi.org/10.1080/10408398.2010.509552>.

Blake, A., Nahtigal, I. 2019. The evolving landscape of cannabis edibles. *Curr. Opin. Food Sci.* 28, 25-31. <https://doi.org/10.1016/j.cofs.2019.03.009>.

Booth, J. K., Bohlmann, J. 2019. Terpenes in Cannabis sativa—From plant genome to humans. *Plant Sci.* 284, 67-72. <https://doi.org/10.1016/j.plantsci.2019.03.022>.

Brighenti, V., Pellati, F., Steinbach, M., Maran, D., Benvenuti, S., 2017. Development of a new extraction technique and HPLC method for the analysis of non-psychoactive cannabinoids in fibre-type Cannabis sativa L.(hemp). *J. Pharm. Biomed. Anal.* 143, 228-236. <https://doi.org/10.1016/j.jpba.2017.05.049>.

Challa, S.K.R., Misra, N., Martynenko, A., 2021. Drying of cannabis— State of the practices and future needs. *Dry. Technol.* 39, 2055-2064. <https://doi.org/10.1080/07373937.2020.1752230>.

Chang, C.-W., Yen, C.-C., Wu, M.-T., Hsu, M.-C., Wu, Y.-T., 2017. Microwave-assisted extraction of cannabinoids in hemp nut using response surface methodology: Optimization and comparative study. *Molecules* 22, 1894. <https://doi.org/10.3390/molecules22111894>.

Chen, C., Pan, Z., 2021. Cannabidiol and terpenes from hemp—ingredients for future foods and processing technologies. *J. Future Foods* 1, 113-127. <https://doi.org/10.1093/annweh/wxaa013>.

Couch, J.R., Grimes, G.R., Green, B.J., Wiegand, D.M., King, B., Methner, M.M., 2020. Review of NIOSH cannabis-related health hazard evaluations and research. *Annals of work exposures and health* 64, 693-704. <https://doi.org/10.1093/annweh/wxaa013>.

del Valle, J.M., Uquiche, E.L., 2002. Particle size effects on supercritical CO<sub>2</sub> extraction of oil-containing seeds. *J. Am. Oil Chem. Soc.* 79, 1261-1266. <https://doi.org/10.1007/s11746-002-0637-9>.

Desaulniers Brousseau, V., Wu, B.-S., MacPherson, S., Morello, V., Lefsrud, M., 2021. Cannabinoids and terpenes: how production of photo-protectants can be manipulated to enhance Cannabis sativa L. phytochemistry. *Front. Plant Sci.* 12, 620021. <https://doi.org/10.3389/fpls.2021.620021>.

Eichhorn Bilodeau, S., Wu, B.-S., Rufyikiri, A.-S., MacPherson, S., Lefsrud, M., 2019. An update on plant photobiology and implications for cannabis production. *Front. Plant Sci.* 10, 296. <https://doi.org/10.3389/fpls.2019.00296>.



- Esmaeilzadeh Kenari, R., Dehghan, B., 2020. Optimization of ultrasound-assisted solvent extraction of hemp (*Cannabis sativa* L.) seed oil using RSM: Evaluation of oxidative stability and physicochemical properties of oil. *Food Sci. Nutr.* 8, 4976-4986.  
<https://doi.org/10.1002/fsn3.1796>.
- Fischedick, J.T., 2017. Identification of terpenoid chemotypes among high (–)-trans- $\Delta^9$ -tetrahydrocannabinol-producing *Cannabis sativa* L. cultivars. *Cannabis Cannabinoid Res.* 2, 34-47. <https://doi.org/10.1089/can.2016.0040>.
- Friesen, L. To Grind or Not To Grind. 2020 [accessed 19 March 2023]; Available from: <https://www.cannabissciencetech.com/view/to-grind-or-not-to-grind>.
- Grijo, D.R., Bidoia, D.L., Nakamura, C.V., Osorio, I.V., Cardozo-Filho, L., 2019. Analysis of the antitumor activity of bioactive compounds of *Cannabis* flowers extracted by green solvents. *The Journal of Supercritical Fluids* 149, 20-25.
- Grijó, D.R., Osorio, I.A.V., Cardozo-Filho, L., 2018. Supercritical extraction strategies using CO<sub>2</sub> and ethanol to obtain cannabinoid compounds from *Cannabis* hybrid flowers. *Journal of CO<sub>2</sub> Utilization* 28, 174-180.
- Gupta, A., Soni, R., Ganguli, M., 2021. Frostbite—manifestation and mitigation. *Burns Open* 5, 96-103. <https://doi.org/10.1016/j.burnso.2021.04.002>.
- Halim, R., Gladman, B., Danquah, M.K., Webley, P.A., 2011. Oil extraction from microalgae for biodiesel production. *Bioresour. Technol.* 102, 178-185.  
<https://doi.org/10.1016/j.biortech.2010.06.136>.
- Hartsel, J.A., Eades, J., Hickory, B., Makriyannis, A., 2016. *Cannabis sativa* and Hemp, Nutraceuticals. Elsevier, pp. 735-754. <https://doi.org/10.1016/B978-0-12-802147-7.00053-X>.
- Hashemi, B., Shiri, F., Švec, F., Nováková, L., 2022. Green solvents and approaches recently applied for extraction of natural bioactive compounds. *TrAC-Trend Anal. Chem.*, 116732.  
<https://doi.org/10.1016/j.trac.2022.116732>.
- Hidalgo, P., Ciudad, G., Navia, R., 2016. Evaluation of different solvent mixtures in esterifiable lipids extraction from microalgae *Botryococcus braunii* for biodiesel production. *Bioresour. Technol.* 201, 360-364. <https://doi.org/10.1016/j.biortech.2015.11.031>.
- Jin, D., Dai, K., Xie, Z., Chen, J., 2020. Secondary metabolites profiled in cannabis inflorescences, leaves, stem barks, and roots for medicinal purposes. *Sci. Rep.* 10, 1-14.  
<https://doi.org/10.1038/s41598-020-60172-6>.

Kim, S.B., Bisson, J., Friesen, J.B., Pauli, G.F., Simmler, C., 2020. Selective chlorophyll removal method to “degreen” botanical extracts. *J. Nat. Prod.* 83, 1846-1858. <https://doi.org/10.1021/acs.jnatprod.0c00005>.

Li, H., Pordesimo, L., Weiss, J., 2004. High intensity ultrasound-assisted extraction of oil from soybeans. *Food Res. Int.* 37, 731-738. <https://doi.org/10.1016/j.foodres.2004.02.016>.

Li, Y., Fine, F., Fabiano-Tixier, A.-S., Abert-Vian, M., Carre, P., Pages, X., Chemat, F., 2014. Evaluation of alternative solvents for improvement of oil extraction from rapeseeds. *C. R. Chim.* 17, 242-251. <https://doi.org/10.1016/j.crci.2013.09.002>.

Liang, J., Aachary, A.A., Hydamaka, A., Eskin, N.M., Eck, P., Thiyam-Holländer, U., 2018. Reduction of chlorophyll in cold-pressed hemp (*Cannabis sativa*) seed oil by ultrasonic bleaching and enhancement of oxidative stability. *Eur. J. Lipid Sci. Technol.* 120, 1700349. <https://doi.org/10.1002/ejlt.201700349>.

Livingston, S.J., Quilichini, T.D., Booth, J.K., Wong, D.C., Rensing, K.H., Laflamme-Yonkman, J., Castellarin, S.D., Bohlmann, J., Page, J.E., Samuels, A.L., 2020. Cannabis glandular trichomes alter morphology and metabolite content during flower maturation. *Plant J.* 101, 37-56. <https://doi.org/10.1111/tpj.14516>.

Maaroufi, C., Melcion, J.-P., De Monredon, F., Giboulot, B., Guibert, D., Le Guen, M.-P., 2000. Fractionation of pea flour with pilot scale sieving. I. Physical and chemical characteristics of pea seed fractions. *Anim. Feed Sci. Technol.* 85, 61-78. [https://doi.org/10.1016/S0377-8401\(00\)00127-9](https://doi.org/10.1016/S0377-8401(00)00127-9).

Makanjuola, S.A., 2017. Influence of particle size and extraction solvent on antioxidant properties of extracts of tea, ginger, and tea-ginger blend. *Food Sci. Nutr.* 5, 1179-1185. <https://doi.org/10.1002/fsn3.509>.

Meziane, S., Kadi, H., Lamrous, O., 2006. Kinetic study of oil extraction from olive foot cake. *Grasas Aceites.* 57, 175-179. <https://doi.org/10.3989/gya.2006.v57.i2.34>.

Morales, I., Keshavamurthy, J., Patel, N., Thomson, N., 2017. Inert gas asphyxiation: A liquid nitrogen accident. *Chest* 152, A378. <https://doi.org/10.1016/j.chest.2017.08.404>.

Morello, V., Brousseau, V.D., Wu, N., Wu, B.-S., MacPherson, S., Lefsrud, M., 2022. Light Quality Impacts Vertical Growth Rate, Phytochemical Yield and Cannabinoid Production Efficiency in *Cannabis sativa*. *Plants* 11, 2982. <https://doi.org/10.3390/plants11212982>.

Nahar, L., Uddin, S.J., Alam, M.A., Sarker, S.D., 2021. Extraction of naturally occurring cannabinoids: an update. *Phytochem. Anal.* 32, 228-241. <https://doi.org/10.1002/pca.2987>.

Nakach, M., Authelin, J.-R., Chamayou, A., Dodds, J., 2004. Comparison of various milling technologies for grinding pharmaceutical powders. *Int. J. Miner. Process.* 74, S173-S181. <https://doi.org/10.1016/j.minpro.2004.07.039>.

Nieh, C., Snyder, H., 1991. Solvent extraction of oil from soybean flour I—extraction rate, a countercurrent extraction system, and oil quality. *J. Am. Oil Chem. Soc.* 68, 246-249. <https://doi.org/10.1007/BF02657618>.

Panneton, B., Pillion, H., Dutilleul, P., Thériault, R., Khelifi, M., 1999. Full factorial design versus central composite design: statistical comparison and implications for spray droplet deposition experiments. *Trans. ASABE* 42, 877-884. <https://doi.org/10.13031/2013.13267>.

Paterakis, P., Korakianiti, E., Dallas, P., Rekkas, D., 2002. Evaluation and simultaneous optimization of some pellets characteristics using a 33 factorial design and the desirability function. *Int. J. Pharm.* 248, 51-60. [https://doi.org/10.1016/S0378-5173\(02\)00341-1](https://doi.org/10.1016/S0378-5173(02)00341-1).

Péres, V.F., Saffi, J., Melecchi, M.I.S., Abad, F.C., de Assis Jacques, R., Martinez, M.M., Oliveira, E.C., Caramão, E.B., 2006. Comparison of soxhlet, ultrasound-assisted and pressurized liquid extraction of terpenes, fatty acids and Vitamin E from *Piper gaudichaudianum* Kunth. *J. Chromatogr. A* 1105, 115-118. <https://doi.org/10.1016/j.chroma.2005.07.113>.

Pesek, C., Wilson, L., Hammond, E., 1985. Spice quality: Effect of cryogenic and ambient grinding on volatiles. *J. Food Sci.* 50, 599-601. <https://doi.org/10.1111/j.1365-2621.1985.tb13753.x>.

Pusiak, R.J., Cox, C., Harris, C.S., 2021. Growing pains: An overview of cannabis quality control and quality assurance in Canada. *Int. J. Drug Policy* 93, 103111. <https://doi.org/10.1016/j.drugpo.2021.103111>.

Romano, L.L., Hazekamp, A., 2013. Cannabis oil: chemical evaluation of an upcoming cannabis-based medicine. *Cannabinoids* 1, 1-11. <https://www.researchgate.net/publication/297707359>.

Rovetto, L.J., Aieta, N.V., 2017. Supercritical carbon dioxide extraction of cannabinoids from *Cannabis sativa* L. *J. Supercrit. Fluids* 129, 16-27. <https://doi.org/10.1016/j.supflu.2017.03.014>.

Russin, T.A., Arcand, Y., Boye, J.I., 2007. Particle size effect on soy protein isolate extraction. *J. Food Process. Preserv.* 31, 308-319. <https://doi.org/10.1111/j.1745-4549.2007.00127.x>.

Sagili, S.U.K.R., Addo, P.W., Gladu-Gallant, F.-A., Bilodeau, S.E., MacPherson, S., Paris, M., Lefsrud, M., Orsat, V., 2023. Optimization of wiped-film short path molecular distillation for recovery of cannabinoids from cannabis oil using response surface methodology. *Ind. Crops Prod.* 195, 116442. <https://doi.org/10.1016/j.indcrop.2023.116442>.

Schilling, S., Dowling, C.A., Shi, J., Ryan, L., Hunt, D., O'Reilly, E., Perry, A.S., Kinnane, O., McCabe, P.F., Melzer, R., 2020. The cream of the crop: Biology, breeding and applications of *Cannabis sativa*. *Authorea Preprints*. <https://doi.org/10.22541/au.160139712.25104053/v2>.

Shi, B., Ma, L., Dong, W., Zhou, F., 2015. Application of a novel liquid nitrogen control technique for heat stress and fire prevention in underground mines. *J. Occup. Environ. Hyg.* 12, D168-D177. <https://doi.org/10.1080/15459624.2015.1019074>.

Singh, K., Goswami, T., 1999a. Design of a cryogenic grinding system for spices. *J. Food Eng.* 39, 359-368. [https://doi.org/10.1016/S0260-8774\(98\)00172-1](https://doi.org/10.1016/S0260-8774(98)00172-1).

Tzima, K., Brunton, N.P., Rai, D.K., 2020. Evaluation of the impact of chlorophyll removal techniques on polyphenols in rosemary and thyme by-products. *J. Food Biochem.* 44, e13148. <https://doi.org/10.1111/jfbc.13148>.

Uoonlue, N., Muangrat, R., 2019. Effect of different solvents on subcritical solvent extraction of oil from Assam tea seeds (*Camellia sinensis* var. *assamica*): Optimization of oil extraction and physicochemical analysis. *J. Food Process Eng.* 42, e12960. <https://doi.org/10.1111/jfpe.12960>.

Valizadehderakhshan, M., Shahbazi, A., Kazem-Rostami, M., Todd, M.S., Bhowmik, A., Wang, L., 2021. Extraction of cannabinoids from *Cannabis sativa* L.(Hemp). *Agric.* 11, 384. <https://doi.org/10.3390/agriculture11050384>.

Vega, G.A., Dávila, J.A., 2022. Use of non-psychoactive residual biomass from *Cannabis sativa* L. for obtaining phenolic rich-extracts with antioxidant capacity. *Nat. Prod. Res.* 36, 4193-4199. <https://doi.org/10.1080/14786419.2021.1969562>.

Wilczek, M., Bertling, J., Hintemann, D., 2004. Optimised technologies for cryogenic grinding. *Int. J. Miner. Process.* 74, S425-S434. <https://doi.org/10.1016/j.minpro.2004.07.032>.

Yunus, M.A.C., Hasan, M., Othman, N., Mohd-Setapar, S.H., Salleh, L.M.-., Ahmad-Zaini, M.A., Idham, Z., Zhari, S., 2013. Effect of particle size on the oil yield and catechin compound using accelerated solvent extraction. *J. Teknol.* 60, 21-25. <https://doi.org/10.11113/jt.v60.1436>.

Zaiter, A., Becker, L., Karam, M.-C., Dicko, A., 2016. Effect of particle size on antioxidant activity and catechin content of green tea powders. *J. Food Sci. Technol.* 53, 2025-2032.  
<https://doi.org/10.1007/s13197-016-2201-4>.

### **Connecting text**

Chapter 3 emphasized the significance of reducing particle size, using appropriate extraction solvent and temperature to enhance the yield of crude cannabis oil and the concentration of cannabinoids and terpenes in the crude oil extracts. Crude cannabis oil typically contains a substantial amount of acidic cannabinoids. To produce medical- or pharmaceutical-grade products, it is crucial to undergo decarboxylation, which converts acidic cannabinoids into neutral cannabinoids. Chapter 4 focused on studying the optimal temperature and time required for complete decarboxylation of CBDA to CBD in crude cannabis oil, while ensuring minimal degradation.

Chapter 4 has been submitted for publication and is cited as the following:

**Sagili, S.U.K.R.,** Addo, P.W., Shearer, M., Taylor, N., Gladu-Gallant, F.-A., Bilodeau, S.E., MacPherson, S., Paris, M., Lefsrud, M., Orsat, V., 2023. Cannabinoid decarboxylation in crude cannabis oil: A kinetic study (Submitted to Journal of Applied Research on Medicinal and Aromatic Plants, Elsevier).

## Chapter 4: Cannabinoid decarboxylation in crude cannabis oil: a kinetic study

### Abstract

Valued *Cannabis sativa* cannabinoids undergo decarboxylation when heated. Cannabidiol (CBD) is obtained by decarboxylation of its acid analogue cannabidiolic acid (CBDA). The CBDA to CBD decarboxylation process in cannabis crude oil was monitored to examine effects of temperature and time. A rotary evaporator was used at 95 °C to 155 °C, for 0 to 180 min. Results indicate that a shorter time is optimal at high temperatures and vice versa. Complete CBDA decarboxylation was observed in 30 min at high temperatures of 135 °C and 155 °C compared to 60 min at 115 °C. Total CBD remained unchanged, suggesting that neither CBDA was converted to unknown cannabinoids nor CBD lost by evaporation. A kinetic study determined rate constants and activation energy required for decarboxylation. Calculated activation energy for CBDA is 84.64 kJ mol<sup>-1</sup>. Findings identify optimal temperatures and processing times required for efficient decarboxylation that reduce CBD loss and degradation in oil intended for further processing.

## 4.1 Introduction

*Cannabis sativa* has been grown for various purposes such as food, fibre, oil, medicine, recreational, and religious for centuries (Piluzza et al., 2013). The cannabinoid content is commonly used to classify different varieties of cannabis. Type I, THC-dominant, is the most common offering in both the medicinal and recreational markets. Type II cannabis includes both THC and cannabidiol (CBD), whereas Type III is CBD-rich. Types II and III with CBD- and terpene-rich profiles have the potential to enhance the effectiveness of THC and reduce its detrimental effects (Lewis et al., 2018). Synergistic interactions of terpenoids with cannabinoids include several complementary functions that increase therapeutic effectiveness of treatment for a range of health issues, including cancer, mental disorders, pain, and a variety of other conditions (Russo and Marcu, 2017). Some of the adverse psychological effects of THC can be reduced by the anxiolytic properties of CBD (Englund et al., 2013; Morgan et al., 2010). Hemp and marijuana can be distinguished by the presence of less than 0.3 % and more than 0.3 % of  $\Delta^9$ -tetrahydrocannabinol ( $\Delta^9$ -THC) on mass./mass. Basis, respectively (Aiello et al., 2016).

The cannabis plant has over 400 bioactive compounds, the majority of which are cannabinoids (phytocannabinoids), terpenoids, polyphenols, flavonoids, fatty acids, oils, and waxes (Ashton, 2001; Mahlberg and Kim, 2004). The most important phytocannabinoids are  $\Delta^9$ -THC, CBD, and cannabigerol (CBG), which are produced in the presence of heat, light or alkaline conditions via the decarboxylation of their carboxylic acid forms THCA, CBDA, and cannabigerolic acid (CBGA), respectively (Figure 4.1) (Taschwer and Schmid, 2015; Wang et al., 2016b). Biosynthesis studies show that the alkylation of olivetolic acid leads to the formation of CBGA, the precursor molecules for phytocannabinoids. THCA and CBDA are biosynthesized from CBGA by the action of oxidoreductases, THCA synthase and CBDA synthase, respectively (Sirikantaramas and Taura, 2017b).



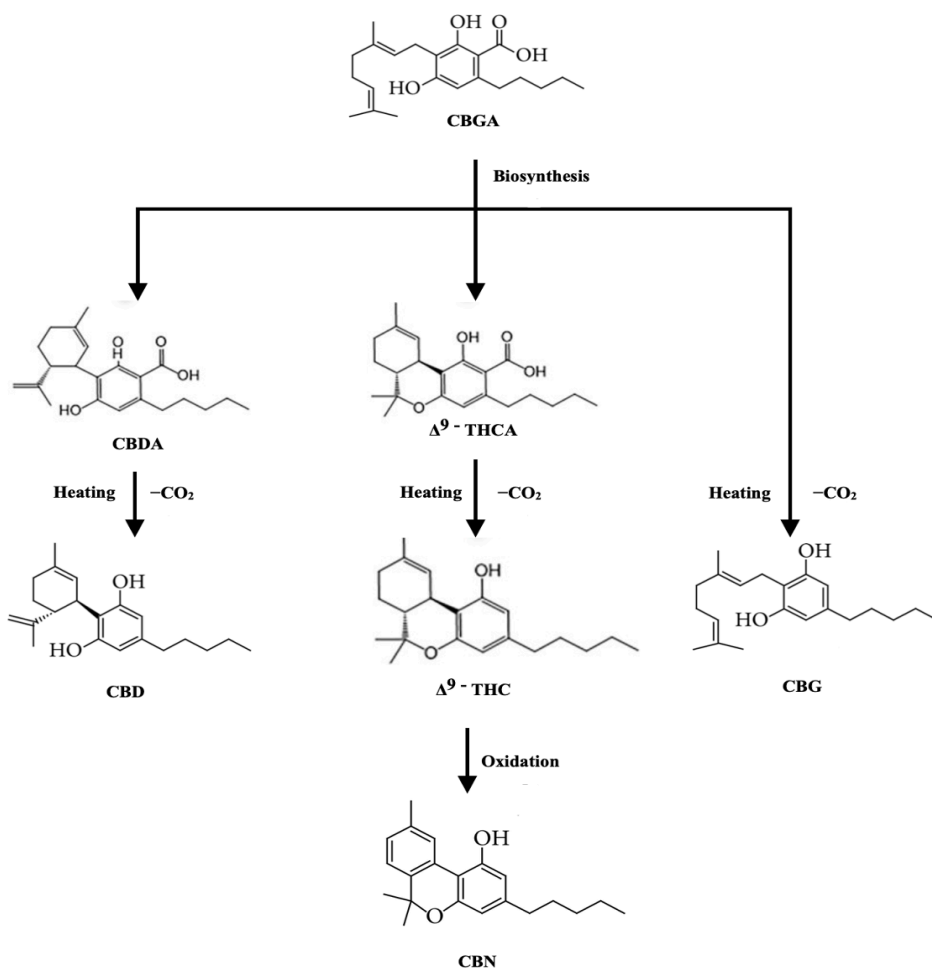


Figure 4.1. Molecular structure of major cannabinoids and their simplified biosynthetic, decarboxylation, and oxidation pathways.

Efficient production and development of cannabis products comprising neutral cannabinoids (i.e., THC, CBD, and CBG) are essential for assuring quality and safety for consumers. Acidic cannabinoids differ from neutral cannabinoids with the presence of carboxylic acid (COOH) in their chemical structure. Inhaling the volatiles produced by combusting or vaporizing cannabis is the primary method of administration for both medical and recreational purposes. Cannabinoids mostly exist in the non-psychoactive carboxylic acid forms in raw unheated cannabis material. When cannabis material undergoes combustion, the carboxylic acids are converted into their neutral forms (Elzinga et al., 2015). Decarboxylation has emerged as a critical stage in the cannabis supply chain (Moreno et al., 2020a), as these desired cannabinoids occur as carboxylic acids in the cannabis plant. Optimal post-harvest operations maintaining uniformity are required for the growing field of medicinal cannabis and cannabinoid research

(Addo et al., 2021). To obtain pharmaceutical or food-grade THC-, CBD-, or CBG-containing products, drying, grinding, extraction, decarboxylation, molecular distillation, and chromatographic analyses are typically required. Decarboxylation is generally carried out either before or after crude cannabis oil extraction, and a controlled process is critical for regulatory requirements and consistent product quality (Reason et al., 2022a). Unintentional decarboxylation of acidic cannabinoids occurs during various post-harvest processing stages, including long-term storage, drying and extraction at higher temperatures, as well as during molecular distillation of acidic cannabinoids. Decarboxylation additionally occurs by means of smoking, vaping, or baking. When compared to the production of acidic cannabinoids by enzymatic biosynthesis in the plant, decarboxylation of the acidic to the neutral cannabinoid form is a non-enzymatic solid-state reaction involving the release of CO<sub>2</sub> by splitting of the carboxyl group (Moreno et al., 2020a; Reason et al., 2022a).

Optimizing the decarboxylation process could help improve cannabinoid yields and reduce handling costs for large-scale operations (Reason et al., 2022a). In this study, thermal decarboxylation of crude cannabis oil was investigated to optimize the temperature and time parameters required for the efficient conversion of CBDA to CBD. Kinetic analysis was performed by measuring the rate constants and activation energies of the decarboxylation reaction based on the time-dependent decrease in acidic cannabinoids concentration.

## **4.2 Materials and methods**

### **4.2.1 Sample processing**

A licensed producer (EXKA Inc., Mirabel, Qc, Canada) provided air-dried and ground (2-mm particle size) cannabis biomass. Analytical tests and a certificate of analysis showed that the harvested cannabis biomass contained total CBD and total THC contents of 7.45 % and 0.03 % mass/mass, respectively. The steps followed in sample preparation are shown in Figure 4.2. Quick-wash cold ethanol extraction was performed in batches using biomass (kg) to ethanol (kg) ratio of 1:3 at -40 °C and flushed over the ground biomass for 20 min. The lower temperatures used during extraction prevent cannabinoid decarboxylation (Addo et al., 2022a). Before ethanol evaporation at 65 °C under vacuum, extracted crude cannabis oil was filtered through a 3-micron mesh to eliminate any particulate material. The oil was then stored at -40 °C to prevent thermal decarboxylation.

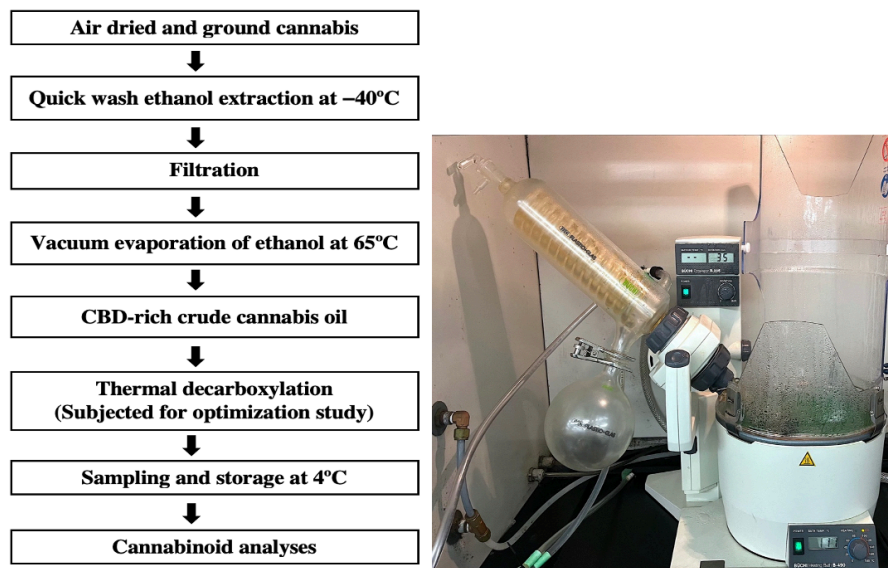


Figure 4.2. Left: Sample preparation flowchart; Right: rotary evaporator setup used for the decarboxylation study.

#### 4.2.2 Decarboxylation method

Decarboxylation of CBDA to CBD was conducted using a rotary evaporator (Büchi Rotavapor, R-205, USA) at 95 °C, 115 °C, 135 °C, and 155 °C for different lengths of time (30, 60, 90, 120, 150, and 180 minutes). The rotary evaporator consisted of a condenser connected to a vacuum, receiving and evaporating flasks, a heating water bath (Büchi, B-490, USA) (maximum temperature of 180 °C), a vapour duct, an action jack lift for manually elevating the evaporating flask, and a rotation speed that can be manually adjusted up to 280 rpm. Samples were placed in the evaporator flask in a heating bath containing ethylene glycol. Ethylene glycol was used because of its higher heating capacity compared to water. The rotation speed for the evaporator flask containing the crude cannabis oil was set at 35 rpm. A thermometer attached to the retort stand and an infrared thermometer was used to monitor the temperature of the heating bath during each experimental run. The vacuum duct was connected to the vacuum unit, and a low vacuum (50 mbar) was maintained throughout the study. A condenser with a cold trap was connected to the sample flask to trap metabolites escaping from the system and prevent damage to the vacuum unit. Approximately 50 g of crude cannabis oil was used for each experimental run. Preheating of crude cannabis oil was carried out using an electric heating mantle to reach the desired temperature. Once the temperature was reached, the oil was subjected to the

decarboxylation. Samples were collected before and after each experimental run and stored at 4 °C before cannabinoid analyses. Each experimental condition was run three times.

#### **4.2.3 Cannabinoid analyses**

Approximately 0.1 g oil extract was transferred to a 50 mL conical tube, and 40 mL of HPLC grade methanol (Thermo Fisher Scientific, Waltham, Massachusetts, US) was added. The sample was vortexed (Thermo Scientific vortex, Waltham, Massachusetts, US) for 5 min to ensure the extract was dissolved in the solvent. For analysis of major cannabinoids, 200 µL each extract sample was transferred into a volumetric flask, and the volume was made up to 5 mL using HPLC grade methanol. A total of 250 µL sample was transferred into a 2 mL micro vial, and the volume made up to 1 mL for minor cannabinoid analyses. The Waters Acquity Ultra High-Performance Liquid Chromatography (UPLC) coupled with a tunable ultraviolet (TUV) detector (Waters™, Mississauga, Ontario, Canada) was used for cannabinoid analyses. Cannabinoids were separated using a Waters Cortex column with a column temperature and sample injection volume of 30 °C and 2 µL, respectively, equipped with an isocratic gradient pump (Agilent Technologies, Inc). A 22 % reverse osmosis water and 0.1 % formic acid (Sigma-Aldrich, St. Louis, Missouri, US) made up mobile phase A. Mobile phase B consisted of 78 % HPLC grade acetonitrile (Thermo Fisher Scientific, Waltham, Massachusetts, US). An external calibration curve was developed for cannabinoid quantification using 4 standard cannabinoids (GC standards, Manchester, New Hampshire, US and Sigma Aldrich, St. Louis, Missouri, US).

#### **4.2.4 Experimental design to determine optimal decarboxylation**

A 4 x 7 full factorial temperature-time series was used for this study (Table 4.1). A total of 28 experimental runs were conducted to optimize the decarboxylation process. The total CBD content (mg/100 g dry matter) was calculated using Equation 4.1. This was considered to observe potential cannabinoid loss due to stoichiometric cannabinoid conversions other than acid-neutral cannabinoid conversion as described in previous literature (Moreno et al., 2020a; Reason et al., 2022a; Wang et al., 2016b). The run order of experiments within the temperature range was randomized to prevent systematic errors. Data collected from the samples were analyzed, and the statistical significance of the generated models was assessed by performing a one-way analysis of variance (ANOVA).

$$\text{Total CBD (mg 100 g dry matter}^{-1}\text{)} = \text{CBD (mg 100 g dry matter}^{-1}\text{)} + (0.877 \times \text{CBDA (mg 100 g dry matter}^{-1}\text{)}) \quad (4.1)$$

Table 4.1. Range of temperatures (°C) and time (min) used for thermal decarboxylation in this experiment.

Independent variables							
Temperature (°C)	Time (min)						
95	0	30	60	90	120	150	180
115	0	30	60	90	120	150	180
135	0	30	60	90	120	150	180
155	0	30	60	90	120	150	180

#### 4.2.5 Statistical analyses

JMP software (JMP 4.3 SAS Institute Inc.) was used to examine the statistical significance of the independent variables using one-way analysis of variance (ANOVA) with the Fisher's F-test at a 99 % confidence level.

### 4.3 Results and discussion

Optimization of the CBDA to CBD decarboxylation process and the development of a decarboxylation model for cannabis biomass can prevent loss of acidic cannabinoids and degradation or conversion of neutral cannabinoids into undesired forms from prolonged exposure to higher temperatures, eventually improving product quality and translating to cost savings for licensed producers in this relatively nascent industry. Crude cannabis oil was used for this experiment to determine the effects of temperature and time on the CBDA decarboxylation using a rotary evaporator and ethylene glycol as a bath solvent due to its high boiling point of 197 °C.

Some licensed cannabis processing facilities use large-scale rotary evaporators for decarboxylation of crude cannabis oil as the presence of a vacuum prevents degradation of cannabis oil by oxygen during the decarboxylation process. The main focus of this investigation was on the abundant acidic cannabinoid CBDA since initial cannabinoid analyses revealed that

CBGA (<limit of detection (LOD) by the instrument) and THCA (<0.03 % mass/mass) were present in low amounts in both the initial cannabis biomass and crude cannabis oil. Cannabinoid concentrations (mg 100 g dry matter<sup>-1</sup>) of the decarboxylated samples are presented in Table 4.2.

Table 4.2. Cannabinoid concentrations (mg 100 g dry matter<sup>-1</sup>) with different experimental conditions for decarboxylation of crude cannabis oil.

Temperature (°C)	Time (min)	Concentration (mg 100 g dry matter <sup>-1</sup> )				
		CBDA	CBD	CBGA	CBG	Total CBD
95	0	21.75	37.30	0.00	2.43	56.37
	30	6.43	49.85	0.00	3.28	55.49
	60	1.71	57.13	0.00	3.56	58.63
	90	0.79	56.43	0.00	3.75	57.12
	120	0.56	58.57	0.00	4.19	59.06
	150	0.88	57.98	0.00	3.94	58.75
	180	0.41	56.98	0.00	3.70	57.34
115	0	21.75	37.30	0.00	2.43	56.37
	30	5.02	57.81	0.00	3.49	62.21
	60	0.00	58.29	2.23	4.09	58.29
	90	0.00	59.71	1.97	3.76	59.71
	120	0.00	59.31	2.13	4.36	59.31
	150	0.00	58.52	2.03	4.19	58.52
	180	0.00	59.52	2.20	4.67	59.52
135	0	21.75	37.30	0.00	2.43	56.37
	30	0.00	59.99	1.70	3.59	59.99
	60	0.00	61.89	2.00	4.45	61.89
	90	0.00	60.51	1.72	3.94	60.51
	120	0.00	59.62	1.75	4.10	59.62
	150	0.00	59.64	1.89	4.37	59.64
	180	0.00	61.56	1.76	4.23	61.56
155	0	21.75	37.30	0.00	2.43	56.37
	30	0.00	59.31	1.75	3.86	59.31
	60	0.00	59.24	1.54	3.64	59.24
	90	0.00	60.18	1.75	4.35	60.18
	120	0.00	59.74	1.59	4.03	59.74
	150	0.00	60.08	1.58	4.04	60.08
	180	0.00	61.01	1.59	4.04	61.01

#### **4.3.1 Decarboxylation studies**

The difference in total CBD concentrations for the initial cannabis biomass and initial crude cannabis oil (0 min) can be attributed to the loss of cannabinoids during the extraction process. Figure 4.3 illustrates how the decarboxylation process resulted in a linear reduction in CBDA while simultaneously leading to an increase in CBD. This was consistent with the findings presented by a study on the decarboxylation of hemp seed oil in a closed reactor at 120 °C, where a simultaneous production of CBD and a linear decrease of CBDA were observed (Citti et al., 2018).



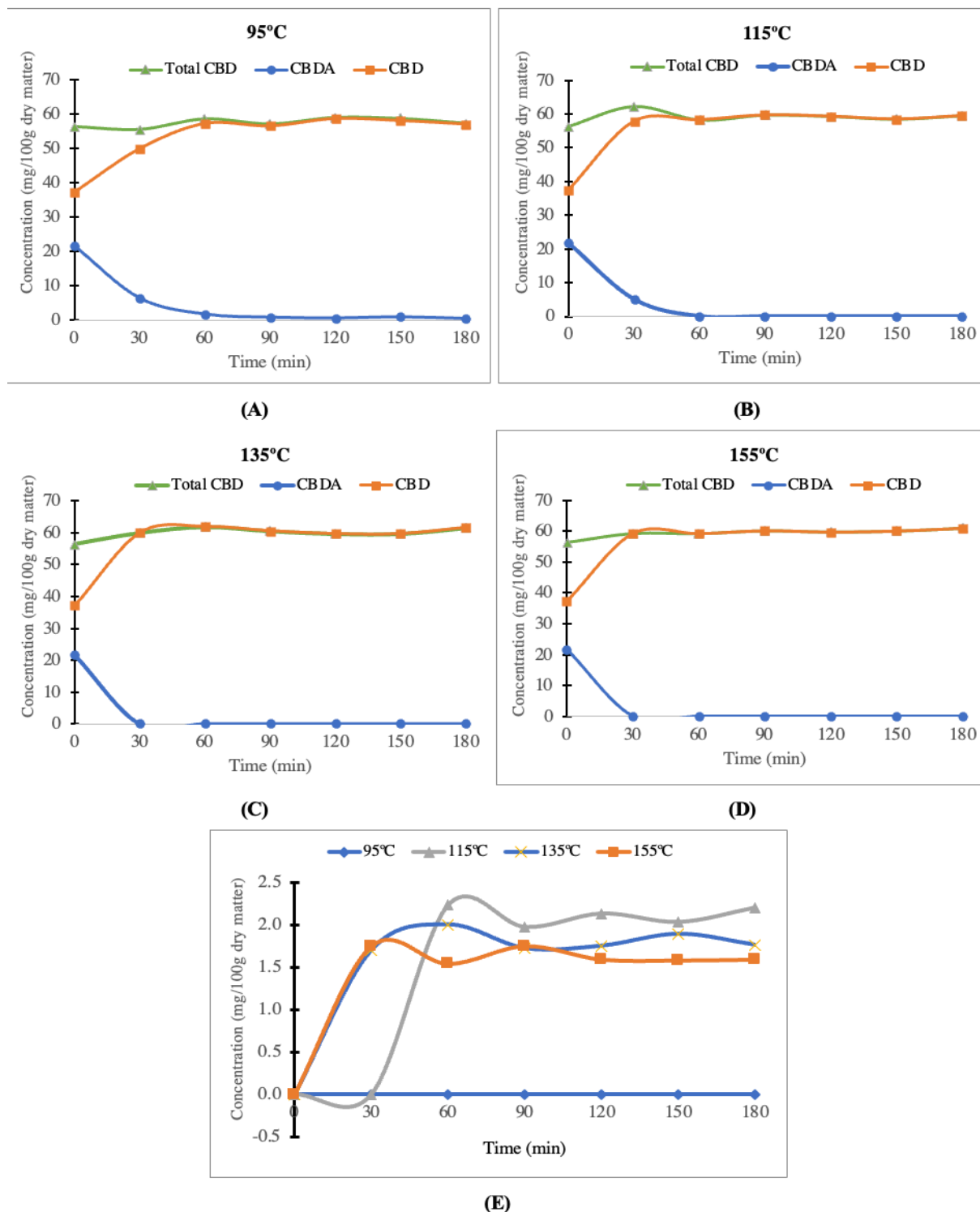


Figure 4.3. Concentrations ( $\text{mg } 100 \text{ g dry matter}^{-1}$ ) of Total CBD, CBD, CBDA (A, B, C, D), and CBGA (E) as a function of time (min) during the decarboxylation process.

At a lower temperature of  $95^\circ\text{C}$ , the time required for the decarboxylation of CBDA to CBD requires more than 180 min (Figure 4.3A). The time needed for complete decarboxylation

of CBDA was halved from 60 minutes at 115 °C (Figure 4.3B) to 30 minutes at 135 °C and 155 °C (Figure 4.3C, 4.3D). Therefore, increasing the temperature to greater than 135 °C is not suggested, and the results imply that less time is required at higher temperatures and vice versa. When the temperature was increased from 95 °C to 115 °C for 30 min, concentrations of CBDA and CBD decreased and increased by 28 % and 15.8 %, respectively.

When decarboxylation was complete, the concentration of CBD remained nearly constant throughout the duration of the experiment after the concentration of CBDA approached 0, except at 95 °C, due to the incomplete decarboxylation. Total CBD remained unchanged, suggesting that neither CBDA was converted to unknown cannabinoids nor CBD was lost by evaporation under all tested conditions. This may be explained by two factors; first, the vacuum eliminates oxygen during the experiment, preventing any possible oxidative degradation of CBD, and second, the studied low-temperature range prevented CBD from evaporating. These results are supportive of a comparable study in which the rate of disappearance of total cannabinoid concentration was reduced significantly during a decarboxylation reaction performed in sealed containers compared to open beakers (Moreno et al., 2020a). Other studies have reported cannabinoid loss during decarboxylation (Citti et al., 2018; Wang et al., 2016b). Similarly, a study on hemp seed oil reported that 60 % of total CBD molar concentration was lost after the decarboxylation of CBDA in an open reactor at 120 °C (Citti et al., 2018). When time and temperature were increased, Wang et al. (2016b) noticed an unexpected decrease in the total CBD molar concentrations during decarboxylation in the vacuum oven at 110 °C and 130 °C. This difference in results could be possibly due to the methodology utilized; in our research, 50 g of crude cannabis oil in the rotary evaporator was used, whereas Wang et al. (2016) used small vials containing small amounts of concentrated extracts in a vacuum oven. One limitation of this study was such that the effect of the shorter preheating time of the crude cannabis oil on cannabinoid content was not examined. However, the initial cannabinoid concentrations in the samples collected immediately (0 min) after preheating of oil at different temperatures were similar, indicating that it had no significant effect on the results.

Although CBGA was initially present in minimal amounts in the crude cannabis oil sample (<LOD), CBGA production was surprisingly observed (Figure 4.3E) after 60 min at 115 °C and 30 min at 135 °C and 155 °C. The results were observed after analyses were performed at two independent laboratories. Addo et al. (2023b) recently reported a similar outcome of

unexpected CBGA production resulting from the use of higher temperatures. One possible explanation is that increased temperature triggered the biochemical pathway of precursor molecules, leading to the production of CBGA or the transformation of some unknown cannabinoids into CBGA. Further studies could be conducted to examine how temperature and time affect the molecular biosynthesis of CBGA, as this minor cannabinoid and its decarboxylated form have garnered some interest in therapeutical research and could be of value.

#### 4.3.2 Kinetic analyses

It is essential to take into account both the chemical characteristics of acidic cannabinoids and the reaction environment to get a complete understanding of the decarboxylation reaction (Wang et al., 2016b). It has been previously reported that the decarboxylation of CBDA into CBD follows first-order reaction kinetics (Citti et al., 2018; Moreno et al., 2020a; Veress et al., 1990b; Wang et al., 2016b). The relationship between the concentration of CBDA and the decarboxylation rate constant can be obtained using Equation (4.2)

$$\ln \frac{[CBDA]_0}{[CBDA]_t} = kt \quad (4.2)$$

where  $[CBDA]_0$  and  $[CBDA]_t$  are the concentration of CBDA at time 0, and t (min), respectively, and k is the decarboxylation rate constant ( $s^{-1}$ ) calculated from the gradient of  $\ln \frac{[CBDA]_0}{[CBDA]_t}$  over time. Figure 4.4 demonstrates that first-order kinetics were obtained at 95 °C over 180 min and at 115 °C until complete decarboxylation occurred. High reaction rates made it difficult to determine the reaction order at the higher temperatures of 135 °C and 155 °C. This was consistent with a reported study performed at 145 °C (Wang et al., 2016b).

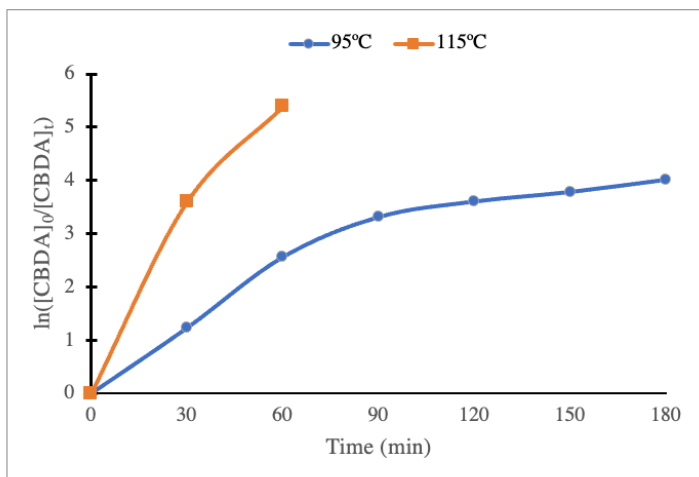


Figure 4.4. Decarboxylation kinetics of CBDA in crude cannabis oil at 95 °C and 115 °C.

The Arrhenius equation was used to calculate the activation energy ( $E_A$ ) based on kinetic rate constants ( $k$ ) obtained at each temperature. The activation energy ( $E_A$ ) ( $\text{kJ mol}^{-1}$ ) is the minimum energy required for the reaction to occur and was calculated using Equation (4.3)

$$\ln k = \ln A - \frac{E_A}{RT} \quad (4.3)$$

where  $R$  represents the universal gas constant ( $8.314 \text{ J mol}^{-1} \text{ K}^{-1}$ ),  $T$  is the temperature (K), and  $A$  is the pre-exponential factor or frequency. After plotting the natural logarithmic values of rate constants ( $k$ ) over the inverse of the temperature ( $\text{K}^{-1}$ ), the slope of the equation correlates to  $-\frac{E_A}{R}$  and  $\ln A$  is the intercept.

The calculated values of the kinetic rate constants at 95 °C and 115 °C and the activation energy ( $E_A$ ) of CBDA are included in Table 4.3. The Arrhenius plot was used to calculate the activation energy ( $E_A$ ), which resulted in  $84.64 \text{ kJ mol}^{-1}$ . This value was consistent with the activation energy ( $89.5 \text{ kJ mol}^{-1}$ ) reported by the Citti et al. (2018) during the decarboxylation of CBDA in hemp seed oil in open and closed reactor with temperatures varying from 80 °C to 120 °C. The higher rate constants and different activation energies ( $112 \text{ kJ mol}^{-1}$  and  $60 \text{ kJ mol}^{-1}$ ) obtained by Wang et al. (2016b) and Moreno et al. (2020a), respectively for CBDA could be due to different methodologies, where Wang employed a vacuum oven and a smaller quantity of extracts, and Moreno used 10 g of ground hemp biomass in an oven as opposed to our study's use of rotary evaporator and a large quantity of crude cannabis oil (50 g).

Table 4.3. Kinetic rate constants (k) and Activation energies ( $E_A$ ) for the CBDA decarboxylation.

Acidic cannabinoid	Kinetic rate constants ( $k \times 10^3$ ) ( $\text{sec}^{-1}$ )		Activation energies ( $E_A$ ) ( $\text{kJ mol}^{-1}$ )
	95 °C	115 °C	
CBDA	0.022	0.09	84.64

At the same temperatures, the time has a highly significant effect ( $p < 0.01$ ) on the concentrations of CBDA and CBD. This was evident by a strong negative correlation of -0.99 between the concentrations of CBDA and CBD at all studied time periods for the same temperature condition. Higher coefficients of determination ( $R^2$ ) and adjusted ( $R^2$ ) values of 0.97 and 0.96 for CBDA and 0.90 and 0.88 for CBD, respectively, indicate the suitability of the tested model and relate to the effective fitting of experimental data with a low variation from mean values.

#### 4.4 Conclusion

This study aimed to find out the optimal conditions for the decarboxylation of CBDA to CBD in cannabis crude oil. In doing so, the efficient production of CBD with minimal losses due to temperature and time combinations during the reaction was investigated. Decarboxylation of CBDA in cannabis crude oil was studied at temperatures between 95 °C and 155 °C, from 0 min to 180 min with 30 min time intervals. A shorter process time was required for the complete decarboxylation at higher temperatures and vice versa. For example, only 30 min is required at 135 °C and 155 °C, compared to 95 °C and 115 °C, which took more than 180 min and 60 min, respectively. Kinetic studies were conducted, and rate constants were determined at lower temperatures, while it was not possible at 135 °C and 155 °C due to the higher reaction rates. The decarboxylation conditions reported herein provide information about the temperature and time period that may be useful to cannabis processing operations, but scale-up tests will be required. Complete CBD decarboxylation was achieved while simultaneously preventing further CBD degradation losses with prolonged exposure at higher temperatures. Future research must be done to find the exact time and temperature required for the complete decarboxylation of CBDA to CBD using response surface methodology.

#### 4.5 References

- Addo, P.W., Brousseau, V.D., Morello, V., MacPherson, S., Paris, M., Lefsrud, M., 2021. Cannabis chemistry, post-harvest processing methods and secondary metabolite profiling: A review. *Ind. Crops Prod.* 170, 113743. <https://doi.org/10.1016/j.indcrop.2021.113743>.
- Addo, P.W., Poudineh, Z., Shearer, M., Taylor, N., MacPherson, S., Raghavan, V., Orsat, V., Lefsrud, M., 2023b. Relationship between Total Antioxidant Capacity, Cannabinoids and Terpenoids in Hops and Cannabis. *Plants* 12, 1225. <https://doi.org/10.3390/plants12061225>.
- Addo, P. W., Sagili, S. U. K. R., Bilodeau, S. E., Gladu-Gallant, F.-A., MacKenzie, D. A., Bates, J., McRae, G., MacPherson, S., Paris, M., Raghavan, V., Orsat, V., Lefsrud, M. 2022. Cold Ethanol Extraction of Cannabinoids and Terpenes from Cannabis Using Response Surface Methodology: Optimization and Comparative Study. *Molecules*. 27 (24), 8780. <https://doi.org/10.3390/molecules27248780>.
- Aiello, G., Fasoli, E., Boschini, G., Lammi, C., Zanoni, C., Citterio, A., Arnoldi, A., 2016. Proteomic characterization of hempseed (*Cannabis sativa* L.). *J. Proteomics* 147, 187-196. <https://doi.org/10.1016/j.jprot.2016.05.033>.
- Ashton, C.H., 2001. Pharmacology and effects of cannabis: a brief review. *Br. J. Psychiatry* 178, 101-106. <https://doi.org/10.1192/bjp.178.2.101>.
- Citti, C., Pacchetti, B., Vandelli, M.A., Forni, F., Cannazza, G., 2018. Analysis of cannabinoids in commercial hemp seed oil and decarboxylation kinetics studies of cannabidiolic acid (CBDA). *J. Pharm. Biomed. Anal.* 149, 532-540. <https://doi.org/10.1016/j.jpba.2017.11.044>.
- Elzinga, S., Ortiz, O., Raber, J.C., 2015. The conversion and transfer of cannabinoids from cannabis to smoke stream in cigarettes. *Nat Prod Chem Res.* <https://doi.org/10.4172/2329-6836.1000163>.
- Elzinga, S., Ortiz, O., Raber, J.C., 2015. The conversion and transfer of cannabinoids from cannabis to smoke stream in cigarettes. *Nat Prod Chem Res.* <https://doi.org/10.1177/0269881112460109>.
- Lewis, M.A., Russo, E.B., Smith, K.M., 2018. Pharmacological foundations of cannabis chemovars. *Planta Med.* 84, 225-233. <https://doi.org/10.1055/s-0043-122240>.
- Mahlberg, P.G., Kim, E.S., 2004. Accumulation of cannabinoids in glandular trichomes of Cannabis (*Cannabaceae*). *J. Ind. Hemp.* 9, 15-36. [https://doi.org/10.1300/J237v09n01\\_04](https://doi.org/10.1300/J237v09n01_04).

Moreno, T., Dyer, P., Tallon, S., 2020a. Cannabinoid decarboxylation: a comparative kinetic study. *Ind. Eng. Chem. Res.* 59, 20307-20315. <https://doi.org/10.1021/acs.iecr.0c03791>.

Morgan, C.J., Schafer, G., Freeman, T.P., Curran, H.V., 2010. Impact of cannabidiol on the acute memory and psychotomimetic effects of smoked cannabis: naturalistic study. *Br. J. Psychiatry* 197, 285-290. <https://doi.org/10.1192/bjp.bp.110.077503>.

Piluzza, G., Delogu, G., Cabras, A., Marceddu, S., Bullitta, S., 2013. Differentiation between fiber and drug types of hemp (*Cannabis sativa* L.) from a collection of wild and domesticated accessions. *Genet. Resour. Crop Evol.* 60, 2331-2342. <https://doi.org/10.1007/s10722-013-0001-5>.

Reason, D.A., Grainger, M.N., Lane, J.R., 2022. Optimization of the Decarboxylation of Cannabis for Commercial Applications. *Ind. Eng. Chem. Res.* <https://doi.org/10.1021/acs.iecr.2c00826>.

Russo, E.B., Marcu, J., 2017. Cannabis pharmacology: the usual suspects and a few promising leads. *Adv. Pharmacol.* 80, 67-134. <https://doi.org/10.1016/bs.apha.2017.03.004>.

Sirikantaramas, S., Taura, F., 2017b. Cannabinoids: biosynthesis and biotechnological applications, in: Chandra, S., Lata, H., ElSohly, M., Eds.; (Ed.), *Cannabis sativa* L.-Botany and biotechnology. Springer, University of Illinois Press, Champaign, Illinois, United States, pp. 183-206. [https://doi.org/10.1007/978-3-319-54564-6\\_8](https://doi.org/10.1007/978-3-319-54564-6_8).

Taschwer, M.; Schmid, M. G. Determination of the relative percentage distribution of THCA and  $\Delta^9$ -THC in herbal cannabis seized in Austria–Impact of different storage temperatures on stability. *Forensic Sci. Int.* 2015, 254, 167-171. <https://doi.org/10.1016/j.forsciint.2015.07.019>.

Veress, T., Szanto, J., Leisztner, L., 1990. Determination of cannabinoid acids by high-performance liquid chromatography of their neutral derivatives formed by thermal decarboxylation: I. Study of the decarboxylation process in open reactors. *J. Chromatogr. A.* 520, 339-347. [https://doi.org/10.1016/0021-9673\(90\)85118-F](https://doi.org/10.1016/0021-9673(90)85118-F).

Wang, M., Wang, Y.-H., Avula, B., Radwan, M.M., Wanas, A.S., van Antwerp, J., Parcher, J.F., ElSohly, M.A., Khan, I.A., 2016b. Decarboxylation study of acidic cannabinoids: a novel approach using ultra-high-performance supercritical fluid chromatography/photodiode array-mass spectrometry. *Cannabis Cannabinoid Res.* 1, 262-271. <https://doi.org/10.1089/can.2016.0020>.

### **Connecting text**

Chapters 3 and 4 enhanced the yield and concentration of cannabinoids and terpenes in the extracted crude cannabis oil and determined the optimal conditions for complete decarboxylation of acidic cannabinoids without degradation. The separation of cannabinoids from terpenes and other heavy compounds in decarboxylated crude cannabis oil, and the subsequent increase in their mass in the distillate, is vital for the production of cannabis products containing neutral cannabinoids. Chapter 5 investigated the impact of feed flow rate and internal condensation temperature on maximizing the mass of neutral cannabinoids in the distillate stream, while ensuring the quality of cannabinoids remained unaffected, using wiped-film short path molecular distillation.

Chapter 5 has been published and is cited as the following:

**Sagili, S.U.K.R.**, Addo, P.W., Gladu-Gallant, F.-A., Bilodeau, S.E., MacPherson, S., Paris, M., Lefsrud, M., Orsat, V., 2023. Optimization of wiped-film short path molecular distillation for recovery of cannabinoids from cannabis oil using response surface methodology. *Ind. Crops Prod.* 195, 116442.



## **Chapter 5: Optimization of wiped-film short path molecular distillation for recovery of cannabinoids from cannabis oil using response surface methodology**

### **Abstract**

Few studies have explored the molecular distillation techniques that can improve the recovery of cannabinoids from crude cannabis oil with scale-up potential. Wiped-film short path molecular distillation is commonly employed in the cannabis industry for separating cannabinoids from terpenes and heavy compounds. It is a two-cut process, where the distillation of terpenes and cannabinoids occurs at the first and second cuts, respectively. In this experiment, the effects of the distillation parameters in the second cut, including feed flow rate (35 to 55 Hz) (41.6 to 71.3 mL min<sup>-1</sup>) and internal condensation temperature (60 to 90 °C), were examined and optimized using a central composite rotatable design towards maximizing cannabinoid mass and recovery efficiency in the distillate and minimizing cannabinoid mass in the residue. Results show that irrespective of internal condensation temperature, reducing feed flow rate increased the cannabinoid's yield and recovery. Although long distillation time was observed at low feed flow rates, the quality of cannabinoids remained unaffected. Response surface methodology was used to optimize the wiped-film short path molecular distillation of cannabis oil. The predicted optimal conditions were a feed flow rate of 35 Hz (41.6 mL min<sup>-1</sup>) and an internal condensation temperature of 75 °C. At these optimized conditions, the recovery efficiency of tetrahydrocannabinol was 93.4 % in the distillate. To this end, this study provides distillation conditions to be considered by the cannabis industry if aiming for a cannabinoid-rich distillate from the molecular distillation process without affecting cannabinoid quality.

## 5.1 Introduction

Cannabis (*Cannabis sativa*) is a dioecious, rarely monoecious, annual flowering plant that belongs to the family Cannabaceae (Micalizzi et al., 2021). Stalked glandular trichomes are distributed on the cannabis inflorescence and, to a minor extent, on the epidermis of cannabis leaves (Benelli et al., 2018). These sites are where phytochemicals (valuable metabolic products) such as cannabinoids, terpenes, and flavonoids are secreted and accumulate (ElSohly and Slade, 2005; Flores-Sanchez and Verpoorte, 2008). Terpenes are the most prevalent volatile fraction among the bioactive phytochemicals of cannabis essential oil, which are made up of monoterpenes, including myrcene,  $\alpha$ -pinene, and terpinolene and bitter-tasting sesquiterpenes like humulene, caryophyllene, and caryophyllene oxide (Happyana and Kayser, 2016). The least volatile fraction of cannabis essential oil is the cannabinoids (Calzolari et al., 2017), among which  $\Delta^9$ -tetrahydrocannabinol (THC), cannabidiol (CBD), cannabichromene (CBC), and cannabinol (CBN) are the major cannabinoids (Callado et al., 2018). CBN is the degraded product of THC in the presence of oxygen (Hartsel et al., 2016).

With the legalization of medicinal and adult use (or recreational) cannabis in many countries, product development and optimized extraction, separation, and purification methods have become developmental focal points for the cannabis industry. Vacuum evaporation and distillation are widely used to process thermolabile blends of valued plant metabolites, among other separating techniques. Both techniques use vapor pressure to enable the boiling of various components at lower temperatures (Valizadehderakhshan et al., 2022a). The distillation process involves selective evaporation and condensation to separate components from the liquid mixture (Kinsara and Demirbas, 2016). Separation of desired chemical components under distillation occurs because of the relative volatility of different components at various temperatures. Short path distillation (SPD) and wiped-film short path (WFSP) molecular distillation are the most commonly employed techniques in the cannabis industry. Although cannabinoid recovery is low, SPD systems are smaller and easy to operate with reduced operational costs compared with the WFSP systems for small-scale operations (Valizadehderakhshan et al., 2022a). In WFSP molecular distillation, the heating and cooling surfaces are incorporated into a single chamber with a short travel path for molecules from the heating medium to the condenser, rendering this system very effective in separation and preventing thermal degradation losses (Chen et al., 2021; Martins et al., 2006; Martins et al., 2012). This chamber allows vapor molecules to move freely

between the evaporator and the condenser. The spacing between the evaporator and condenser must be smaller than the mean free path of the evaporating molecules (Fregolente et al., 2007b). The agitation of wiper blades supports the heat and mass transfer process by forming a thin layer with a substantial heat-transfer surface with a short residence time at reduced pressures.

There are very few studies performed on the molecular distillation of cannabis oil, and there is a need to develop an optimized process using a scientific approach. One study recently reported that internal condensation temperature (ICT) had no effect on recovered CBD amounts from hemp extracts and that increasing WFMD evaporation and condensation temperatures increase CBD concentrations (Valizadehderakhshan et al., 2022a). Other research has shown that increasing feed flow rate (FFR) of sugarcane (*Saccharum officinarum*) molasses reduced the residence time of the molecules on the evaporator surface, ultimately resulting in a lower mass ratio (distillate/feed) (Fregolente et al., 2007b). The aim of this experiment was to optimize other operating parameters for the WFSP molecular distillation system using decarboxylated cannabis oil. Specifically, to determine the influence of independent variables, including FFR and ICT, on the cannabinoid profile, recovery, distillate, and residue yields.

## **5.2 Materials and methods**

### **5.2.1 Sample processing**

Dried and ground cannabis biomass of 2-mm particle size was obtained from a licensed producer (EXKA Inc., Mirabel, Qc, Canada). Ethanol was used as an extraction solvent because of its low toxicity and ease of recovery (Valizadehderakhshan et al., 2022a). Cold ethanol extraction was performed at -40 °C in batches using the quick wash ethanol extraction process (Figure 5.1). The ratio of cannabis biomass (kg) to ethanol (kg) was set as 1:3. The temperature of ethanol was lowered to -40 °C and flushed over the ground cannabis biomass for 20 minutes. Extracted crude cannabis oil was filtered using a 3-micron mesh to remove any particulate content before ethanol evaporation at 65 °C under vacuum. Thermal decarboxylation of crude cannabis oil was done at 110 °C for 90 minutes to convert the acidic to neutral cannabinoid forms before distillation. Samples collected were stored at 4 °C before cannabinoid analyses.

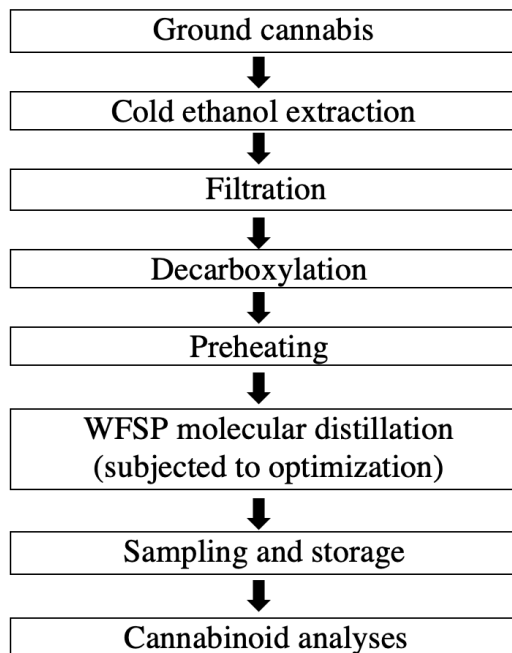


Figure 5.1. Sample preparation flowchart used for optimizing wiped-film short path (WFSP) molecular distillation in this study.

### 5.2.2 Reagents

Food-grade ethanol, methanol, and acetonitrile were purchased from Thermo Fisher Scientific (Waltham, Massachusetts, US). Reverse osmosis water and formic acid were brought from Sigma-Aldrich (St. Louis, Missouri, US). Reference cannabinoids were purchased from LGC standards (Manchester, New Hampshire, US) and Sigma Aldrich (St. Louis, Missouri, US). Both acidic cannabinoids, tetrahydrocannabinolic acid (THCA) and cannabidiolic acid (CBDA), were supplied at  $1.0 \text{ mg mL}^{-1}$  in acetonitrile. All neutral cannabinoids, including THC, CBD, CBC, CBG, and CBN, were provided at  $1.0 \text{ mg mL}^{-1}$  in methanol.

### 5.2.3 WFSP molecular distillation of cannabis oil

Distillation of decarboxylated cannabis oil was performed using a WFSP molecular distillation system (VKS 70-5 RS, Root Sciences, Washington, US) that consisted of a feed tank connected to a frequency inverter and a short path evaporator (Figure 5.2). The frequency inverter modulates the FFR. The short path evaporator comprised a combined evaporator and an internal condenser section with surface areas of  $0.1 \text{ m}^2$  and  $0.15 \text{ m}^2$ , respectively. This system was equipped with a wiper basket and three-stranded wipers with controllable speed (rpm) to

regulate spreading of cannabis oil on the evaporator. Two cold trap units, glycol and liquid nitrogen, were used to prevent the vapor escaping the distillation unit from damaging the vacuum pump. The WFSP unit has distillate and residue discharge units with adjustable speeds. The system was covered with a heating jacket to prevent heat loss during molecular distillation. Marlotherm SH thermic oil ensured proper control over temperature and maintains constant feed temperature throughout the distillation process.

A total of 8724 g decarboxylated THC-rich ( $74.2 \text{ g } 100 \text{ g dry matter}^{-1}$ ) cannabis oil was preheated at  $90^{\circ}\text{C}$  using an electric heating mantle and transferred to the feed tank of the WFSP for the distillation of terpenes (first cut). The FFR of 50 Hz and wiper speed of 400 rpm combined with a feed temperature, evaporator temperature, and ICT of  $115^{\circ}\text{C}$ ,  $158^{\circ}\text{C}$ , and  $48^{\circ}\text{C}$ , respectively, were used to distill the terpenes. The distillation unit was maintained at 57 Pa pressure to ensure low vacuum throughout the process. The cold glycol trap was maintained at  $-40^{\circ}\text{C}$  while the liquid nitrogen cold trap was set at  $-196^{\circ}\text{C}$ . The residue of the first cut served as the feed for cannabinoid distillation (second cut). Approximately 250 ml (232 g) of cannabis oil was used for each second-cut experimental run. To reduce the effect of the experimental conditions on each other, 100 ml cannabis oil was used to clean the distillation system before an experimental run. For cannabinoid distillation, the sys'em's pressure was reduced to 0.73 Pa with an increased evaporator temperature of  $172^{\circ}\text{C}$ . However, the FFR and ICT for the second cut were varied for the optimization study. When subjected to different operating conditions, two significant separate fractions were obtained, namely, the distillate stream rich in cannabinoids and the residue stream containing heavy compounds (waxes, chlorophyll, etc.). Samples were collected from both distillate and residue streams separately and sent for cannabinoid analyses to understand the effect of two operating conditions (FFR and ICT) on cannabinoid mass (g) in the distillate and residue, as well as cannabinoid recovery efficiency (%) in the distillate.

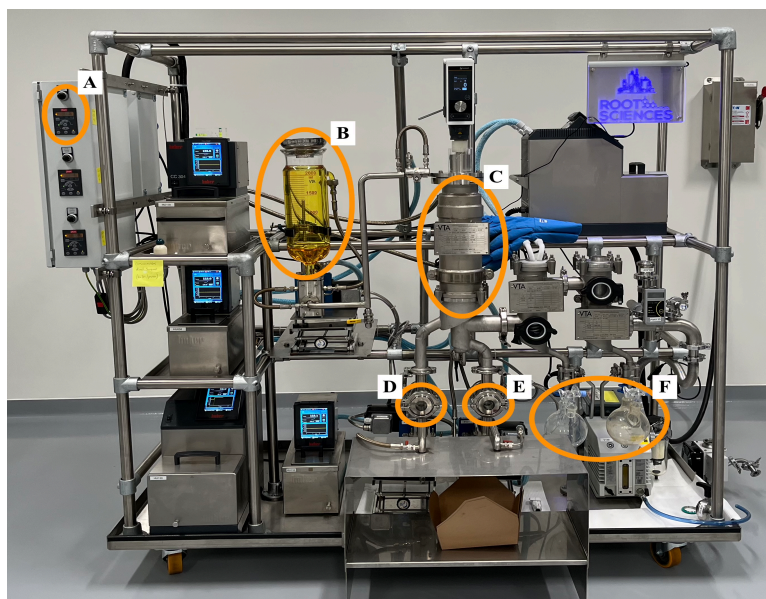


Figure 5.2. Wiped-film short path (WFSP) molecular distillation equipment used for this study. (A) Feed flow rate regulator, (B) Feed tank, (C) Combined evaporator and internal condenser section, (D) Distillate discharge unit, and (E) Residue discharge unit, and (F) Cold traps.

#### 5.2.4 Experimental design

Two variables of five-level central composite rotatable statistical design (CCRD) with uniform precision was used to optimize the independent variables for WFSP molecular distillation with response surface methodology (RSM). RSM is a set of statistical and mathematical approaches used to model and analyze a problem when the desired response is impacted by several variables (Amini et al., 2009; Bajpai et al., 2012). CCRD is highly efficient in providing helpful information on the effects of process parameters for optimization purposes with a reduced number of total experimental runs compared with factorial designs (Routray and Orsat, 2014). The study assessed and compared the effects of the two operating parameters on the responses including mass of cannabinoids (g) in distillate ( $Y_1$ ) and residue ( $Y_2$ ), and recovery efficiency (%) of cannabinoids in the distillate ( $Y_3$ ) of the second cut. Equipment measures the FFR in Hz and nominal capacity conversion of Hz to  $\text{mL min}^{-1}$  were based on viscosity, temperature, and pressure (Table 5.1).

Cannabinoid mass (g) in the distillate and residue was calculated separately by multiplying the quantity of cannabis oil (g) collected at the distillate and residue portion of each experimental

run with the concentration of particular cannabinoid (g g dry matter<sup>-1</sup>) measured at distillate and residue portion of each run respectively by using Equation (5.1):

$$\text{Mass of cannabinoids in the distillate (or) residue (g)} = Q \times C \quad (5.1)$$

where Q = quantity of cannabis oil (g) collected at the distillate (or) residue portion of each run

C = concentration of particular cannabinoid (g g dry matter<sup>-1</sup>) measured at distillate (or) residue portion of each run. The recovery efficiency (%) of cannabinoids in distillate was calculated by using Equation (5.2):

$$\text{Recovery efficiency (\%)} = \frac{\text{Mass of cannabinoid (g) in second cut distillate}}{\text{Mass of cannabinoid (g) in second cut feed}} \times 100 \quad (5.2)$$

A total of 13 experimental runs were generated using JMP software (JMP 4.3 SAS Institute Inc.). The experimental design (CCRD) was based on the complete factorial design (2<sup>2</sup>) described previously (Demim et al., 2013) with five center and star points (Table 5.1). To ensure rotatability, the distance for the axial points was fixed from the center ( $\alpha = 2^{k/4}$ , where k is the number of variables). The star points were fixed based on the rotatability conditions (Demim et al., 2013). The central point was coded as 0, the low and high factor settings were coded as -1 and +1, respectively, and the low and high star points were coded as -1.414 or +1.414, respectively (Koo et al., 2011). Quadratic terms can be included in the response surface model using axial combinations. The replication of the central point ensures a more consistent level of precision in response estimates across the experimental design. The run order of experiments was randomized to prevent systematic errors. Samples of the distillates and residues were collected after each experimental run, and data collected were analyzed and fit into second-order polynomial equations. Analysis of variance (ANOVA) was performed to determine the significance of the generated models.

Table 5.1. Uncoded levels of the independent variables with WFSP molecular distillation of cannabis oil.

Parameters	Symbol	Coded levels				
		$-\alpha$	Low	Medium	High	$+\alpha$
		-1.414	-1	0	+1	+1.414
Independent variables						
FFR (Hz)	$X_l$	30.9	35	45	55	59.1
FFR (mL min <sup>-1</sup> )	$X_l$	36.7	41.6	53.5	71.3	70.2
ICT (°C)	$X_2$	53.8	60	75	90	96.2

### 5.2.5 Cannabinoid analyses

Using HPLC-grade methanol, each extracted sample was further diluted to a 1:50 ratio for major cannabinoid analyses and 1:4 ratio for minor cannabinoid analyses. One millilitre volumes of each extract were pipetted into HPLC vials and the Waters Acquity Ultra High-Performance Liquid Chromatography (UPLC) coupled to a tunable ultraviolet (TUV) detector (Waters™, Mississauga, Ontario, Canada) were employed for cannabinoid analyses. Separation of cannabinoids was achieved using an isocratic gradient pump and a Waters Cortex column with an injection volume of 2 µL and a column temperature of 30 °C. The components of mobile phase A were 22 % reverse osmosis water and 0.1 % formic acid. 78 % HPLC-grade acetonitrile was used for mobile phase B. Cannabinoids were quantified using a calibration curve derived from seven standard cannabinoids.

### 5.2.6 Statistical analysis

JMP software (JMP 4.3 SAS Institute Inc.) was used to assess the data for the effects of independent variables on the responses. The least squares regression methodology was used to obtain the parameter estimators for the mathematical model. Based on the experimental results, the second-order polynomial model was fitted using a multiple regression equation (Equation 5.3):

$$Y_j = \beta_0 + \beta_1 X_1 + \beta_2 X_2 + \beta_{11} X_1 X_1 + \beta_{22} X_2 X_2 + \beta_{12} X_1 X_2 \quad (5.3)$$



Where  $Y_j$  is the predicted response (dependent variable),  $X_1$  (FFR) and  $X_2$  (ICT) are the independent variables,  $\beta_0$  is the model intercept,  $\beta_1$  and  $\beta_2$  are the linear terms,  $\beta_{11}$  and  $\beta_{22}$  are the quadratic terms, and  $\beta_{12}$  is the interaction term.

The second-order polynomial model used for the study was to test the significance ( $p < 0.05$ ) of the FFR ( $X_1$ ), ICT ( $X_2$ ), and the interaction of the FFR and ICT ( $X_1X_2$ ) on the responses. This was to help with scale-up purposes for the cannabis industry. The Fisher's  $F$ -test with a 95 % confidence level was performed to examine the statistical significance of the regression coefficients using ANOVA. By eliminating non-significant dependent factors ( $p > 0.05$ ) in a "backward elimination" procedure, the model's statistical significance was increased. Response surface plots were produced from the experimental data to overview the effects of independent variables. The optimum conditions for WFSP molecular distillation of cannabis oil for the two operating conditions were obtained based on modelling and the highest desired function.

### **5.2.7 Verification of model**

To validate the model, three experiments were carried out using the optimal extraction conditions. The model's validity was assessed by comparing the experimental and predicted values.

## **5.3 Results**

### **5.3.1 Terpene cut (first cut)**

Two distillation parameters were investigated to optimize WFSP molecular distillation for cannabis oil, including FFR and ICT. Data (Table 5.2) indicate that out of a total of 8724 g decarboxylated cannabis oil used for the first cut, 584 g (6.7 %), 7712 g (88.4 %), and 402 g (4.61 %) cannabis oil were in the terpene distillate, residue, and cold traps, respectively and 26 g (0.29 %) oil was lost by vapor during the process. Major cannabinoid concentrations (g 100 g dry matter<sup>-1</sup>) in the decarboxylated cannabis oil and in the distillate, residue, and cold trap collections produced by the first cut is presented in Table 5.2. The THC concentration in the residue (feed for cannabinoid distillation) was significantly ( $p < 0.05$ ) higher than in the distillate and THC concentration increased 7.8 % in the residue compared with the decarboxylated oil (the feed of the first cut).

Table 5.2. Cannabinoid analysis of decarboxylated cannabis oil and distillate, residue, and cold trap collections from the terpene distillation (first cut).

Sample	Decarboxylated cannabis oil	Terpenes (distillate)	2 <sup>nd</sup> cut feed (residue)	Glycol cold trap	Liquid nitrogen cold trap
Yield (g)	8724	584	7712	364	38
Concentration of cannabinoids (g 100 g dry matter <sup>-1</sup> )					
THC	74.2	23.3	80.5	3.6	1.3
THCA	0.43	0.43	0.12	0.16	0.12
Total THC	74.6	23.7	80.6	3.78	0.14
CBD	0.13	0.28	0.12	< 0.1	< 0.1
CBDA	0.12	0.14	0.11	< 0.1	< 0.1
Total CBD	0.23	0.4	0.22	< 0.1	< 0.1
CBG	2.7	0.54	2.96	< 0.1	< 0.1
CBN	0.32	< 0.1	0.36	< 0.1	< 0.1

### 5.3.2 Effect of operating parameters on cannabinoid distillation (second cut)

RSM was used to optimize operating conditions for cannabinoid distillation. The influence of the independent distillation parameters on the responses is presented in Table 5.3. THCA and CBDA in the distillates and THCA and CBD in the residues were below the detection limit of the methodology and instrument. Statistical significance of linear, interactive, and quadratic coefficients for all parameters and each response are presented in Table A.1 (Appendix). Negative regression coefficients of the developed models indicate a negative correlation between the independent variable and the response. Thus, a decrease in FFR results in a significant ( $p < 0.05$ ) increase in the cannabinoids' mass and recovery in the distillate of the second cut, demonstrated by an increase of 6.51 % – 10.97 % for THC concentration in the distillate compared with the feed.

Table 5.3. Matrix of the CCRD and observed responses ( $Y_j$ ) for different experimental conditions for WFSP molecular distillation of cannabis oil.

Independent variables		Responses							
$X_1$ (Hz)	$X_2$ (°C)	THC	Total THC	CBD	CBDA	Total CBD	CBG	CBC	CBN
Mass of cannabinoids in the distillate (g) $\pm$ Standard deviation									
35	60	177.49 $\pm$ 2.31	177.49 $\pm$ 2.65	0.33 $\pm$ 0.02	<LOD	0.33 $\pm$ 0.03	5.98 $\pm$ 0.49	1.27 $\pm$ 0.07	0.76 $\pm$ 0.02
35	90	175.75 $\pm$ 1.64	177.75 $\pm$ 2.59	0.34 $\pm$ 0.02	<LOD	0.34 $\pm$ 0.02	6.09 $\pm$ 0.51	1.27 $\pm$ 0.06	0.86 $\pm$ 0.04
55	60	132.21 $\pm$ 1.15	132.21 $\pm$ 1.72	0.29 $\pm$ 0.00	<LOD	0.29 $\pm$ 0.02	4.14 $\pm$ 0.52	0.99 $\pm$ 0.03	0.57 $\pm$ 0.02
55	90	119.23 $\pm$ 1.21	119.23 $\pm$ 1.04	0.26 $\pm$ 0.01	<LOD	0.26 $\pm$ 0.01	3.78 $\pm$ 0.34	0.91 $\pm$ 0.01	0.57 $\pm$ 0.01
30.8	75	177.36 $\pm$ 0.69	177.36 $\pm$ 2.44	0.36 $\pm$ 0.01	<LOD	0.36 $\pm$ 0.02	6.13 $\pm$ 0.58	1.35 $\pm$ 0.02	0.75 $\pm$ 0.03
59.1	75	123.67 $\pm$ 0.81	123.86 $\pm$ 1.01	0.28 $\pm$ 0.01	<LOD	0.28 $\pm$ 0.01	4.03 $\pm$ 0.59	1.00 $\pm$ 0.02	0.49 $\pm$ 0.01
45	53.8	150.19 $\pm$ 0.95	150.19 $\pm$ 2.41	0.29 $\pm$ 0.02	<LOD	0.29 $\pm$ 0.00	4.96 $\pm$ 0.05	1.11 $\pm$ 0.04	0.66 $\pm$ 0.03
45	96.2	152.3 $\pm$ 0.83	152.3 $\pm$ 1.11	0.32 $\pm$ 0.01	<LOD	0.32 $\pm$ 0.02	5.01 $\pm$ 0.54	0.97 $\pm$ 0.02	0.66 $\pm$ 0.02
45	75	151.73 $\pm$ 0.97	151.73 $\pm$ 0.89	0.26 $\pm$ 0.01	<LOD	0.26 $\pm$ 0.03	4.92 $\pm$ 0.23	1.04 $\pm$ 0.01	0.64 $\pm$ 0.01
45	75	154.51 $\pm$ 0.88	154.51 $\pm$ 0.98	0.33 $\pm$ 0.03	<LOD	0.33 $\pm$ 0.02	5.08 $\pm$ 0.36	1.01 $\pm$ 0.01	0.63 $\pm$ 0.01
45	75	155.53 $\pm$ 1.10	155.53 $\pm$ 0.95	0.33 $\pm$ 0.01	<LOD	0.33 $\pm$ 0.01	5.23 $\pm$ 0.26	1.01 $\pm$ 0.02	0.63 $\pm$ 0.02
45	75	155.4 $\pm$ 0.92	155.4 $\pm$ 1.22	0.32 $\pm$ 0.01	<LOD	0.32 $\pm$ 0.01	5.16 $\pm$ 0.38	1.09 $\pm$ 0.03	0.61 $\pm$ 0.02
45	75	146.21 $\pm$ 1.01	146.21 $\pm$ 1.32	0.30 $\pm$ 0.01	<LOD	0.30 $\pm$ 0.02	4.81 $\pm$ 0.21	1.02 $\pm$ 0.02	0.61 $\pm$ 0.01
Mass of cannabinoids in the residue (g) $\pm$ Standard deviation									

35	60	31.47 ± 1.12	31.66 ± 0.98	<LOD	0.32 ± 0.02	0.28 ± 0.03	1.60 ± 0.02	0.15 ± 0.02	0.20 ± 0.01
35	90	38.10 ± 0.29	38.22 ± 0.36	<LOD	0.18 ± 0.01	0.16 ± 0.02	1.67 ± 0.01	0.21 ± 0.02	0.18 ± 0.02
55	60	74.96 ± 0.58	75.23 ± 0.73	<LOD	0.28 ± 0.01	0.25 ± 0.02	3.30 ± 0.06	0.38 ± 0.01	0.36 ± 0.01
55	90	78.31 ± 0.62	78.51 ± 0.55	<LOD	0.28 ± 0.03	0.24 ± 0.02	3.43 ± 0.09	0.40 ± 0.02	0.40 ± 0.03
30.8	75	31.08 ± 0.06	31.25 ± 0.18	<LOD	0.21 ± 0.02	0.19 ± 0.01	1.46 ± 0.03	0.17 ± 0.01	0.16 ± 0.02
59.1	75	90.06 ± 0.68	90.37 ± 0.52	<LOD	0.30 ± 0.02	0.26 ± 0.01	3.91 ± 0.01	0.50 ± 0.01	0.46 ± 0.02
45	53.8	53.61 ± 0.81	53.56 ± 0.39	<LOD	0.29 ± 0.01	0.26 ± 0.02	2.53 ± 0.02	0.26 ± 0.00	0.30 ± 0.03
45	96.2	57.20 ± 0.79	57.37 ± 0.54	<LOD	0.26 ± 0.03	0.24 ± 0.02	2.56 ± 0.02	0.26 ± 0.00	0.32 ± 0.01
45	75	46.89 ± 0.75	47.06 ± 0.35	<LOD	0.27 ± 0.01	0.23 ± 0.02	2.20 ± 0.01	0.22 ± 0.02	0.27 ± 0.02
45	75	56.62 ± 0.78	56.82 ± 0.30	<LOD	0.31 ± 0.03	0.27 ± 0.01	2.68 ± 0.03	0.24 ± 0.01	0.30 ± 0.02
45	75	53.05 ± 0.81	53.22 ± 0.36	<LOD	0.27 ± 0.03	0.24 ± 0.02	2.44 ± 0.02	0.23 ± 0.02	0.26 ± 0.01
45	75	50.25 ± 0.84	50.40 ± 0.34	<LOD	0.23 ± 0.02	0.20 ± 0.00	2.26 ± 0.02	0.25 ± 0.02	0.25 ± 0.02
45	75	53.93 ± 0.77	54.13 ± 0.36	<LOD	0.36 ± 0.03	0.32 ± 0.01	2.54 ± 0.01	0.23 ± 0.01	0.29 ± 0.02

---

Recovery efficiency of cannabinoids in the distillate (%) ± Standard deviation

---

35	60	95.06 ± 1.07	95.06 ± 0.99	117.23 ± 1.58	<LOD	64.05 ± 0.82	87.10 ± 0.91	109.11 ± 1.44	89.92 ± 0.82
35	90	95.20 ± 0.93	95.20 ± 0.94	122.77 ± 1.21	<LOD	67.02 ± 0.76	88.71 ± 1.05	109.19 ± 1.15	102.92 ± 0.99
55	60	70.81 ± 0.89	70.81 ± 0.81	104.36 ± 0.87	<LOD	56.97 ± 0.71	60.35 ± 0.64	85.69 ± 0.64	67.36 ± 1.02
55	90	63.86 ± 0.54	63.86 ± 0.68	94.58 ± 0.91	<LOD	51.63 ± 0.84	55.09 ± 0.29	78.85 ± 0.61	67.64 ± 1.00
30.8	75	94.83 ± 1.02	94.99 ± 1.09	130.4 ± 1.96	<LOD	71.19 ± 0.70	89.29 ± 1.02	116.50 ± 0.92	88.85 ± 0.66
59.1	75	66.23 ± 0.47	66.34 ± 0.62	100.8 ± 1.08	<LOD	55.05 ± 0.45	58.66 ± 0.48	85.92 ± 0.68	58.49 ± 0.23
45	53.8	80.44 ± 0.62	80.44 ± 0.55	105.4 ± 0.52	<LOD	57.58 ± 0.29	72.19 ± 0.78	95.30 ± 0.81	78.14 ± 0.61

45	96.2	$81.57 \pm 0.69$	$81.57 \pm 0.48$	$114.5 \pm 0.81$	<LOD	$62.50 \pm 0.68$	$72.98 \pm 0.21$	$83.97 \pm 0.69$	$78.00 \pm 0.59$
45	75	$81.26 \pm 0.70$	$81.26 \pm 0.63$	$95.07 \pm 0.96$	<LOD	$51.90 \pm 0.64$	$71.69 \pm 0.45$	$89.75 \pm 0.55$	$75.62 \pm 0.42$
45	75	$82.75 \pm 0.72$	$82.86 \pm 0.67$	$116.7 \pm 1.00$	<LOD	$63.74 \pm 0.63$	$73.99 \pm 0.49$	$87.02 \pm 0.50$	$75.36 \pm 0.39$
45	75	$83.30 \pm 0.70$	$83.30 \pm 0.59$	$116.9 \pm 0.95$	<LOD	$63.83 \pm 0.69$	$76.11 \pm 0.48$	$87.31 \pm 0.51$	$75.35 \pm 0.45$
45	75	$83.23 \pm 0.76$	$83.23 \pm 0.64$	$115.8 \pm 0.94$	<LOD	$63.25 \pm 0.63$	$75.16 \pm 0.43$	$94.24 \pm 0.68$	$72.54 \pm 0.41$
45	75	$78.31 \pm 0.73$	$78.31 \pm 0.61$	$109.5 \pm 0.98$	<LOD	$59.80 \pm 0.67$	$70.07 \pm 0.44$	$87.64 \pm 0.53$	$72.62 \pm 0.42$

---

$X_1$  is the FFR (Hz), and  $X_2$  is the ICT (°C). LOD is the limit of detection by the instrument or methodology.

### 5.3.3 The FFR effect

FFR is defined as the rate at which the volume of fluid flows per unit of time. FFR had a linearly significant ( $p < 0.05$ ) effect on the mass of all cannabinoids measured in the distillates (Figure 5.3), and the mass of THC, total THC, CBG, CBC, and CBN in the residue (Figure 5.4). The quadratic effect of FFR significantly ( $p < 0.05$ ) influenced the CBC yields in the distillates and THC, total THC, and CBC in the residue. The interactive effects ( $\beta_{12}$ ) of the independent parameters did not play a role in the yields of the distillates, residue, and concentration of cannabinoids. Decreasing FFR from 59.1 Hz to 30.9 Hz at a constant ICT (75 °C) increased THC and total THC yield in the distillate by 30.3 % and 30.2 %, respectively; this was decreased by 65.5 % and 65.4 %, respectively, in the residue. Similar observations were made for CBD (22.2 %), total CBD (34.3 %), CBG (26 %), and CBC (25.9 %) in the distillates. Decreasing FFR (59.1 Hz to 30.8 Hz) additionally caused a significant increase in the yield of CBN by 34.67 % at a constant ICT of 75 °C. The recovery efficiency of THC significantly ( $p < 0.05$ ) increased by 30.2 % and 19.0 % when FFR decreased from 59.1 Hz to 45 Hz or 30.8 Hz, respectively, at a constant ICT (75 °C). Recovery efficiency had a significant ( $p < 0.05$ ) linear effect on all cannabinoids in the distillate (Table A.1 in Appendix). However, CBC was significantly ( $p < 0.05$ ) influenced by the quadratic effect of FFR and the linear effect of ICT.

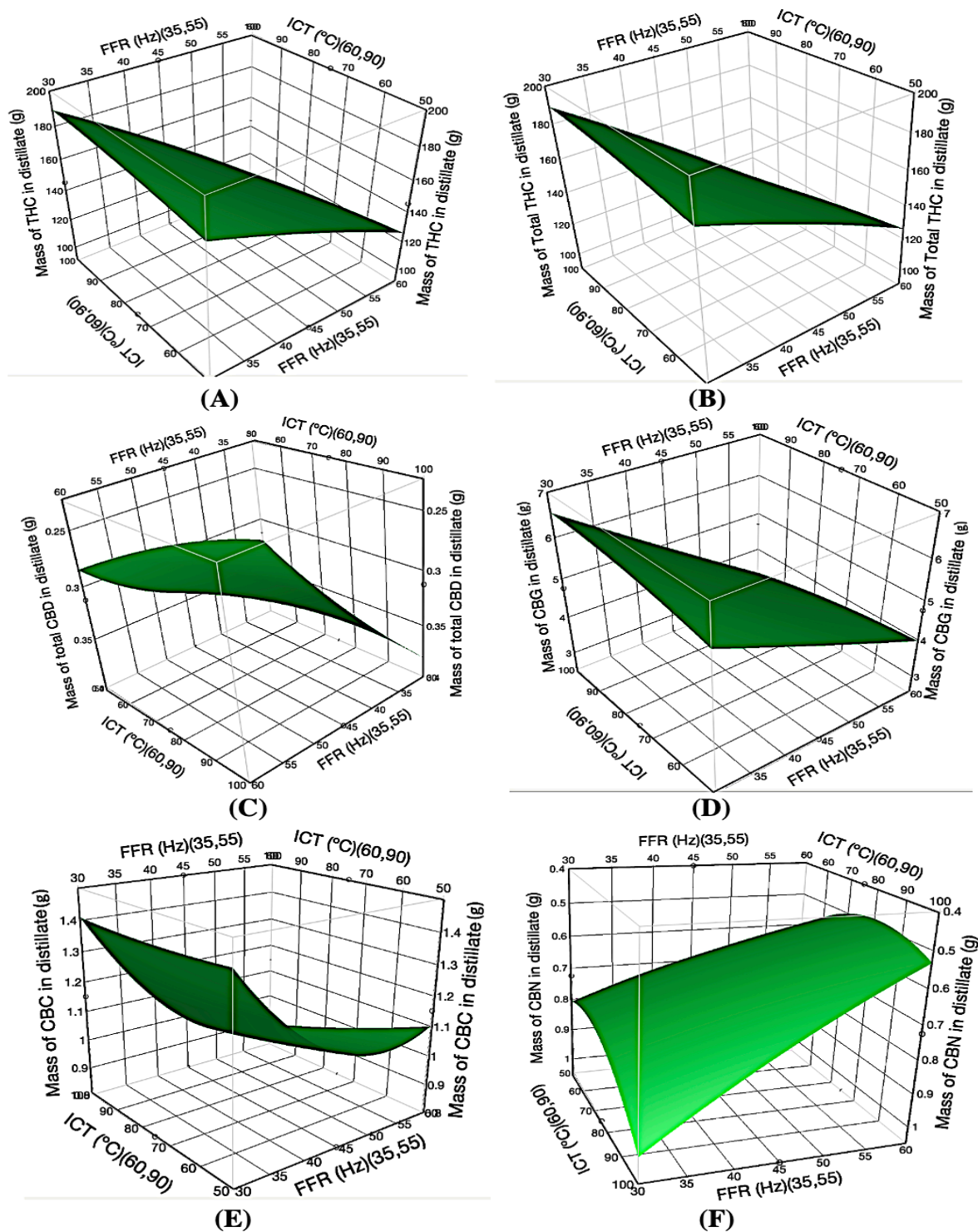


Figure 5.3. 3D response surface plots demonstrating the combined effects of FFR (Hz) and ICT (°C) on the mass (g) of THC (A), Total THC (B), Total CBD (C), CBG (D), CBC (E), CBN (F) in the distillate of the second cut.

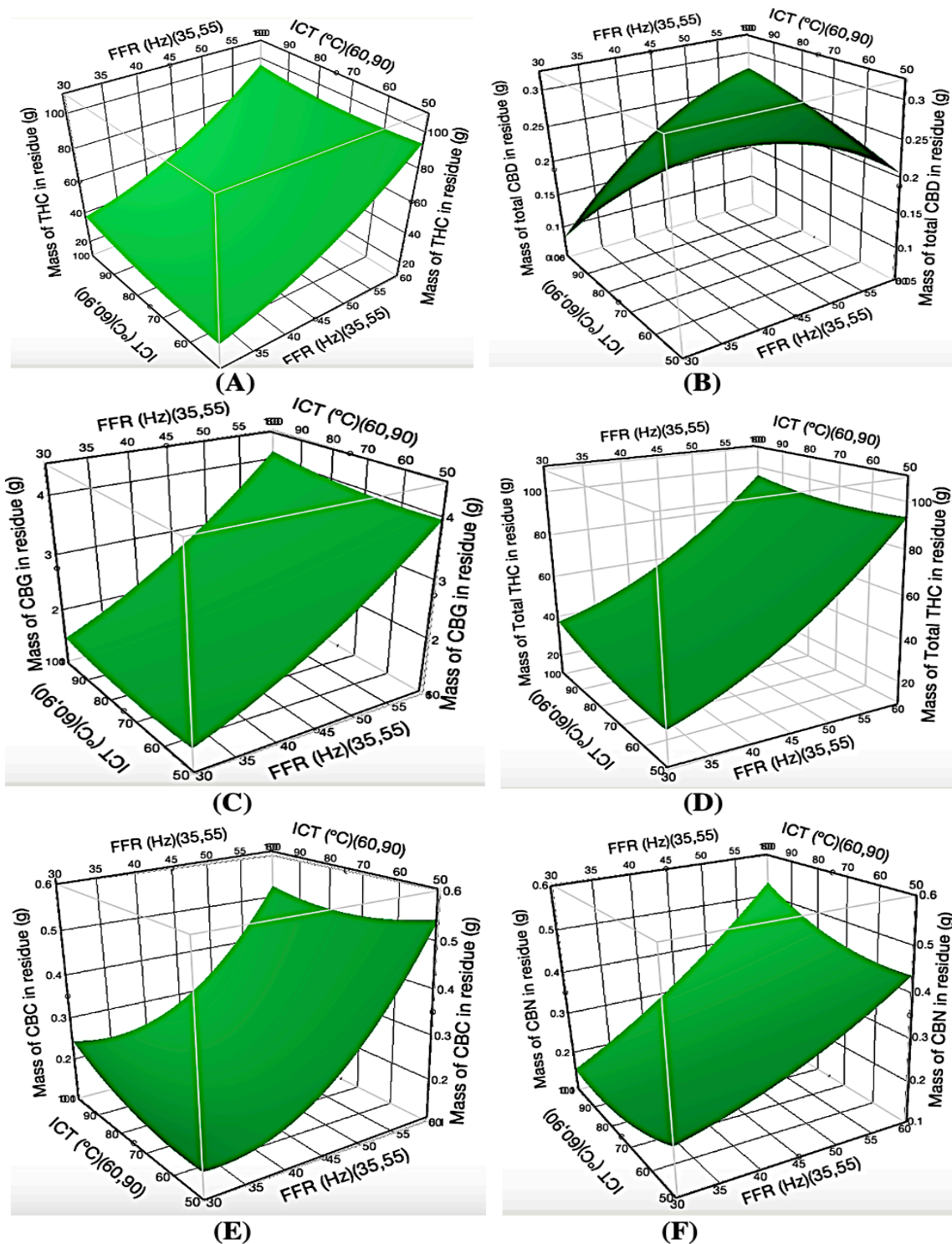


Figure 5.4. 3D response surface plots demonstrating the combined effects of FFR (Hz) and ICT (°C) on the mass (g) of THC (A), Total THC (B), Total CBD (C), CBG (D), CBC (E), CBN (F) in the residue of the second cut.



### 5.3.4 The ICT effect

ICT refers to the temperature of the internal condenser at which a specific gas-phase component condenses into a liquid. This did not play a significant role ( $p > 0.05$ ) on the mass of cannabinoids in the distillate, residue, and recovery efficiency of cannabinoids in the distillate, except for a linear effect on CBC yield in the distillate and recovery efficiency, in addition to an interaction effect for CBC in the residue (Supplementary Table S1). This was evident by the high correlation (1) between CBC yield in the distillate and recovery efficiency for the experimental runs. Negative regression coefficients show that a decrease in the ICT and FFR caused a significant ( $p < 0.05$ ) decrease in the distillate and residue yield of CBC. Decreasing ICT from 90 °C to 60 °C using a constant FFR of 55 Hz increased CBC content by 8.1 % and 8.0 % in the distillate and residue, respectively.

### 5.3.5 Optimal conditions for WFSP molecular distillation of cannabis oil

To optimize the operating parameters for WFSP molecular distillation of cannabis oil, two variables were kept in range: FFR (30.8 Hz to 59.1 Hz) and ICT (53.8 °C to 96.2 °C). The aim was to maximize cannabinoid mass (g) and cannabinoid recovery efficiency (%) in the distillate, while minimizing cannabinoid mass (g) in the residue. The experimental design was additionally set to minimize mass (g) and recovery efficiency (%) of CBN in the distillate for the purpose of reducing THC degradation to CBN. The desirability value ranged from 0 (unacceptable for one or more product characteristics) to 1 (all product characteristics on target), where values close to 1 have maximum desirability. Optimal independent experimental conditions and desirability for each cannabinoid at each response are presented in Table 5.4, along with the predicted response values. WFSP molecular distillation using an FFR of 35 Hz (41.6 mL min<sup>-1</sup>) and ICT of 75 °C, respectively, described as the optimal conditions with highest desirability values of 0.72, 0.84 and 0.70 for cannabinoid mass (g) in the distillate, residue, and recovery efficiency (%) of cannabinoids in the distillate.

Table 5.4. Optimal experimental conditions for WFSP molecular distillation of cannabis oil and the predicted response values.

Responses	Mass of cannabinoids (g)		Recovery efficiency of cannabinoids in the distillate (%)
	Distillate	Residue	
Desirability	0.72	0.84	0.70
Optimal independent experimental conditions			
FFR (Hz)	35	35	35
FFR (mL min <sup>-1</sup> )	41.6	41.6	41.6
ICT (°C)	76	75	77
Predicted response values at optimal conditions			
THC	174.4	38.8	93.44
Total THC	177.4	38.8	93.51
CBD	0.34	<LOD	123.6
CBDA	<LOD	0.18	<LOD
Total CBD	0.34	0.17	67.46
CBG	5.95	1.71	86.74
CBC	1.25	0.2	107.23
CBN	0.74	0.19	88.94

### 5.3.6 Model fitting

Experimental observations indicate that a low FFR could efficiently increase cannabinoid mass and recovery in distillate and decrease cannabinoid mass in residue, except for CBD, CBDA, and total CBD. Values for these three experimental responses were analyzed using ANOVA (Table 5.5). The reduced model (model B), where FFR was an independent parameter, demonstrated a significant effect ( $p < 0.05$ ) on the mass (g) and recovery efficiency (%) of CBD

and total CBD in the distillate. Coefficients of determination ( $R^2$ ) and adjusted  $R^2$  estimate the adequacy test of the models and values ranging from 0.51 to 0.98 and 0.16 to 0.97, respectively (Table 5.5). Higher  $R^2$  values and adjusted  $R^2$  correspond to the fitting of experimental data successfully with a low deviation from mean values. Data indicate that lack-of-fit is non-significant ( $p > 0.05$ ) except for the mass (g) and recovery efficiency (%) of CBN in the distillate.

Table 5.5. ANOVA for responses at different experimental conditions.

Response	Source			Residual			<i>F</i>	Prob > <i>F</i>	Lack-of-fit	<i>R</i> <sup>2</sup>	Adjusted	CV %
	Model						ratio		(Prob > <i>F</i> )		<i>R</i> <sup>2</sup>	
	<i>df</i>	SS	MS	<i>df</i>	SS	MS						
Cannabinoid mass in the distillate												
THC	5	4081.59	816.32	7	194.03	27.72	29.45	0.0001*	0.17	0.95	0.92	3.46
Total THC	5	4088.02	817.6	7	193.35	27.62	29.6	0.0001*	0.17	0.95	0.92	3.46
CBD	5	0.0075	0.0015	7	0.004	0.0006	2.56	0.1258	0.87	0.65	0.39	7.83
								(0.0102*)	(0.85)			
Total CBD	5	0.0075	0.0015	7	0.004	0.0006	2.56	0.1258	0.87	0.65	0.39	7.83
								(0.0102*)	(0.85)			
CBG	5	6.407	1.28	7	0.309	0.044	29.05	0.0002*	0.24	0.95	0.92	4.18
CBC	5	0.208	0.041	7	0.009	0.0013	32.66	0.0001*	0.39	0.96	0.93	3.3
CBN	5	0.1003	0.02	7	0.008	0.0012	16.44	0.0010*	0.0129*	0.92	0.86	5.38
Cannabinoid mass in the residue												
THC	5	3616.42	723.28	7	68.63	9.8	73.77	<0.0001*	0.81	0.98	0.97	5.63
Total THC	5	3630.45	726.1	7	67.75	9.68	75.02	<0.0001*	0.82	0.98	0.97	5.63
CBDA	5	0.0155	0.003	7	0.011	0.002	1.89	0.21	0.86	0.57	0.27	14.76
								(0.27)	(0.88)			
Total CBD	5	0.0104	0.0021	7	0.01	0.0014	1.47	0.31	0.85	0.51	0.16	15.59
								(0.31)	(0.91)			
CBG	5	6.078	1.215	7	0.186	0.026	45.77	<0.0001*	0.86	0.97	0.95	6.5

CBC	5	0.115	0.023	7	0.002	0.0003	84.65	<0.001*	0.13	0.98	0.97	6.13
CBN	5	0.087	0.017	7	0.0032	0.0005	36.37	<0.0001*	0.43	0.96	0.94	7.44
Recovery efficiency of cannabinoids in the distillate												
THC	5	1170.89	234.178	7	55.599	7.943	29.48	0.0001*	0.17	0.95	0.92	3.47
Total THC	5	1172.42	234.48	7	55.44	7.92	29.6	0.0001*	0.17	0.95	0.92	3.46
CBD	5	960.24	192.048	7	403.1196	57.589	3.335	0.074	0.88	0.70	0.49	6.83
								(0.0054*)	(0.79)			
Total CBD	5	286.02	57.205	7	120.018	17.145	3.34	0.074	0.88	0.70	0.49	6.83
								(0.0054*)	(0.79)			
CBG	5	1358.81	271.762	7	64.4297	9.204	29.53	0.0001*	0.24	0.95	0.92	4.14
CBC	5	1512.14	302.428	7	61.169	8.738	34.6	<0.0001*	0.51	0.96	0.93	3.17
CBN	5	1416.25	283.25	7	134.5396	19.22	14.74	0.0013*	0.0099*	0.91	0.85	5.68

Effects are statistically significant if  $p$  value  $* < 0.05$ .  $p$ -values for ANOVA and Lack-of-fit for the revised model B only has FFR as an independent parameter.  $df$ : Degrees of freedom; SS: Sum of squares; MS: Mean square;  $F$ -ratio: Fisher ratio; and Prob: Probability.

### **5.3.7 Actual and predicted plots**

Actual (experimental) values were plotted against predicted values to validate the model for the three experimental responses, namely cannabinoid mass in the distillate and residue, as well as the recovery efficiency of cannabinoids in the distillate (Figures A.1, A.2, and A.3, in Appendix). Actual experimental points for THC, total THC, CBG, CBC, and CBN, were within the range of predicted data points for the three experimental responses. This closeness suggests the suitability of the predicted model. Actual data points for the recovery efficiency of CBD in distillate (Figure A.3D) and total CBD for the three experimental responses (Figures A.1C, A.2C, A.3C) are not in the predicted zone, demonstrating that the model does not fit for these particular cannabinoids.

### **5.3.8 Verification of model**

An experiment with an optimal FFR of 35 Hz ( $41.6 \text{ mL min}^{-1}$ ) and an ICT of  $75^\circ\text{C}$  was conducted to verify the model. Under these conditions, corresponding experimental values for cannabinoid mass (g) in the distillate and residue, as well as recovery efficiency (%) in the distillate, were determined after WFSP molecular distillation of decarboxylated cannabis oil. Experimental values were in agreement with the predicted values, and a strong correlation from 0.85 to 0.92 was obtained, proving that this model is suitable for increasing cannabinoid mass (g) and recovery efficiency (%) in the distillate and reducing cannabinoid mass (g) in the residue of the second cut during WFSP molecular distillation.

## **5.4 Discussion**

### **5.4.1 Terpene cut**

WFSP molecular distillation is a two-stage process that involves the distillation of terpenes followed by cannabinoids. Licensed producers of cannabis products conventionally remove terpenes from the crude cannabis oil before cannabinoid distillation to produce a cannabinoid-rich oil. Operating conditions during the first (terpene) cut likely caused thermal decarboxylation of THCA, resulting in increased THC concentration in the residue of the first (terpene) cut compared to the feed. Future research must be conducted to investigate the effects of the distillation parameters on cannabinoid biosynthesis and optimize terpene distillation to decrease THC concentrations in the terpene distillate.

### 5.4.2 Cannabinoid cut (second cut)

FFR was determined as the most critical parameter affecting molecular distillation, and data collected in this study support this finding. This was because a reduced FFR increases the retention time of the biomass on the evaporator surface of a distillation system, which improves the evaporation of the desired metabolites. During second cut distillation, decarboxylation of acidic cannabinoids was observed which was evident by low concentrations of THCA and CBDA compared with the feed of second cut (residue of the first cut). Decarboxylation of THC to CBN was observed while decreasing the FFR.

Various studies have explored the effect of FFR on the distillate yield and reported similar results. Decreasing FFR from 15 to 5 ml min<sup>-1</sup> at 200 °C resulted in a 67.8 % increase of monoglycerides in distillate per feed (Fregolente et al., 2007b), and increased FFR for soybean (*Glycine max*) oil from 1.87 to 10.57 g min<sup>-1</sup> and reduced the tocopherol concentration in the distillate by 70.6 % (Martins et al., 2006). One study on the molecular distillation of tocotrienols from palm fatty acid distillates showed that yield (g) of free fatty acids (FFA) in the distillate was increased by 3.6 % when FFR was decreased from 0.25 kg h<sup>-1</sup> to 0.1 kg h<sup>-1</sup> at 130 °C (Posada et al., 2007).

Recovery efficiency reported herein are supportive of a comparable study, where the deacidification rate (%) in low-calorie cocoa (*Theobroma cacao*) butter increased by 4.9 % with a decrease in FFR from 3 mL min<sup>-1</sup> to 1 mL min<sup>-1</sup> at 180 °C and 2 Pa (Wu et al., 2012). The recovery efficiencies of tocopherol from rapeseed (*Brassica napus*) oil was increased by 3.3 % when FFR was decreased from 150 mL min<sup>-1</sup> to 30 mL min<sup>-1</sup> using an evaporator temperature and wiper rolling speed of 473 °C and 50 rpm, respectively (Shao et al., 2007). One study conducted to improve the purification of benzene from volatile waste gas reported that average recovery efficiency of benzene was increased from 70.8 % to 90.2 % when inlet flow rate was decreased to 50 mL min<sup>-1</sup> from 100 mL min<sup>-1</sup> by using 1 % KOH-AC (coconut shell activated-carbon modified by 1 % KOH) (Deng et al., 2021). Recovery efficiencies higher than 100 % can be explained by the formation of neutral cannabinoids acidic cannabinoids during the cannabinoid molecular distillation process.

When enriching patchoulol from patchouli (*Pogostemon cablin*) with molecular distillation, one study reported that decreasing ICT did not affect the distilled yield (67.8 % at 15 °C to 69.8 % at 5 °C) at the constant evaporator temperature (70 °C) and wiper speed (200 rpm)

(Dantas et al., 2020). When using wiped-film molecular distillation to refine CBD from hemp extracts with high concentration and maximum recovery, where evaporator temperature and pressure were significant and at 170 °C and 40 Pa, the CBD concentration and recovery achieved were high with 80.19 % mass and 92.66 % mass, respectively. CBD concentration was not significantly affected by the ICT when it was increased from -10 °C (45.63 % mass dry matter) to 50 °C (48.54 % mass dry matter) at an evaporator temperature and pressure of 110 °C and 220 Pa, respectively (Valizadehderakhshan et al., 2022a).

## **5.5 Conclusion**

This study optimized the operating parameters, including FFR and ICT, for WFSP molecular distillation system using RSM. Among the different experimental conditions tested, the optimal setting includes an FFR of 35 Hz (41.6 mL min<sup>-1</sup>) and ICT of 75 °C. Although ICT did not play a significant role within the range of the tested parameters, reducing the FFR maximizes the cannabinoid mass and recovery in the distillate. At the same time, it minimizes the cannabinoid mass in the residue of the second cut. Furthermore, varying the FFR influences the distillation time, but the quality of cannabinoids remains unaffected. An increase in THC concentration was observed during the distillation process but was not limited to decarboxylation/conversion of THCA, CBGA, and CBG. Future research must be done to reduce the cannabinoid mass in the terpene distillate of the first cut.



## 5.6 References

- Amini, M., Younesi, H., Bahramifar, N., 2009. Statistical modeling and optimization of the cadmium biosorption process in an aqueous solution using *Aspergillus niger*. *Colloids Surf. Physicochem. Eng. Aspects* 337, 67-73. <https://doi.org/10.1016/j.colsurfa.2008.11.053>.
- Bajpai, S., Gupta, S., Dey, A., Jha, M., Bajpai, V., Joshi, S., Gupta, A., 2012. Application of central composite design approach for removal of chromium (VI) from aqueous solution using weakly anionic resin: modeling, optimization, and study of interactive variables. *J. Hazard. Mater.* 227, 436-444. <https://doi.org/10.1016/j.jhazmat.2012.05.016>.
- Benelli, G., Pavela, R., Petrelli, R., Cappellacci, L., Santini, G., Fiorini, D., Sut, S., Dall'Acqua, S., Canale, A., Maggi, F., 2018. The essential oil from industrial hemp (*Cannabis sativa* L.) by-products as an effective tool for insect pest management in organic crops. *Ind. Crops Prod.* 122, 308-315. <https://doi.org/10.1016/j.indcrop.2018.05.032>.
- Callado, C.S.-C., Núñez-Sánchez, N., Casano, S., Ferreiro-Vera, C., 2018. The potential of near infrared spectroscopy to estimate the content of cannabinoids in *Cannabis sativa* L.: A comparative study. *Talanta* 190, 147-157. <https://doi.org/10.1016/j.talanta.2018.07.085>.
- Calzolari, D., Magagnini, G., Lucini, L., Grassi, G., Appendino, G., Amaducci, S., 2017. High added-value compounds from *Cannabis* threshing residues. *Ind. Crops Prod.* 108, 558-563. <https://doi.org/10.1016/j.indcrop.2017.06.063>.
- Chen, Z., Zhang, Z., Zhou, J., Chen, H., Li, C., Li, X., Li, H., Gao, X., 2021. Efficient synthesis of isobutylene dimerization by catalytic distillation with advanced heat-integrated technology. *Ind. Eng. Chem. Res.* 60, 6121-6136. <https://doi.org/10.1021/acs.iecr.1c00945>.
- Dantas, T., Cabral, T., Neto, A.D., Moura, M., 2020. Enrichment of patchoulol extracted from patchouli (*Pogostemon cablin*) oil by molecular distillation using response surface and artificial neural network models. *J. Ind. Eng. Chem.* 81, 219-227. <https://doi.org/10.1016/j.jiec.2019.09.011>.
- Demim, S., Drouiche, N., Aouabed, A., Benayad, T., Dendene-Badache, O., Semsari, S., 2013. Cadmium and nickel: Assessment of the physiological effects and heavy metal removal using a response surface approach by L. gibba. *Ecol. Eng.* 61, 426-435. <https://doi.org/10.1016/j.ecoleng.2013.10.016>.

Deng, Z., Deng, Q., Wang, L., Xiang, P., Lin, J., Murugadoss, V., Song, G., 2021. Modifying coconut shell activated carbon for improved purification of benzene from volatile organic waste gas. *Adv. Compos. Hybrid Mater.* 4, 751-760. <https://doi.org/10.1007/s42114-021-00273-6>.

ElSohly, M.A., Slade, D., 2005. Chemical constituents of marijuana: the complex mixture of natural cannabinoids. *Life Sci.* 78, 539-548. <https://doi.org/10.1016/j.lfs.2005.09.011>.

Flores-Sanchez, I.J., Verpoorte, R., 2008. Secondary metabolism in cannabis. *Phytochem. Rev.* 7, 615-639. <https://doi.org/10.1007/s11101-008-9094-4>.

Fregolente, L.V., Fregolente, P.B.L., Chicuta, A., Batistella, C., Maciel Filho, R., Wolf-Maciel, M., 2007. Effect of operating conditions on the concentration of monoglycerides using molecular distillation. *Chem. Eng. Res. Des.* 85, 1524-1528. <https://doi.org/10.1205/cherd07024>.

Happyana, N., Kayser, O., 2016. Monitoring metabolite profiles of *Cannabis sativa* L. trichomes during flowering period using <sup>1</sup>H NMR-based metabolomics and real-time PCR. *Planta Med.* 82, 1217-1223. <https://doi.org/10.1055/s-0042-108058>.

Hartsel, J.A., Eades, J., Hickory, B., Makriyannis, A., 2016. *Cannabis sativa* and Hemp, *Nutraceuticals*. Elsevier, pp. 735-754. <https://doi.org/10.1016/B978-0-12-802147-7.00053-X>.

Kinsara, R.A., Demirbas, A., 2016. Upgrading of crude oil via distillation processes. *Pet. Sci. Technol.* 34, 1300-1306. <https://doi.org/10.1080/10916466.2016.1200080>.

Koo, N., Jo, H.-J., Lee, S.-H., Kim, J.-G., 2011. Using response surface methodology to assess the effects of iron and spent mushroom substrate on arsenic phytotoxicity in lettuce (*Lactuca sativa* L.). *J. Hazard. Mater.* 192, 381-387. <https://doi.org/10.1016/j.jhazmat.2011.05.032>.

Martins, P., Ito, V., Batistella, C., Maciel, M.W., 2006. Free fatty acid separation from vegetable oil deodorizer distillate using molecular distillation process. *Sep. Purif. Technol.* 48, 78-84. <https://doi.org/10.1016/j.seppur.2005.07.028>.

Martins, P.F., Carmona, C., Martinez, E.L., Sbaite, P., Maciel Filho, R., Maciel, M.R.W., 2012. Short path evaporation for methyl chavicol enrichment from basil essential oil. *Sep. Purif. Technol.* 87, 71-78. <https://doi.org/10.1016/j.seppur.2011.11.024>.

Micalizzi, G., Alibrando, F., Vento, F., Trovato, E., Zoccali, M., Guarnaccia, P., Dugo, P., Mondello, L., 2021. Development of a novel microwave distillation technique for the isolation of *Cannabis sativa* L. essential oil and gas chromatography analyses for the comprehensive characterization of terpenes and terpenoids, including their enantio-distribution. *Molecules* 26, 1588. <https://doi.org/10.3390/molecules26061588>.

Posada, L.R., Shi, J., Kakuda, Y., Xue, S.J., 2007. Extraction of tocotrienols from palm fatty acid distillates using molecular distillation. *Sep. Purif. Technol.* 57, 220-229.

<https://doi.org/10.1016/j.seppur.2007.04.016>.

Routray, W., Orsat, V., 2014. MAE of phenolic compounds from blueberry leaves and comparison with other extraction methods. *Ind. Crops Prod.* 58, 36-45.

<https://doi.org/10.1016/j.indcrop.2014.03.038>.

Shao, P., Jiang, S., Ying, Y., 2007. Optimization of molecular distillation for recovery of tocopherol from rapeseed oil deodorizer distillate using response surface and artificial neural network models. *Food Bioprod. Process.* 85, 85-92. <https://doi.org/10.1205/fbp06048>.

Valizadehderakhshan, M., Kazem-Rostami, M., Shahbazi, A., Azami, M., Bhowmik, A., Wang, L., 2022. Refining Cannabidiol Using Wiped-Film Molecular Distillation: Experimentation, Process Modeling, and Prediction. *Ind. Eng. Chem. Res.*

<https://doi.org/10.1021/acs.iecr.2c00290>.

Wu, W., Wang, C., Zheng, J., 2012. Optimization of deacidification of low-calorie cocoa butter by molecular distillation. *LWT--Food Sci. Technol.* 46, 563-570.

<https://doi.org/10.1016/j.lwt.2011.10.028>.

**Connecting text**

Chapters 3, 4, and 5 detailed the research conducted to enhance and optimize the postharvest processing of the cannabis plant. Chapter 6 provides a brief summary and discussion of the significant findings.

## Chapter 6: General discussion

This research project aimed to optimize and increase the efficiency of post-harvest handling operations by preserving the secondary metabolites of the cannabis plant. Preserving and extracting secondary metabolites is vital because of their advantageous health benefits such as anticancer, antifungal, analgesic, antimicrobial, anti-inflammatory, antiviral, and antiparasitic properties (Ojeda-Sana et al., 2013; Rufino et al., 2015).

The effects of particle size reduction [coarse (2-4 mm), medium (0.5-2 mm), fine (0.25–0.5 mm)] and extraction conditions, including solvent type (ethanol, butanol, hexane), and extraction temperature (–20 °C, 4 °C, RT), on the extraction yield and secondary metabolite concentration was evaluated. Results show that oil yield with ethanol extraction using finely (0.25 – 0.5 mm) ground biomass at 4°C and RT presented the highest oil yield with 28 % and 25.7 % extracted oil, respectively. Ethanol and butanol are highly effective in promoting a substantial oil yield from fine-sized particles compared to hexane, a non-polar solvent. For each solvent type, fine particles resulted in higher concentrations of THCA, CBGA, and THC. This is due to the fact that particle size reduction breaks the cell walls and increases the specific area (surface area-to-volume ratio), and the surface of smaller particles exposes larger specific areas to release more oil (del Valle and Uquiche, 2002). When comparing different solvents at the same temperature and particle size, ethanol extracted a higher concentration of total terpenes. The terpenes are predominantly polar in nature, making them more easily extractable by a polar solvent such as ethanol. The extraction temperature is not playing a significant ( $p > 0.05$ ) role in this extraction study. Following extraction, marked differences in color between extracts obtained with each solvent were observed. Extracts had a dark green, green, and yellow color for ethanol, butanol, and hexane extraction solvents, respectively. The difference in the color of extracts obtained with different solvents can be attributed to the affinity of the solvents for chlorophyll and its derivatives.

Optimizing the decarboxylation process could help improve cannabinoid yields and reduce handling costs for large-scale operations (Reason et al., 2022a). In this study, thermal decarboxylation of crude cannabis oil was investigated to optimize the temperature (95 °C to 155 °C) and time (0 to 180 min) parameters required for the efficient conversion of CBDA to CBD. Results indicate that at a lower temperature of 95 °C, the time required for the decarboxylation of

CBDA to CBD requires more than 180 min. The time needed for complete decarboxylation of CBDA was halved from 60 minutes at 115 °C to 30 minutes at 135 °C and 155 °C. This is due to the increased temperatures favour the faster decarboxylation reaction. Total CBD remained unchanged, suggesting that neither CBDA was converted to unknown cannabinoids nor CBD was lost by evaporation under all tested conditions. This may be explained by two factors; first, the vacuum eliminates oxygen during the experiment, preventing any possible oxidative degradation of CBD, and second, the studied low-temperature range prevented CBD from evaporating. Although CBGA was initially present in minimal amounts in the crude cannabis oil sample (<LOD), CBGA production was surprisingly observed after 60 min at 115 °C and 30 min at 135 °C and 155 °C.

The molecular distillation experiment was conducted to optimize the effects of operating parameters, including FFR (35 to 55 Hz) (41.6 to 71.3 mL min<sup>-1</sup>) and ICT (60 to 90 °C) on the mass and recovery of cannabinoids in the distillate and residue streams of second cut using decarboxylated crude cannabis oil. Results showed that ICT is not playing a significant effect in this study. Decreasing FFR from 59.1 Hz to 30.9 Hz at a constant ICT (75 °C) increased THC and total THC yield in the distillate by 30.3 % and 30.2 %, respectively and was decreased by 65.5 % and 65.4 %, respectively, in the residue. The recovery efficiency of THC significantly ( $p < 0.05$ ) increased by 30.16 % and 19 % when FFR decreased from 59.1 Hz to 45 Hz or 30.8 Hz, respectively, at a constant ICT (75 °C). Using CCRD, the optimal conditions of 35 Hz (41.6 mL min<sup>-1</sup>) for FFR and 75 °C for ICT were predicted, and the recovery efficiency of THC was 93.4 % in the distillate was observed under these conditions. This was because a reduced FFR increases the retention time of the biomass on the evaporator surface of a distillation system, which improves the evaporation of the desired metabolites. The reported findings contribute essential industry-relevant knowledge, to help optimize post-harvest handling and enhance process efficiencies for this regulated crop.

## **Chapter 7: Conclusion and future studies**

### **7.1 General conclusion**

This study evaluated the effects of particle size reduction, extraction, decarboxylation, and molecular distillation conditions on the secondary metabolite profile of cannabis. In doing so, particle size reduction of dried cannabis biomass was preserved and increased cannabinoid concentration during extraction. Extraction yield is positively correlated with a reduction in particle size. Optimal conditions for extracting the highest yield of crude cannabis oil with significant concentrations of THCA, CBGA, and total terpenes involve using finely ground biomass in ethanol at a temperature of 4 °C. This data may prove useful for feasible evaluation in an industrial setting to improve extraction and achieve the highest yield of crude cannabis oil containing significant concentrations of cannabinoids and terpenes. For decarboxylation, a total of 30 min was required for the complete conversion of CBDA to CBD at temperatures of 135 °C. Complete CBD decarboxylation was achieved while simultaneously preventing further CBD degradation losses with prolonged exposure at higher temperatures. The decarboxylation conditions reported provide information about the temperature and time period that may be useful to cannabis processing operations, but scale-up tests will be required. For the WFSP molecular distillation, reducing the FFR maximizes the cannabinoid mass and recovery in the distillate. At the same time, it minimizes the cannabinoid mass in the residue of the second cut. Optimal conditions of FFR of 35 Hz (41.6 mL min<sup>-1</sup>) and ICT of 75 °C were determined. Furthermore, varying the FFR influenced the distillation time, but the quality or concentration of cannabinoids remained unaffected. This study provides distillation conditions to be considered by the cannabis industry when aiming for a cannabinoid-rich distillate from the molecular distillation process without affecting cannabinoid quality.

## **7.2 Future suggested studies**

The following suggestions are developed based on the results obtained throughout the course of the research. Further knowledge is required on the:

1. Effect of micronization of cannabis biomass on the extraction yield and concentration of cannabinoids and terpenes.
2. Effects of increased temperature on the decarboxylation time and THC concentration during THCA decarboxylation. Evaluating and controlling the degradation of THC to CBN and could help understand the thermal stability of cannabinoids.
3. Optimization of operating parameters to reduce the cannabinoid mass in the distillate of terpene cut of the molecular distillation process.
4. Optimization and evaluation of the effects of operating parameters, including evaporator temperature and pressure, on the concentration of cannabinoids during the cannabinoid cut of the WFSP molecular distillation process.
5. Effects of evaporator temperature and pressure on the distillation of acidic cannabinoids using WFSP molecular distillation process.



## 8. Master Reference List

- Addo, P.W., Brousseau, V.D., Morello, V., MacPherson, S., Paris, M., Lefsrud, M., 2021. Cannabis chemistry, post-harvest processing methods and secondary metabolite profiling: A review. *Ind. Crops Prod.* 170, 113743. <https://doi.org/10.1016/j.indcrop.2021.113743>.
- Addo, P.W., Chauvin-Bossé, T., Taylor, N., MacPherson, S., Paris, M., Lefsrud, M., 2023a. Freeze-drying *Cannabis sativa* L. using real-time relative humidity monitoring and mathematical modeling for the cannabis industry. *Ind. Crops Prod.* 199, 116754. <https://doi.org/10.1016/j.indcrop.2023.116754>.
- Addo, P.W., Poudineh, Z., Shearer, M., Taylor, N., MacPherson, S., Raghavan, V., Orsat, V., Lefsrud, M., 2023b. Relationship between Total Antioxidant Capacity, Cannabinoids and Terpenoids in Hops and Cannabis. *Plants* 12, 1225. <https://doi.org/10.3390/plants12061225>.
- Addo, P. W., Sagili, S. U. K. R., Bilodeau, S. E., Gladu-Gallant, F.-A., MacKenzie, D. A., Bates, J., McRae, G., MacPherson, S., Paris, M., Raghavan, V., Orsat, V., Lefsrud, M. 2022. Cold Ethanol Extraction of Cannabinoids and Terpenes from Cannabis Using Response Surface Methodology: Optimization and Comparative Study. *Molecules*. 27 (24), 8780. <https://doi.org/10.3390/molecules27248780>.
- Addo, P.W., Sagili, S.U.K.R., Bilodeau, S.E., Gladu-Gallant, F.-A., MacKenzie, D.A., Bates, J., McRae, G., MacPherson, S., Paris, M., Raghavan, V., Orsat, V., Lefsrud, M., 2022b. Microwave-and ultrasound-assisted extraction of cannabinoids and terpenes from cannabis using response surface methodology. *Molecules* 27, 8803. <https://doi.org/10.3390/molecules27248803>.
- Addo, P.W., Taylor, N., MacPherson, S., Raghavan, V., Orsat, V., Lefsrud, M., 2022c. Impact of pre-freezing and microwaves on drying behavior and terpenes in hops (*Humulus lupulus*). *J. Appl. Res. Med. Aromat. Plants* 31, 100436. <https://doi.org/10.1016/j.jarmap.2022.100436>.
- Agarwal, C., Máthé, K., Hofmann, T., Csóka, L., 2018. Ultrasound-assisted extraction of cannabinoids from *Cannabis sativa* L. optimized by response surface methodology. *J. Food Sci.* 83, 700-710. <https://doi.org/10.1111/1750-3841.14075>.
- Aguiar, G.P.S., Arcari, B.D., Chaves, L.M., Dal Magro, C., Boschetto, D.L., Piato, A.L., Lanza, M., Oliveira, J.V., 2018. Micronization of trans-resveratrol by supercritical fluid: Dissolution, solubility and in vitro antioxidant activity. *Ind. Crops Prod.* 112, 1-5. <https://doi.org/10.1016/j.indcrop.2017.11.008>.

Aiello, G., Fasoli, E., Boschini, G., Lammi, C., Zanoni, C., Citterio, A., Arnoldi, A., 2016. Proteomic characterization of hempseed (*Cannabis sativa* L.). *J. Proteomics* 147, 187-196. <https://doi.org/10.1016/j.jprot.2016.05.033>.

Aizpurua-Olaizola, O., Soydaner, U., Öztürk, E., Schibano, D., Simsir, Y., Navarro, P., Etxebarria, N., Usobiaga, A., 2016. Evolution of the cannabinoid and terpene content during the growth of *Cannabis sativa* plants from different chemotypes. *J. Nat. Prod.* 79, 324-331. <https://doi.org/10.1021/acs.jnatprod.5b00949>.

Al Ubeed, H.M.S., Bhuyan, D.J., Alsherbiny, M.A., Basu, A., Vuong, Q.V., 2022. A comprehensive review on the techniques for extraction of bioactive compounds from medicinal cannabis. *Molecules* 27, 604. <https://doi.org/10.3390/molecules27030604>.

Alexandri, F., Papadopoulou, L., Tsolaki, A., Papantoniou, G., Athanasiadis, L., Tsolaki, M., 2023. The Effect of Cannabidiol 3% on Neuropsychiatric Symptoms in Dementia—Six-Month Follow-Up. *Clin. Gerontol.*, 1-8. <https://doi.org/10.1080/07317115.2023.2209563>.

Amini, M., Younesi, H., Bahramifar, N., 2009. Statistical modeling and optimization of the cadmium biosorption process in an aqueous solution using *Aspergillus niger*. *Colloids Surf. Physicochem. Eng. Aspects* 337, 67-73. <https://doi.org/10.1016/j.colsurfa.2008.11.053>.

Andre, C.M., Hausman, J.-F., Guerriero, G., 2016a. Cannabis sativa: the plant of the thousand and one molecules. *Frontiers in plant science* 7, 19. <https://doi.org/10.3389/fpls.2016.00019>.

Andre, C.M., Hausman, J.-F., Guerriero, G., 2016b. Cannabis sativa: the plant of the thousand and one molecules. *Front. Plant Sci.* 7, 19. <https://doi.org/10.3389/fpls.2016.00019>.

Appendino, G., Chianese, G., Tagliatela-Scafati, O., 2011. Cannabinoids: occurrence and medicinal chemistry. *Curr. Med. Chem.* 18, 1085-1099. <https://doi.org/10.2174/092986711794940888>.

Ashour, M., Wink, M., Gershenzon, J., 2018. Biochemistry of terpenoids: monoterpenes, sesquiterpenes and diterpenes. *Ann. Plant Rev.* 40, 258-303. <https://doi.org/10.1002/9781119312994.apr0427>.

Ashton, C.H., 2001. Pharmacology and effects of cannabis: a brief review. *Br. J. Psychiatry* 178, 101-106. <https://doi.org/10.1192/bjp.178.2.101>.

ASTM-WK84667. 2023. New Guide for Working with Ground Cannabis and Kief. [accessed 16 March 2023; Available from: <https://www.astm.org/workitem-wk84667>].

Atkins, P.L., 2019. Sample processing and preparation considerations for solid cannabis products. *J. AOAC Int.* 102, 427-433. <https://doi.org/10.5740/jaoacint.18-0203>.

Azmir, J., Zaidul, I.S.M., Rahman, M.M., Sharif, K., Mohamed, A., Sahena, F., Jahurul, M., Ghafoor, K., Norulaini, N., Omar, A., 2013. Techniques for extraction of bioactive compounds from plant materials: A review. *J. Food Eng.* 117, 426-436. <https://doi.org/10.1016/j.jfoodeng.2013.01.014>.

Badi, H.N., Yazdani, D., Ali, S.M., Nazari, F., 2004. Effects of spacing and harvesting time on herbage yield and quality/quantity of oil in thyme, *Thymus vulgaris* L. *Ind. Crops Prod.* 19, 231-236. <https://doi.org/10.1016/j.indcrop.2003.10.005>.

Bahji, A., Stephenson, C., 2019. International perspectives on the implications of cannabis legalization: a systematic review & thematic analysis. *Int. J. Environ. Res. Public Health.* 16, 3095. <https://doi.org/10.3390/ijerph16173095>.

Bajpai, S., Gupta, S., Dey, A., Jha, M., Bajpai, V., Joshi, S., Gupta, A., 2012. Application of central composite design approach for removal of chromium (VI) from aqueous solution using weakly anionic resin: modeling, optimization, and study of interactive variables. *J. Hazard. Mater.* 227, 436-444. <https://doi.org/10.1016/j.jhazmat.2012.05.016>.

Balasubramanian, S., Gupta, M.K., Singh, K., 2012. Cryogenics and its application with reference to spice grinding: a review. *Crit. Rev. Food Sci. Nutr.* 52, 781-794. <https://doi.org/10.1080/10408398.2010.509552>.

Bandini, S., Gostoli, C., Sarti, G., 1992. Separation efficiency in vacuum membrane distillation. *J. Membr. Sci.* 73, 217-229. [https://doi.org/10.1016/0376-7388\(92\)80131-3](https://doi.org/10.1016/0376-7388(92)80131-3).

Bantle, M., Kolsaker, K., Eikevik, T.M., 2011. Modification of the Weibull distribution for modeling atmospheric freeze-drying of food. *Drying Technol.* 29, 1161-1169. <https://doi.org/10.1080/07373937.2011.574242>.

Barbosa-Cánovas, G.V., Ortega-Rivas, E., Juliano, P., Yan, H., 2005. Food powders: physical properties, processing, and functionality. Springer. <https://doi.org/10.1007/0-387-27613-0>.

Batistella, C., Maciel, M.W., 1998. Recovery of carotenoids from palm oil by molecular distillation. *Comput. Chem. Eng.* 22, S53-S60. [https://doi.org/10.1016/S0098-1354\(98\)00038-6](https://doi.org/10.1016/S0098-1354(98)00038-6).

Batistella, C.B., Moraes, E., Filho, R.M., Maciel, M.W., 2002. Molecular distillation: rigorous modeling and simulation for recovering vitamin E from vegetal oils. *Biotechnology for Fuels and*

Chemicals: The Twenty–Third Symposium, 1187-1206. [https://doi.org/10.1007/978-1-4612-0119-9\\_96](https://doi.org/10.1007/978-1-4612-0119-9_96).

Battisti, R., Machado, R.A., Marangoni, C., 2020. A background review on falling film distillation in wetted-wall columns: from fundamentals towards intensified technologies. *Chem. Eng. Process.* 150, 107873. <https://doi.org/10.1016/j.cep.2020.107873>.

Bellik, F.-Z., Benkaci-Ali, F., Alsaфра, Z., Eppe, G., Tata, S., Sabaou, N., Zidani, R., 2019. Chemical composition, kinetic study and antimicrobial activity of essential oils from *Cymbopogon schoenanthus* L. Spreng extracted by conventional and microwave-assisted techniques using cryogenic grinding. *Ind. Crops Prod.* 139, 111505. <https://doi.org/10.1016/j.indcrop.2019.111505>.

Bender, A.B.B., Speroni, C.S., Moro, K.I.B., Morisso, F.D.P., dos Santos, D.R., da Silva, L.P., Penna, N.G., 2020. Effects of micronization on dietary fiber composition, physicochemical properties, phenolic compounds, and antioxidant capacity of grape pomace and its dietary fiber concentrate. *LWT-Food Sci. Technol.* 117, 108652. <https://doi.org/10.1016/j.lwt.2019.108652>.

Benelli, G., Pavela, R., Petrelli, R., Cappellacci, L., Santini, G., Fiorini, D., Sut, S., Dall'Acqua, S., Canale, A., Maggi, F., 2018. The essential oil from industrial hemp (*Cannabis sativa* L.) by-products as an effective tool for insect pest management in organic crops. *Ind. Crops Prod.* 122, 308-315. <https://doi.org/10.1016/j.indcrop.2018.05.032>.

Bethge, D., 2014. Short path and molecular distillation. *Vacuum Technol. Chem. Ind.*, 281-294. <https://doi.org/10.1002/9783527653898.ch15>.

Blake, A., Nahtigal, I. 2019. The evolving landscape of cannabis edibles. *Curr. Opin. Food Sci.* 28, 25-31. <https://doi.org/10.1016/j.cofs.2019.03.009>.

Blessing, E.M., Steenkamp, M.M., Manzanares, J., Marmar, C.R., 2015. Cannabidiol as a Potential Treatment for Anxiety Disorders. *Neurotherapeutics* 12, 825-36. <https://doi.org/10.1007/s13311-015-0387-1>.

Boggs, D.L., Surti, T., Gupta, A., Gupta, S., Niciu, M., Pittman, B., Schnakenberg Martin, A.M., Thurnauer, H., Davies, A., D'Souza, D.C., 2018. The effects of cannabidiol (CBD) on cognition and symptoms in outpatients with chronic schizophrenia a randomized placebo controlled trial. *Psychopharmacology* 235, 1923-1932. <https://doi.org/10.1007/s00213-018-4885-9>.

Booth, J. K., Bohlmann, J. 2019. Terpenes in *Cannabis sativa*—From plant genome to humans. *Plant Sci.* 284, 67-72. <https://doi.org/10.1016/j.plantsci.2019.03.022>.

- Booth, J.K., Page, J.E., Bohlmann, J., 2017. Terpene synthases from *Cannabis sativa*. Plos one 12, e0173911. <https://doi.org/10.1371/journal.pone.0173911>.
- Brighenti, V., Pellati, F., Steinbach, M., Maran, D., Benvenuti, S., 2017. Development of a new extraction technique and HPLC method for the analysis of non-psychoactive cannabinoids in fibre-type *Cannabis sativa* L.(hemp). J. Pharm. Biomed. Anal. 143, 228-236. <https://doi.org/10.1016/j.jpba.2017.05.049>.
- Bu, X., Chen, Y., Ma, G., Sun, Y., Ni, C., Xie, G., 2020. Wet and dry grinding of coal in a laboratory-scale ball mill: Particle-size distributions. Powder Technol. 359, 305-313. <https://doi.org/10.1016/j.powtec.2019.09.062>.
- Callado, C.S.-C., Núñez-Sánchez, N., Casano, S., Ferreiro-Vera, C., 2018. The potential of near infrared spectroscopy to estimate the content of cannabinoids in *Cannabis sativa* L.: A comparative study. Talanta 190, 147-157. <https://doi.org/10.1016/j.talanta.2018.07.085>.
- Calzolari, D., Magagnini, G., Lucini, L., Grassi, G., Appendino, G., Amaducci, S., 2017. High added-value compounds from *Cannabis* threshing residues. Ind. Crops Prod. 108, 558-563. <https://doi.org/10.1016/j.indcrop.2017.06.063>.
- Cao, X., Zhang, F., Zhao, D., Zhu, D., Li, J., 2018. Effects of freezing conditions on quality changes in blueberries. J. Sci. Food Agric. 98, 4673-4679. <https://doi.org/10.1002/jsfa.9000>.
- Challa, S.K.R., Misra, N., Martynenko, A., 2021. Drying of cannabis—State of the practices and future needs. Dry. Technol. 39, 2055-2064. <https://doi.org/10.1080/07373937.2020.1752230>.
- Chandra, S., Lata, H., Khan, I.A., ElSohly, M.A., 2017. *Cannabis sativa* L.: botany and horticulture. *Cannabis sativa* L. Bot. Biotechnol., 79-100. [https://doi.org/10.1007/978-3-319-54564-6\\_3](https://doi.org/10.1007/978-3-319-54564-6_3).
- Chandra, S., Lata, H., ElSohly, M. A., Potter, D., 2017. Cannabis cultivation: methodological issues for obtaining medical-grade product. Epilepsy Behav. 70, 302-312. <https://doi.org/10.1016/j.yebeh.2016.11.029>
- Chandrasekaran, S., Ramanathan, S., Basak, T., 2013. Microwave food processing—A review. Food Res. Int. 52, 243-261. <https://doi.org/10.1016/j.foodres.2013.02.033>.
- Chang, C.-W., Yen, C.-C., Wu, M.-T., Hsu, M.-C., Wu, Y.-T., 2017. Microwave-assisted extraction of cannabinoids in hemp nut using response surface methodology: Optimization and comparative study. Molecules 22, 1894. <https://doi.org/10.3390/molecules22111894>.

Chasiotis, V., Tsakirakis, A., Termentzi, A., Machera, K., Filios, A., 2022. Drying and quality characteristics of *Cannabis sativa* L. inflorescences under constant and time-varying convective drying temperature schemes. *Therm. Sci. Eng. Prog.* 28, 101076.  
<https://doi.org/10.1016/j.tsep.2021.101076>.

Chen, C., Pan, Z., 2021. Cannabidiol and terpenes from hemp—ingredients for future foods and processing technologies. *J. Future Foods* 1, 113-127. <https://doi.org/10.1093/annweh/wxaa013>.

Chen, T., Zhang, M., Bhandari, B., Yang, Z., 2018. Micronization and nanosizing of particles for an enhanced quality of food: A review. *Crit. Rev. Food Sci. Nutr.* 58, 993-1001.  
<https://doi.org/10.1080/10408398.2016.1236238>.

Chen, Z., Zhang, Z., Zhou, J., Chen, H., Li, C., Li, X., Li, H., Gao, X., 2021. Efficient synthesis of isobutylene dimerization by catalytic distillation with advanced heat-integrated technology. *Ind. Eng. Chem. Res.* 60, 6121-6136. <https://doi.org/10.1021/acs.iecr.1c00945>.

Citti, C., Pacchetti, B., Vandelli, M.A., Forni, F., Cannazza, G., 2018. Analysis of cannabinoids in commercial hemp seed oil and decarboxylation kinetics studies of cannabidiolic acid (CBDA). *J. Pharm. Biomed. Anal.* 149, 532-540. <https://doi.org/10.1016/j.jpba.2017.11.044>.

Couch, J.R., Grimes, G.R., Green, B.J., Wiegand, D.M., King, B., Methner, M.M., 2020. Review of NIOSH cannabis-related health hazard evaluations and research. *Annals of work exposures and health* 64, 693-704. <https://doi.org/10.1093/annweh/wxaa013>.

Cvengroš, J., Lutišan, J., Micov, M., 2000. Feed temperature influence on the efficiency of a molecular evaporator. *Chem. Eng. J.* 78, 61-67. [https://doi.org/10.1016/S1385-8947\(99\)00159-X](https://doi.org/10.1016/S1385-8947(99)00159-X).

Cvengroš, J., Pollák, Š., Micov, M., Lutišan, J., 2001. Film wiping in the molecular evaporator. *Chem. Eng. J.* 81, 9-14. [https://doi.org/10.1016/S1385-8947\(00\)00195-9](https://doi.org/10.1016/S1385-8947(00)00195-9).

Dantas, T., Cabral, T., Neto, A.D., Moura, M., 2020. Enrichment of patchoulol extracted from patchouli (*Pogostemon cablin*) oil by molecular distillation using response surface and artificial neural network models. *J. Ind. Eng. Chem.* 81, 219-227.  
<https://doi.org/https://doi.org/10.1016/j.jiec.2019.09.011>.

Dariš, B., Verboten, M.T., Knez, Ž., Ferk, P., 2019. Cannabinoids in cancer treatment: Therapeutic potential and legislation. *Bosn. J. Basic Med. Sci.* 19, 14.  
<https://doi.org/10.17305/bjbms.2018.3532>.

- Das, P.C., Vista, A.R., Tabil, L.G., Baik, O.-D., 2022. Postharvest operations of cannabis and their effect on cannabinoid content: a review. *Bioengineering* 9, 364.  
<https://doi.org/10.3390/bioengineering9080364>.
- De Backer, B., Maebe, K., Verstraete, A.G., Charlier, C., 2012. Evolution of the content of THC and other major cannabinoids in drug-type cannabis cuttings and seedlings during growth of plants. *J. Forensic Sci.* 57, 918-922. <https://doi.org/10.1111/j.1556-4029.2012.02068.x>.
- De Meijer, E.P., 2014. The chemical phenotypes (chemotypes) of Cannabis. *Handbook of cannabis* 89, 110.
- del Valle, J.M., Uquiche, E.L., 2002. Particle size effects on supercritical CO<sub>2</sub> extraction of oil-containing seeds. *J. Am. Oil Chem. Soc.* 79, 1261-1266. <https://doi.org/10.1007/s11746-002-0637-9>.
- Demim, S., Drouiche, N., Aouabed, A., Benayad, T., Dendene-Badache, O., Semsari, S., 2013. Cadmium and nickel: Assessment of the physiological effects and heavy metal removal using a response surface approach by *L. gibba*. *Ecol. Eng.* 61, 426-435.  
<https://doi.org/10.1016/j.ecoleng.2013.10.016>.
- Deng, Z., Deng, Q., Wang, L., Xiang, P., Lin, J., Murugadoss, V., Song, G., 2021. Modifying coconut shell activated carbon for improved purification of benzene from volatile organic waste gas. *Adv. Compos. Hybrid Mater.* 4, 751-760. <https://doi.org/https://doi.org/10.1007/s42114-021-00273-6>.
- Desaulniers Brousseau, V., Wu, B.-S., MacPherson, S., Morello, V., Lefsrud, M., 2021. Cannabinoids and terpenes: how production of photo-protectants can be manipulated to enhance *Cannabis sativa* L. phytochemistry. *Front. Plant Sci.* 12, 620021.  
<https://doi.org/10.3389/fpls.2021.620021>.
- Dhiman, A., Prabhakar, P.K., 2021. Micronization in food processing: A comprehensive review of mechanistic approach, physicochemical, functional properties and self-stability of micronized food materials. *J. Food Eng.* 292, 110248. <https://doi.org/10.1016/j.jfoodeng.2020.110248>.
- Dussy, F.E., Hamberg, C., Luginbühl, M., Schwerzmann, T., Briellmann, T.A., 2005. Isolation of  $\Delta^9$ -THCA-A from hemp and analytical aspects concerning the determination of  $\Delta^9$ -THC in cannabis products. *Forensic science international* 149, 3-10.  
<https://doi.org/https://doi.org/10.1016/j.forsciint.2004.05.015>.
- Eckles, A., Benz, P., Fine, S., 1991. When to use high-vacuum distillation. *Chem. Eng.* 98, 201.



Eichhorn Bilodeau, S., Wu, B.-S., Rufyikiri, A.-S., MacPherson, S., Lefsrud, M., 2019. An update on plant photobiology and implications for cannabis production. *Front. Plant Sci.* 10, 296. <https://doi.org/10.3389/fpls.2019.00296>.

Elsaid, S., Kloiber, S., Le Foll, B., 2019. Effects of cannabidiol (CBD) in neuropsychiatric disorders: A review of pre-clinical and clinical findings. *Prog. Mol. Biol. Transl. Sci.* 167, 25-75. <https://doi.org/10.1016/bs.pmbts.2019.06.005>.

ElSohly, M.A., Slade, D., 2005. Chemical constituents of marijuana: the complex mixture of natural cannabinoids. *Life Sci.* 78, 539-548. <https://doi.org/10.1016/j.lfs.2005.09.011>.

Elzinga, S., Ortiz, O., Raber, J.C., 2015. The conversion and transfer of cannabinoids from cannabis to smoke stream in cigarettes. *Nat Prod Chem Res.* <https://doi.org/10.4172/2329-6836.1000163>.

Englund, A., Morrison, P.D., Nottage, J., Hague, D., Kane, F., Bonaccorso, S., Stone, J.M., Reichenberg, A., Brenneisen, R., Holt, D., 2013. Cannabidiol inhibits THC-elicited paranoid symptoms and hippocampal-dependent memory impairment. *J. Psychopharmacol.* 27, 19-27. <https://doi.org/10.1177/0269881112460109>.

Esmailzadeh Kenari, R., Dehghan, B., 2020. Optimization of ultrasound-assisted solvent extraction of hemp (*Cannabis sativa* L.) seed oil using RSM: Evaluation of oxidative stability and physicochemical properties of oil. *Food Sci. Nutr.* 8, 4976-4986. <https://doi.org/10.1002/fsn3.1796>.

Espínola, F., Moya, M., Fernández, D.G., Castro, E., 2009. Improved extraction of virgin olive oil using calcium carbonate as coadjuvant extractant. *J. Food Eng.* 92, 112-118. <https://doi.org/10.1016/j.jfoodeng.2008.10.038>.

Evans, F.J., 1991. Cannabinoids: the separation of central from peripheral effects on a structural basis. *Planta Med.* 57, S60-S67. <https://doi.org/10.1055/s-2006-960231>.

Fellermeier, M., Zenk, M.H., 1998. Prenylation of olivetolate by a hemp transferase yields cannabigerolic acid, the precursor of tetrahydrocannabinol. *FEBS Lett.* 427, 283-285. [https://doi.org/10.1016/S0014-5793\(98\)00450-5](https://doi.org/10.1016/S0014-5793(98)00450-5).

Ferber, S.G., Namdar, D., Hen-Shoval, D., Eger, G., Koltai, H., Shoval, G., Shbiro, L., Weller, A., 2020. The “entourage effect”: terpenes coupled with cannabinoids for the treatment of mood disorders and anxiety disorders. *Curr. Neuropharmacol.* 18, 87-96. <https://doi.org/10.2174/1570159X17666190903103923>.



Fetterman, P.S., Keith, E.S., Waller, C.W., Guerrero, O., Doorenbos, N.J., Quimby, M.W., 1971. Mississippi-grown *Cannabis sativa* L.: Preliminary observation on chemical definition of phenotype and variations in tetrahydrocannabinol content versus age, sex, and plant part. *J. Pharm. Sci.* 60, 1246-1249. <https://doi.org/10.1002/jps.2600600832>.

Fischedick, J.T., 2017. Identification of terpenoid chemotypes among high (–)-trans- $\Delta^9$ -tetrahydrocannabinol-producing *Cannabis sativa* L. cultivars. *Cannabis Cannabinoid Res.* 2, 34-47. <https://doi.org/10.1089/can.2016.0040>.

Flores-Sanchez, I.J., Verpoorte, R., 2008. Secondary metabolism in cannabis. *Phytochemistry reviews* 7, 615-639.

Forester, B., Lanctôt, K., Mintzer, J., Rosenberg, P., 2022. Cannabinoids and Psychedelics for Neuropsychiatric Symptoms of Alzheimer's: Addressing Disparities Through Clinical Trials. *Am. J. Geriatr. Psychiatry.* 30, S7. <https://doi.org/10.1016/j.jagp.2022.01.261>.

Fregolente, L.V., Fregolente, P.B.L., Chicuta, A., Batistella, C., Maciel Filho, R., Wolf-Maciel, M., 2007a. Effect of operating conditions on the concentration of monoglycerides using molecular distillation. *Chem. Eng. Res. Des.* 85, 1524-1528. <https://doi.org/10.1205/cherd07024>.

Fregolente, L.V., Fregolente, P.B.L., Chicuta, A., Batistella, C., Maciel Filho, R., Wolf-Maciel, M., 2007b. Effect of operating conditions on the concentration of monoglycerides using molecular distillation. *Chem. Eng. Res. Des.* 85, 1524-1528. <https://doi.org/10.1205/cherd07024>.

Friesen, L., 2020. To Grind or Not To Grind. *Cannabis Science and Technology*. [accessed 19 March 2023]; Available from: <https://www.cannabissciencetech.com/view/to-grind-or-not-to-grind>.

Gagne, S.J., Stout, J.M., Liu, E., Boubakir, Z., Clark, S.M., Page, J.E., 2012. Identification of olivetolic acid cyclase from *Cannabis sativa* reveals a unique catalytic route to plant polyketides. *Proc. Natl. Acad. Sci. U.S.A.* 109, 12811-12816. <https://doi.org/10.1073/pnas.1200330109>.

García-Fajardo, J.A., Flores-Méndez, D.A., Suárez-Jacobo, Á., Torres-Martínez, L.G., Granados-Vallejo, M., Corona-González, R.I., Guatemala-Morales, G.M., Arriola-Guevara, E., 2023. Separation of D-Limonene and Other Oxygenated Compounds from Orange Essential Oil by Molecular Distillation and Fractional Distillation with a Wiped Film Evaporator. *Processes* 11, 991. <https://doi.org/10.3390/pr11040991>.

Goswami, T., Singh, M., 2003. Role of feed rate and temperature in attrition grinding of cumin. *J. Food Eng.* 59, 285-290. [https://doi.org/10.1016/S0260-8774\(02\)00469-7](https://doi.org/10.1016/S0260-8774(02)00469-7).

Grijo, D.R., Bidoia, D.L., Nakamura, C.V., Osorio, I.V., Cardozo-Filho, L., 2019. Analysis of the antitumor activity of bioactive compounds of Cannabis flowers extracted by green solvents. *The Journal of Supercritical Fluids* 149, 20-25.

Grijó, D.R., Osorio, I.A.V., Cardozo-Filho, L., 2018. Supercritical extraction strategies using CO<sub>2</sub> and ethanol to obtain cannabinoid compounds from Cannabis hybrid flowers. *Journal of CO<sub>2</sub> Utilization* 28, 174-180.

Gupta, A., Soni, R., Ganguli, M., 2021. Frostbite—manifestation and mitigation. *Burns Open* 5, 96-103. <https://doi.org/10.1016/j.burnso.2021.04.002>.

Halim, R., Gladman, B., Danquah, M.K., Webley, P.A., 2011. Oil extraction from microalgae for biodiesel production. *Bioresour. Technol.* 102, 178-185. <https://doi.org/10.1016/j.biortech.2010.06.136>.

Hammond, C.T., Mahlberg, P.G., 1977. Morphogenesis of capitate glandular hairs of Cannabis sativa (Cannabaceae). *Am. J. Bot.* 64, 1023-1031. <https://doi.org/10.1002/j.1537-2197.1977.tb11948.x>.

Hampson, A., Grimaldi, M., Axelrod, J., Wink, D., 1998. Cannabidiol and (–)  $\Delta^9$ -tetrahydrocannabinol are neuroprotective antioxidants. *Proc. Natl. Acad. Sci. U.S.A.* 95, 8268-8273. <https://doi.org/10.1073/pnas.95.14.8268>.

Hanuš, L.O., Meyer, S.M., Muñoz, E., Tagliatela-Scafati, O., Appendino, G., 2016. Phytocannabinoids: a unified critical inventory. *Nat. Prod. Rep.* 33, 1357-1392. <https://doi.org/10.1039/C6NP00074F>.

Happyana, N., Kayser, O., 2016. Monitoring metabolite profiles of Cannabis sativa L. trichomes during flowering period using <sup>1</sup>H NMR-based metabolomics and real-time PCR. *Planta Med.* 82, 1217-1223. <https://doi.org/10.1055/s-0042-108058>.

Hartsel, J.A., Eades, J., Hickory, B., Makriyannis, A., 2016. Cannabis sativa and Hemp, *Nutraceuticals*. Elsevier, pp. 735-754. <https://doi.org/10.1016/B978-0-12-802147-7.00053-X>.

Hashemi, B., Shiri, F., Švec, F., Nováková, L., 2022. Green solvents and approaches recently applied for extraction of natural bioactive compounds. *TrAC-Trend Anal. Chem.*, 116732. <https://doi.org/10.1016/j.trac.2022.116732>.

Hawes, M.D., Cohen, M.R., 2015. Method of drying cannabis materials. Google Patents.

Heikal, A.A.-E.M., 2017. Variation in the essential oil content and its composition in *Eucalyptus cinerea* leaves and its relation to some environmental factors. *J. Essent. Oil Bear. Plants.* 20, 995-1005. <https://doi.org/10.1080/0972060X.2017.1351896>.

Hemery, Y., Chaurand, M., Holopainen, U., Lampi, A.-M., Lehtinen, P., Piironen, V., Sadoudi, A., Rouau, X., 2011. Potential of dry fractionation of wheat bran for the development of food ingredients, part I: Influence of ultra-fine grinding. *J. Cereal Sci.* 53, 1-8. <https://doi.org/10.1016/j.jcs.2010.09.005>.

Hidalgo, P., Ciudad, G., Navia, R., 2016. Evaluation of different solvent mixtures in esterifiable lipids extraction from microalgae *Botryococcus braunii* for biodiesel production. *Bioresour. Technol.* 201, 360-364. <https://doi.org/10.1016/j.biortech.2015.11.031>.

Hollo, J., Kurucz, E., Borodi, A., 1971. Applications of molecular distillation. <https://agris.fao.org/agris-search/search.do?recordID=US201300483121>.

Hu, J., Chen, Y., Ni, D., 2012. Effect of superfine grinding on quality and antioxidant property of fine green tea powders. *LWT-Food Sci. Technol.* 45, 8-12. <https://doi.org/10.1016/j.lwt.2011.08.002>.

Hunter, W.N., 2007. The non-mevalonate pathway of isoprenoid precursor biosynthesis. *J. Biol. Chem.* 282, 21573-21577. <https://doi.org/10.1074/jbc.R700005200>.

Jin, D., Dai, K., Xie, Z., Chen, J., 2020. Secondary metabolites profiled in cannabis inflorescences, leaves, stem barks, and roots for medicinal purposes. *Sci. Rep.* 10, 1-14. <https://doi.org/10.1038/s41598-020-60172-6>.

Jin, D., Jin, S., Chen, J., 2019. Cannabis indoor growing conditions, management practices, and post-harvest treatment: a review. *Am. J. Plant Sci.* 10, 925. <https://doi.org/10.4236/ajps.2019.106067>.

Joshi, J.T., 2011. A review on micronization techniques. *J. Pharm. Sci. Technol.* 3, 651-81.

Karam, M.C., Petit, J., Zimmer, D., Djantou, E.B., Scher, J., 2016. Effects of drying and grinding in production of fruit and vegetable powders: A review. *J. Food Eng.* 188, 32-49. <https://doi.org/10.1016/j.jfoodeng.2016.05.001>.

Ketenoglu, O., Tekin, A., 2015. Applications of molecular distillation technique in food products. *Ital. J. Food Sci.* 27, 277-281. <https://doi.org/10.14674/1120-1770/ijfs.v269>.

Khan, A.A., Shekh-Ahmad, T., Khalil, A., Walker, M.C., Ali, A.B., 2018. Cannabidiol exerts antiepileptic effects by restoring hippocampal interneuron functions in a temporal lobe epilepsy model. *Br. J. Pharmacol.* 175, 2097-2115. <https://doi.org/10.1111/bph.14202>.

Kienle, A., Groebel, M., Gilles, E.D., 1995. Multiple steady states in binary distillation — Theoretical and experimental results. *Chem. Eng. Sci.* 50, 2691-2703. [https://doi.org/10.1016/0009-2509\(95\)00113-J](https://doi.org/10.1016/0009-2509(95)00113-J).

Kim, S.B., Bisson, J., Friesen, J.B., Pauli, G.F., Simmler, C., 2020. Selective chlorophyll removal method to “degreen” botanical extracts. *J. Nat. Prod.* 83, 1846-1858. <https://doi.org/10.1021/acs.jnatprod.0c00005>.

Kinsara, R.A., Demirbas, A., 2016. Upgrading of crude oil via distillation processes. *Pet. Sci. Technol.* 34, 1300-1306. <https://doi.org/10.1080/10916466.2016.1200080>.

Kogan, N.M., Mechoulam, R., 2022. Cannabinoids in health and disease. *Dialogues Clin. Neurosci.* <https://doi.org/10.31887/DCNS.2007.9.4/nkogan>.

Koo, N., Jo, H.-J., Lee, S.-H., Kim, J.-G., 2011. Using response surface methodology to assess the effects of iron and spent mushroom substrate on arsenic phytotoxicity in lettuce (*Lactuca sativa* L.). *J. Hazard. Mater.* 192, 381-387. <https://doi.org/10.1016/j.jhazmat.2011.05.032>.

Kwaśnica, A., Pachura, N., Masztalerz, K., Figiel, A., Zimmer, A., Kupczyński, R., Wujcikowska, K., Carbonell-Barrachina, A.A., Szumny, A., Rózański, H., 2020. Volatile composition and sensory properties as quality attributes of fresh and dried hemp flowers (*Cannabis sativa* L.). *Foods* 9, 1118. <https://doi.org/10.3390/foods9081118>.

Lazarjani, M.P., Young, O., Kebede, L., Seyfoddin, A., 2021. Processing and extraction methods of medicinal cannabis: A narrative review. *J. Cannabis Res.* 3, 1-15. <https://doi.org/10.1186/s42238-021-00087-9>.

Lehmann, T., Brenneisen, R., 1992. A new chromatographic method for the isolation of (–)- $\Delta^9$ -(trans)-tetrahydrocannabinolic acid A. *Phytochem. Anal.* 3, 88-90. <https://doi.org/10.1002/pca.2800030210>.

Lewis, M.A., Russo, E.B., Smith, K.M., 2018. Pharmacological foundations of cannabis chemovars. *Planta Med.* 84, 225-233. <https://doi.org/10.1055/s-0043-122240>.

Li, H., Pordesimo, L., Weiss, J., 2004. High intensity ultrasound-assisted extraction of oil from soybeans. *Food Res. Int.* 37, 731-738. <https://doi.org/10.1016/j.foodres.2004.02.016>.

Li, P., Gasmalla, M.A.A., Zhang, W., Liu, J., Bing, R., Yang, R., 2016. Effects of roasting temperatures and grinding type on the yields of oil and protein obtained by aqueous extraction processing. *J. Food Eng.* 173, 15-24. <https://doi.org/10.1016/j.jfoodeng.2015.10.031>.

Li, Y., Fine, F., Fabiano-Tixier, A.-S., Abert-Vian, M., Carre, P., Pages, X., Chemat, F., 2014. Evaluation of alternative solvents for improvement of oil extraction from rapeseeds. *C. R. Chim.* 17, 242-251. <https://doi.org/10.1016/j.crci.2013.09.002>.

Liang, J., Aachary, A.A., Hydamaka, A., Eskin, N.M., Eck, P., Thiyam-Holländer, U., 2018. Reduction of chlorophyll in cold-pressed hemp (*Cannabis sativa*) seed oil by ultrasonic bleaching and enhancement of oxidative stability. *Eur. J. Lipid Sci. Technol.* 120, 1700349. <https://doi.org/10.1002/ejlt.201700349>.

Liang, S., Cao, Y., Liu, X., Li, X., Zhao, Y., Wang, Y., Wang, Y., 2017. Insight into pressure-swing distillation from azeotropic phenomenon to dynamic control. *Chem. Eng. Res. Des.* 117, 318-335. <https://doi.org/10.1016/j.cherd.2016.10.040>.

Liu, F., Seo, T.S., 2010. A controllable self-assembly method for large-scale synthesis of graphene sponges and free-standing graphene films. *Adv. Funct. Mater.* 20, 1930-1936. <https://doi.org/10.1002/adfm.201000287>.

Livingston, S.J., Quilichini, T.D., Booth, J.K., Wong, D.C., Rensing, K.H., Laflamme-Yonkman, J., Castellarin, S.D., Bohlmann, J., Page, J.E., Samuels, A.L., 2020. Cannabis glandular trichomes alter morphology and metabolite content during flower maturation. *Plant J.* 101, 37-56. <https://doi.org/10.1111/tpj.14516>.

Maaroufi, C., Melcion, J.-P., De Monredon, F., Giboulot, B., Guibert, D., Le Guen, M.-P., 2000. Fractionation of pea flour with pilot scale sieving. I. Physical and chemical characteristics of pea seed fractions. *Anim. Feed Sci. Technol.* 85, 61-78. [https://doi.org/10.1016/S0377-8401\(00\)00127-9](https://doi.org/10.1016/S0377-8401(00)00127-9).

Mahlberg, P.G., Kim, E.S., 2004. Accumulation of cannabinoids in glandular trichomes of *Cannabis* (Cannabaceae). *J. Ind. Hemp.* 9, 15-36. [https://doi.org/10.1300/J237v09n01\\_04](https://doi.org/10.1300/J237v09n01_04).

Mahrous, E.A., Farag, M.A., 2022. Trends and Applications of Molecular Distillation in Pharmaceutical and Food Industries. *Sep. Purif. Rev.* 51, 300-317. <https://doi.org/10.1080/15422119.2021.1924205>.

Makanjuola, S.A., 2017. Influence of particle size and extraction solvent on antioxidant properties of extracts of tea, ginger, and tea–ginger blend. *Food Sci. Nutr.* 5, 1179-1185. <https://doi.org/10.1002/fsn3.509>.

Mani, S., Tabil, L.G., Sokhansanj, S., 2004. Grinding performance and physical properties of wheat and barley straws, corn stover and switchgrass. *Biomass Bioenergy*. 27, 339-352. <https://doi.org/10.1016/j.biombioe.2004.03.007>.

Manohar, B., Sridhar, B., 2001. Size and shape characterization of conventionally and cryogenically ground turmeric (*Curcuma domestica*) particles. *Powder Technol.* 120, 292-297. [https://doi.org/10.1016/S0032-5910\(01\)00284-4](https://doi.org/10.1016/S0032-5910(01)00284-4).

Manohar, B., Udaya Sankar, K., 2009. Enrichment of bakuchiol in supercritical carbon dioxide extracts of chiba seed (*Psoralea corylifolia* L.) using molecular distillation-Response surface methodology. *Biotechnol. Bioprocess Eng.* 14, 112-117. <https://doi.org/10.1007/s12257-007-0210-x>.

Martins, P., Ito, V., Batistella, C., Maciel, M.W., 2006. Free fatty acid separation from vegetable oil deodorizer distillate using molecular distillation process. *Separation and Purification Technology* 48, 78-84. <https://doi.org/10.1016/j.seppur.2005.07.028>.

Martins, P.F., Carmona, C., Martinez, E.L., Sbaite, P., Maciel Filho, R., Maciel, M.R.W., 2012. Short path evaporation for methyl chavicol enrichment from basil essential oil. *Sep. Purif. Technol.* 87, 71-78. <https://doi.org/10.1016/j.seppur.2011.11.024>.

Mayer-Laigle, C., Blanc, N., Rajaonarivony, R.K., Rouau, X., 2018a. Comminution of dry lignocellulosic biomass, a review: Part I. from fundamental mechanisms to milling behaviour. *Bioengineering* 5, 41. <https://doi.org/10.3390/bioengineering5020041>.

Mayer-Laigle, C., Rajaonarivony, R.K., Blanc, N., Rouau, X., 2018b. Comminution of dry lignocellulosic biomass: Part II. Technologies, improvement of milling performances, and security issues. *Bioengineering* 5, 50. <https://doi.org/10.3390/bioengineering5030050>.

McPartland, J.M., 2018. Cannabis systematics at the levels of family, genus, and species. *Cannabis Cannabinoid Res.* 3, 203-212. <https://doi.org/10.1089/can.2018.0039>.

Merlin, M.D., 2003. Archaeological evidence for the tradition of psychoactive plant use in the old world. *Econ. Bot.* 57, 295-323. [https://doi.org/10.1663/0013-0001\(2003\)057\[0295:AEFTTO\]2.0.CO;2](https://doi.org/10.1663/0013-0001(2003)057[0295:AEFTTO]2.0.CO;2).

Meyer, F., Eggers, R., Oehlke, K., Harbaum-Piayda, B., Schwarz, K., Siddiqi, M.A., 2011. Application of short path distillation for recovery of polyphenols from deodorizer distillate. *Eur. J. Lipid Sci. Technol.* 113, 1363-1374. <https://doi.org/10.1002/ejlt.201000523>.

Meziane, S., Kadi, H., Lamrous, O., 2006. Kinetic study of oil extraction from olive foot cake. *Grasas Aceites*. 57, 175-179. <https://doi.org/10.3989/gya.2006.v57.i2.34>.

Micalizzi, G., Alibrando, F., Vento, F., Trovato, E., Zoccali, M., Guarnaccia, P., Dugo, P., Mondello, L., 2021. Development of a novel microwave distillation technique for the isolation of *Cannabis sativa* L. essential oil and gas chromatography analyses for the comprehensive characterization of terpenes and terpenoids, including their enantio-distribution. *Molecules* 26, 1588. <https://doi.org/10.3390/molecules26061588>.

Micov, M., Lutišan, J., Cvengroš, J., 1997. Balance equations for molecular distillation. *Sep. Sci. Technol.* 32, 3051-3066. <https://doi.org/10.1080/01496399708000795>.

Milay, L., Berman, P., Shapira, A., Guberman, O., Meiri, D., 2020. Metabolic profiling of cannabis secondary metabolites for evaluation of optimal postharvest storage conditions. *Front. Plant Sci.* 11, 1556. <https://doi.org/10.3389/fpls.2020.583605>.

Moiceanu, G., Paraschiv, G., Voicu, G., Dinca, M., Negoita, O., Chitoiu, M., Tudor, P., 2019. Energy consumption at size reduction of lignocellulose biomass for bioenergy. *Sustainability* 11, 2477. <https://doi.org/10.3390/su11092477>.

Montserrat-de la Paz, S., Marín-Aguilar, F., García-Gimenez, M.D., Fernández-Arche, M., 2014. Hemp (*Cannabis sativa* L.) seed oil: Analytical and phytochemical characterization of the unsaponifiable fraction. *J. Agric. Food Chem.* 62, 1105-1110. <https://doi.org/10.1021/jf404278q>.

Morales, I., Keshavamurthy, J., Patel, N., Thomson, N., 2017. Inert gas asphyxiation: A liquid nitrogen accident. *Chest* 152, A378. <https://doi.org/10.1016/j.chest.2017.08.404>.

Morello, V., Brousseau, V.D., Wu, N., Wu, B.-S., MacPherson, S., Lefsrud, M., 2022. Light Quality Impacts Vertical Growth Rate, Phytochemical Yield and Cannabinoid Production Efficiency in *Cannabis sativa*. *Plants* 11, 2982. <https://doi.org/10.3390/plants11212982>.

Moreno, T., Dyer, P., Tallon, S., 2020a. Cannabinoid decarboxylation: a comparative kinetic study. *Ind. Eng. Chem. Res.* 59, 20307-20315. <https://doi.org/10.1021/acs.iecr.0c03791>.

Moreno, T., Montanes, F., Tallon, S.J., Fenton, T., King, J.W., 2020b. Extraction of cannabinoids from hemp (*Cannabis sativa* L.) using high pressure solvents: An overview of



different processing options. *J. Supercrit. Fluids*. 161, 104850.

<https://doi.org/10.1016/j.supflu.2020.104850>.

Morgan, C.J., Schafer, G., Freeman, T.P., Curran, H.V., 2010. Impact of cannabidiol on the acute memory and psychotomimetic effects of smoked cannabis: naturalistic study. *Br. J. Psychiatry* 197, 285-290. <https://doi.org/10.1192/bjp.bp.110.077503>.

Morimoto, S., Komatsu, K., Taura, F., Shoyama, Y., 1998. Purification and characterization of cannabichromenic acid synthase from *Cannabis sativa*. *Phytochemistry* 49, 1525-1529.

[https://doi.org/10.1016/S0031-9422\(98\)00278-7](https://doi.org/10.1016/S0031-9422(98)00278-7).

Murthy, C., Rani, M., Rao, P.S., 1999. Optimal grinding characteristics of black pepper for essential oil yield. *J. Food Process Eng.* 22, 161-173. <https://doi.org/10.1111/j.1745-4530.1999.tb00478.x>.

Nahar, L., Uddin, S.J., Alam, M.A., Sarker, S.D., 2021. Extraction of naturally occurring cannabinoids: an update. *Phytochem. Anal.* 32, 228-241. <https://doi.org/10.1002/pca.2987>.

Nakach, M., Authelin, J.-R., Chamayou, A., Dodds, J., 2004. Comparison of various milling technologies for grinding pharmaceutical powders. *Int. J. Miner. Process.* 74, S173-S181.

<https://doi.org/10.1016/j.minpro.2004.07.039>.

Ngamnikom, P., Songsermpong, S., 2011. The effects of freeze, dry, and wet grinding processes on rice flour properties and their energy consumption. *J. Food Eng.* 104, 632-638.

<https://doi.org/10.1016/j.jfoodeng.2011.02.001>.

Nieh, C., Snyder, H., 1991. Solvent extraction of oil from soybean flour I—extraction rate, a countercurrent extraction system, and oil quality. *J. Am. Oil Chem. Soc.* 68, 246-249.

<https://doi.org/10.1007/BF02657618>.

Ogonowski, S., Wołosiewicz-Głąb, M., Ogonowski, Z., Foszcz, D., Pawełczyk, M., 2018.

Comparison of wet and dry grinding in electromagnetic mill. *Minerals* 8, 138.

<https://doi.org/10.3390/min8040138>.

Ojeda-Sana, A.M., van Baren, C.M., Elechosa, M.A., Juárez, M.A., Moreno, S., 2013. New insights into antibacterial and antioxidant activities of rosemary essential oils and their main components. *Food Contr.* 31, 189-195. <https://doi.org/10.1016/j.foodcont.2012.09.022>.

Pacifico, D., Miselli, F., Carboni, A., Moschella, A., Mandolino, G., 2008. Time course of cannabinoid accumulation and chemotype development during the growth of *Cannabis sativa* L. *Euphytica* 160, 231-240. <https://doi.org/10.1007/s10681-007-9543-y>.



Panneton, B., Pillion, H., Dutilleul, P., Thériault, R., Khelifi, M., 1999. Full factorial design versus central composite design: statistical comparison and implications for spray droplet deposition experiments. *Trans. ASABE* 42, 877-884. <https://doi.org/10.13031/2013.13267>.

Patel, B., Wene, D., Fan, Z.T., 2017. Qualitative and quantitative measurement of cannabinoids in cannabis using modified HPLC/DAD method. *J. Pharm. Biomed. Anal.* 146, 15-23. <https://doi.org/10.1016/j.jpba.2017.07.021>.

Paterakis, P., Korakianiti, E., Dallas, P., Rekkas, D., 2002. Evaluation and simultaneous optimization of some pellets characteristics using a 33 factorial design and the desirability function. *Int. J. Pharm.* 248, 51-60. [https://doi.org/10.1016/S0378-5173\(02\)00341-1](https://doi.org/10.1016/S0378-5173(02)00341-1).

Péres, V.F., Saffi, J., Melecchi, M.I.S., Abad, F.C., de Assis Jacques, R., Martinez, M.M., Oliveira, E.C., Caramão, E.B., 2006. Comparison of soxhlet, ultrasound-assisted and pressurized liquid extraction of terpenes, fatty acids and Vitamin E from *Piper gaudichaudianum* Kunth. *J. Chromatogr. A* 1105, 115-118. <https://doi.org/10.1016/j.chroma.2005.07.113>.

Perrotin-Brunel, H., Buijs, W., Van Spronsen, J., Van Roosmalen, M.J., Peters, C.J., Verpoorte, R., Witkamp, G.-J., 2011. Decarboxylation of  $\Delta^9$ -tetrahydrocannabinol: Kinetics and molecular modeling. *J. Mol. Struct.* 987, 67-73. <https://doi.org/10.1016/j.molstruc.2010.11.061>.

Peschel, W., 2016. Quality control of traditional cannabis tinctures: pattern, markers, and stability. *Sci. Pharm.* 84, 567-584. <https://doi.org/10.3390/scipharm84030567>.

Pesek, C., Wilson, L., Hammond, E., 1985. Spice quality: Effect of cryogenic and ambient grinding on volatiles. *J. Food Sci.* 50, 599-601. <https://doi.org/10.1111/j.1365-2621.1985.tb13753.x>.

Piluzza, G., Delogu, G., Cabras, A., Marceddu, S., Bullitta, S., 2013. Differentiation between fiber and drug types of hemp (*Cannabis sativa* L.) from a collection of wild and domesticated accessions. *Genet. Resour. Crop Evol.* 60, 2331-2342. <https://doi.org/10.1007/s10722-013-0001-5>.

Posada, L.R., Shi, J., Kakuda, Y., Xue, S.J., 2007. Extraction of tocotrienols from palm fatty acid distillates using molecular distillation. *Sep. Purif. Technol.* 57, 220-229. <https://doi.org/10.1016/j.seppur.2007.04.016>.

Potter, D. 2004. Growth and morphology of medicinal cannabis. *Med. Uses Cannabinoids*. 17-54.

Potter, D.J., 2014. A review of the cultivation and processing of cannabis (*Cannabis sativa* L.) for production of prescription medicines in the UK. *Drug Test. Anal.* 6, 31-38. <https://doi.org/10.1002/dta.1531>.

Pou, K.J., Raghavan, V., 2020. Recent advances in the application of high pressure processing-based hurdle approach for enhancement of food safety and quality. *J. Biosyst. Eng.* 45, 175-187. <https://doi.org/10.1007/s42853-020-00059-6>.

Prakash, O., Kumar, A., 2014. Solar greenhouse drying: A review. *Renew. Sustain. Energy Rev.* 29, 905-910. <https://doi.org/10.1016/j.rser.2013.08.084>.

Prost, J., Gonzalez, M.T., Urbicain, M.J., 2006. Determination and correlation of heat transfer coefficients in a falling film evaporator. *J. Food Eng.* 73, 320-326. <https://doi.org/10.1016/j.jfoodeng.2005.01.032>.

Pusiak, R.J., Cox, C., Harris, C.S., 2021. Growing pains: An overview of cannabis quality control and quality assurance in Canada. *Int. J. Drug Policy.* 93, 103111. <https://doi.org/10.1016/j.drugpo.2021.103111>.

Querino, M.V., Machado, R.A., Marangoni, C., 2019. Energy and exergetic evaluation of the multicomponent separation of petrochemical naphtha in falling film distillation columns. *Braz. J. Chem. Eng.* 36, 1357-1365. <https://doi.org/10.1590/0104-6632.20190363s20180379>.

Radwan, M.M., Chandra, S., Gul, S., ElSohly, M.A., 2021. Cannabinoids, phenolics, terpenes and alkaloids of cannabis. *Molecules* 26, 2774. <https://doi.org/10.3390/molecules26092774>.

Rahman, S., Mujumdar, A., 2008. A novel atmospheric freeze-drying system using a vibro-fluidized bed with adsorbent. *Drying Technol.* 26, 393-403. <https://doi.org/10.1080/07373930801928914>.

Raman, V., Lata, H., Chandra, S., Khan, I.A., ElSohly, M.A., 2017. Morpho-anatomy of marijuana (*Cannabis sativa* L.). *Cannabis sativa* L. *Bot. Biotechnol.*, 123-136. [https://doi.org/10.1007/978-3-319-54564-6\\_5](https://doi.org/10.1007/978-3-319-54564-6_5).

Ramirez, C.L., Fanovich, M.A., Churio, M.S., 2019. Cannabinoids: Extraction methods, analysis, and physicochemical characterization. *Stud. Nat. Prod. Chem.* 61, 143-173. <https://doi.org/10.1016/B978-0-444-64183-0.00004-X>.

Ratti, C., 2001. Hot air and freeze-drying of high-value foods: a review. *J. Food Eng.* 49, 311-319. [https://doi.org/10.1016/S0260-8774\(00\)00228-4](https://doi.org/10.1016/S0260-8774(00)00228-4).

- Reason, D.A., Grainger, M.N., Lane, J.R., 2022a. Optimization of the Decarboxylation of Cannabis for Commercial Applications. *Ind. Eng. Chem. Res.* <https://doi.org/10.1021/acs.iecr.2c00826>.
- Reason, D.A., Grainger, M.N., Lane, J.R., 2022b. Optimization of the decarboxylation of cannabis for commercial applications. *Ind. Eng. Chem. Res.* 61, 7823-7832. <https://doi.org/10.1021/acs.iecr.2c00826>.
- Ren, M., Tang, Z., Wu, X., Spengler, R., Jiang, H., Yang, Y., Boivin, N., 2019. The origins of cannabis smoking: Chemical residue evidence from the first millennium BCE in the Pamirs. *Sci. Adv.* 5, eaaw1391. <https://doi.org/10.1126/sciadv.aaw1391>.
- Romano, L.L., Hazekamp, A., 2013. Cannabis oil: chemical evaluation of an upcoming cannabis-based medicine. *Cannabinoids* 1, 1-11. <https://www.researchgate.net/publication/297707359>.
- Routray, W., Orsat, V., 2014. MAE of phenolic compounds from blueberry leaves and comparison with other extraction methods. *Ind. Crops Prod.* 58, 36-45. <https://doi.org/10.1016/j.indcrop.2014.03.038>.
- Rovetto, L.J., Aieta, N.V., 2017. Supercritical carbon dioxide extraction of cannabinoids from Cannabis sativa L. *J. Supercrit. Fluids.* 129, 16-27. <https://doi.org/10.1016/j.supflu.2017.03.014>.
- Rufino, A.T., Ribeiro, M., Sousa, C., Judas, F., Salgueiro, L., Cavaleiro, C., Mendes, A.F., 2015. Evaluation of the anti-inflammatory, anti-catabolic and pro-anabolic effects of E-caryophyllene, myrcene and limonene in a cell model of osteoarthritis. *Eur. J. Pharm.* 750, 141-150. <https://doi.org/10.1016/j.ejphar.2015.01.018>.
- Russin, T.A., Arcand, Y., Boye, J.I., 2007. Particle size effect on soy protein isolate extraction. *J. Food Process. Preserv.* 31, 308-319. <https://doi.org/10.1111/j.1745-4549.2007.00127.x>.
- Russo, E.B., 2011. Taming THC: potential cannabis synergy and phytocannabinoid-terpenoid entourage effects. *Br. J. Pharmacol.* 163, 1344-1364. <https://doi.org/10.1111/j.1476-5381.2011.01238.x>.
- Russo, E.B., Marcu, J., 2017. Cannabis pharmacology: the usual suspects and a few promising leads. *Adv. Pharmacol.* 80, 67-134. <https://doi.org/10.1016/bs.apha.2017.03.004>.
- Sagili, S.U.K.R., Addo, P.W., Gladu-Gallant, F.-A., Bilodeau, S.E., MacPherson, S., Paris, M., Lefsrud, M., Orsat, V., 2023. Optimization of wiped-film short path molecular distillation for

recovery of cannabinoids from cannabis oil using response surface methodology. *Ind. Crops Prod.* 195, 116442. <https://doi.org/10.1016/j.indcrop.2023.116442>.

Sasidharan, S., Chen, Y., Saravanan, D., Sundram, K., Latha, L.Y., 2011. Extraction, isolation and characterization of bioactive compounds from plants' extracts. *Afr. J. Tradit. Complement. Altern. Med.* 8. <https://doi.org/10.4314/ajtcam.v8i1.60483>.

Saxena, S., Sharma, Y., Rathore, S., Singh, K., Barnwal, P., Saxena, R., Upadhyaya, P., Anwer, M., 2015. Effect of cryogenic grinding on volatile oil, oleoresin content and anti-oxidant properties of coriander (*Coriandrum sativum* L.) genotypes. *J. Food Sci. Technol.* 52, 568-573. <https://doi.org/10.1007/s13197-013-1004-0>.

Schilling, S., Dowling, C.A., Shi, J., Ryan, L., Hunt, D., O'Reilly, E., Perry, A.S., Kinnane, O., McCabe, P.F., Melzer, R., 2020. The cream of the crop: Biology, breeding and applications of *Cannabis sativa*. *Authorea Preprints*. <https://doi.org/10.22541/au.160139712.25104053/v2>.

Schultes, R.E., Klein, W.M., Plowman, T., Lockwood, T.E., 1975. Cannabis: an example of taxonomic neglect. *Cannabis Cult.*, 21-38.

Shao, P., Jiang, S., Ying, Y., 2007. Optimization of molecular distillation for recovery of tocopherol from rapeseed oil deodorizer distillate using response surface and artificial neural network models. *Food Bioprod. Process.* 85, 85-92. <https://doi.org/10.1205/fbp06048>.

Sharma, L., 2021. Downstream Processing Stages, Comparative Analysis & Extraction Methodologies in Generation of Cannabinoids from Cannabis Sativa L.(Hemp).

Shi, B., Ma, L., Dong, W., Zhou, F., 2015. Application of a novel liquid nitrogen control technique for heat stress and fire prevention in underground mines. *J. Occup. Environ. Hyg.* 12, D168-D177. <https://doi.org/10.1080/15459624.2015.1019074>.

Shi, J., Posada, L.R., Kakuda, Y., Xue, S.J., 2007. Molecular distillation of palm oil distillates: Evaporation rates, relative volatility, and distribution coefficients of tocotrienols and other minor components. *Sep. Sci. Technol.* 42, 3029-3048. <https://doi.org/10.1080/01496390701589024>.

Singh, K., Goswami, T., 1999a. Design of a cryogenic grinding system for spices. *J. Food Eng.* 39, 359-368. [https://doi.org/10.1016/S0260-8774\(98\)00172-1](https://doi.org/10.1016/S0260-8774(98)00172-1).

Singh, K., Goswami, T., 1999b. Studies on cryogenic grinding of cumin seed. *J. Food Process Eng.* 22, 175-190. <https://doi.org/10.1111/j.1745-4530.1999.tb00479.x>.

Singh, K., Goswami, T., 2000. Cryogenic grinding of cloves. *J. Food Process. Preserv.* 24, 57-71. <https://doi.org/10.1111/j.1745-4549.2000.tb00405.x>.

- Sirikantaramas, S., Taura, F., 2017a. Cannabinoids: biosynthesis and biotechnological applications. *Cannabis sativa L. - Bot. Biotechnol.*, 183-206. [https://doi.org/10.1007/978-3-319-54564-6\\_8](https://doi.org/10.1007/978-3-319-54564-6_8).
- Sirikantaramas, S., Taura, F., 2017b. Cannabinoids: biosynthesis and biotechnological applications, in: Chandra, S., Lata, H., ElSohly, M., Eds.; (Ed.), *Cannabis sativa L.-Botany and biotechnology*. Springer, University of Illinois Press, Champaign, Illinois, United States, pp. 183-206. [https://doi.org/10.1007/978-3-319-54564-6\\_8](https://doi.org/10.1007/978-3-319-54564-6_8).
- Slatkin, D.J., Doorenbos, N.J., Harris, L.S., Masoud, A.N., Quimby, M.W., Schiff, P.L., 1971. Chemical constituents of *Cannabis sativa L.* root. *J. Pharm. Sci.* 60, 1891-1892. <https://doi.org/10.1002/jps.2600601232>.
- Sommano, S.R., Chittasupho, C., Ruksiriwanich, W., Jantrawut, P., 2020. The cannabis terpenes. *Molecules* 25, 5792. <https://doi.org/10.3390/molecules25245792>.
- Speroni, C.S., Stiebe, J., Guerra, D.R., Bender, A.B.B., Ballus, C.A., dos Santos, D.R., Morisso, F.D.P., da Silva, L.P., Emanuelli, T., 2019. Micronization and granulometric fractionation improve polyphenol content and antioxidant capacity of olive pomace. *Ind. Crops Prod.* 137, 347-355. <https://doi.org/10.1016/j.indcrop.2019.05.005>.
- Tang, W.-Q., Li, D.-C., Lv, Y.-X., Jiang, J.-G., 2011. Concentration and drying of tea polyphenols extracted from green tea using molecular distillation and spray drying. *Drying Technol.* 29, 584-590. <https://doi.org/10.1080/07373937.2010.516851>.
- Taschwer, M., Schmid, M.G., 2015. Determination of the relative percentage distribution of THCA and  $\Delta^9$ -THC in herbal cannabis seized in Austria—Impact of different storage temperatures on stability. *Forensic Sci. Int.* 254, 167-171. <https://doi.org/10.1016/j.forsciint.2015.07.019>.
- Taura, F., Morimoto, S., Shoyama, Y., 1996. Purification and characterization of cannabidiolic-acid synthase from *Cannabis sativa L.*: Biochemical analysis of a novel enzyme that catalyzes the oxidocyclization of cannabigerolic acid to cannabidiolic acid. *J. Biol. Chem.* 271, 17411-17416. <https://doi.org/10.1074/jbc.271.29.17411>.
- Taura, F., Morimoto, S., Shoyama, Y., Mechoulam, R., 1995. First direct evidence for the mechanism of  $\Delta^9$ -1-tetrahydrocannabinolic acid biosynthesis. *J. Am. Chem. Soc.* 117, 9766-9767. <https://doi.org/10.1021/ja00143a024>.

Taura, F., Tanaka, S., Taguchi, C., Fukamizu, T., Tanaka, H., Shoyama, Y., Morimoto, S., 2009. Characterization of olivetol synthase, a polyketide synthase putatively involved in cannabinoid biosynthetic pathway. *FEBS Lett.* 583, 2061-2066. <https://doi.org/10.1016/j.febslet.2009.05.024>.

Ternelli, M., Brighenti, V., Anceschi, L., Poto, M., Bertelli, D., Licata, M., Pellati, F., 2020. Innovative methods for the preparation of medical Cannabis oils with a high content of both cannabinoids and terpenes. *J. Pharm. Biomed. Anal.* 186, 113296. <https://doi.org/10.1016/j.jpba.2020.113296>.

Thomas, B.F., Elsohly, M., 2015. The analytical chemistry of cannabis: Quality assessment, assurance, and regulation of medicinal marijuana and cannabinoid preparations. Elsevier.

Tovar, L.P., Maciel, M.R.W., Winter, A., Batistella, C.B., Filho, R.M., Medina, L.C., 2012. Reliability-based optimization using surface response methodology to split heavy petroleum fractions by centrifugal molecular distillation process. *Sep. Sci. Technol.* 47, 1213-1233. <https://doi.org/10.1080/01496395.2011.644612>.

Treybal, R.E., 1980. Mass transfer operations. New York 466.

Tsinontides, S., Rajniak, P., Pham, D., Hunke, W., Placek, J., Reynolds, S., 2004. Freeze drying—principles and practice for successful scale-up to manufacturing. *Int. J. Pharm.* 280, 1-16. <https://doi.org/10.1016/j.ijpharm.2004.04.018>.

Tzima, K., Brunton, N.P., Rai, D.K., 2020. Evaluation of the impact of chlorophyll removal techniques on polyphenols in rosemary and thyme by-products. *J. Food Biochem.* 44, e13148. <https://doi.org/10.1111/jfbc.13148>.

Uoonlue, N., Muangrat, R., 2019. Effect of different solvents on subcritical solvent extraction of oil from Assam tea seeds (*Camellia sinensis* var. *assamica*): Optimization of oil extraction and physicochemical analysis. *J. Food Process Eng.* 42, e12960. <https://doi.org/10.1111/jfpe.12960>.

Valizadehderakhshan, M., 2022. Extraction and Purification of Cannabinoids from Hemp—Experimentation and Process Modeling. <https://www.proquest.com/docview/2695368678>

Valizadehderakhshan, M., Kazem-Rostami, M., Shahbazi, A., Azami, M., Bhowmik, A., Wang, L., 2022a. Refining Cannabidiol Using Wiped-Film Molecular Distillation: Experimentation, Process Modeling, and Prediction. *Ind. Eng. Chem. Res.* <https://doi.org/10.1021/acs.iecr.2c00290>.

Valizadehderakhshan, M., Kazem-Rostami, M., Shahbazi, A., Azami, M., Bhowmik, A., Wang, L., 2022b. Refining cannabidiol using wiped-film molecular distillation: Experimentation,

process modeling, and prediction. *Ind. Eng. Chem. Res.* 61, 6628-6639.

<https://doi.org/10.1021/acs.iecr.2c00290>.

Valizadehderakhshan, M., Shahbazi, A., Kazem-Rostami, M., Todd, M.S., Bhowmik, A., Wang, L., 2021. Extraction of cannabinoids from *Cannabis sativa* L.(Hemp). *Agric.* 11, 384.

<https://doi.org/10.3390/agriculture11050384>.

Vanhove, W., Van Damme, P., Meert, N., 2011. Factors determining yield and quality of illicit indoor cannabis (*Cannabis* spp.) production. *Forensic Sci. Int.* 212 (1-3), 158-163.

<https://doi.org/10.1016/j.forsciint.2011.06.006>

Vega, G.A., Dávila, J.A., 2022. Use of non-psychoactive residual biomass from *Cannabis sativa* L. for obtaining phenolic rich-extracts with antioxidant capacity. *Nat. Prod. Res.* 36, 4193-4199.

<https://doi.org/10.1080/14786419.2021.1969562>.

Veress, T., Szanto, J., Leisztner, L., 1990a. Determination of cannabinoid acids by high-performance liquid chromatography of their neutral derivatives formed by thermal decarboxylation: I. Study of the decarboxylation process in open reactors. *J. Chromatogr. A.* 520, 339-347. [https://doi.org/10.1016/0021-9673\(90\)85118-F](https://doi.org/10.1016/0021-9673(90)85118-F).

Veress, T., Szanto, J., Leisztner, L., 1990b. Determination of cannabinoid acids by high-performance liquid chromatography of their neutral derivatives formed by thermal decarboxylation: I. Study of the decarboxylation process in open reactors. *J. Chromatogr. A* 520, 339-347. [https://doi.org/10.1016/0021-9673\(90\)85118-F](https://doi.org/10.1016/0021-9673(90)85118-F).

VijayaVenkataRaman, S., Iniyan, S., Goic, R., 2012. A review of solar drying technologies. *Renew. Sustain. Energy Rev.* 16, 2652-2670. <https://doi.org/10.1016/j.rser.2012.01.007>.

Wang, J., Wang, C., Li, W., Pan, Y., Yuan, G., Chen, H., 2016a. Ball milling improves extractability and antioxidant properties of the active constituents of mushroom *Inonotus obliquus* powders. *Int. J. Food Sci. Technol.* 51, 2193-2200. <https://doi.org/10.1111/ijfs.13180>.

Wang, M., Wang, Y.-H., Avula, B., Radwan, M.M., Wanas, A.S., van Antwerp, J., Parcher, J.F., ElSohly, M.A., Khan, I.A., 2016b. Decarboxylation study of acidic cannabinoids: a novel approach using ultra-high-performance supercritical fluid chromatography/photodiode array-mass spectrometry. *Cannabis Cannabinoid Res.* 1, 262-271.

<https://doi.org/10.1089/can.2016.0020>.

Wilczek, M., Bertling, J., Hintemann, D., 2004. Optimised technologies for cryogenic grinding. *Int. J. Miner. Process.* 74, S425-S434. <https://doi.org/10.1016/j.minpro.2004.07.032>.

Williams, S., Hartley, J., Graham, J., 1976. Bronchodilator effect of delta1-tetrahydrocannabinol administered by aerosol of asthmatic patients. *Thorax* 31, 720-723.

<https://doi.org/10.1136/thx.31.6.720>.

Wu, W., Wang, C., Zheng, J., 2012. Optimization of deacidification of low-calorie cocoa butter by molecular distillation. *LWT--Food Sci. Technol.* 46, 563-570.

<https://doi.org/10.1016/j.lwt.2011.10.028>.

Xu, C., Zhang, Y., Wang, J., Lu, J., 2010. Extraction, distribution and characterisation of phenolic compounds and oil in grapeseeds. *Food Chem.* 122, 688-694.

<https://doi.org/10.1016/j.foodchem.2010.03.037>.

Xubin, Z., Chunjian, X., Ming, Z., 2005. Modeling of falling film molecular distillator.

*Separation science and technology* 40, 1371-1386. [https://doi.org/https://doi.org/10.1081/SS-200053027](https://doi.org/10.1081/SS-200053027).

Yunus, M.A.C., Hasan, M., Othman, N., Mohd-Setapar, S.H., Salleh, L.M.-., Ahmad-Zaini, M.A., Idham, Z., Zhari, S., 2013. Effect of particle size on the oil yield and catechin compound using accelerated solvent extraction. *J. Teknol.* 60, 21â€“25.

<https://doi.org/10.11113/jt.v60.1436>.

Zaiter, A., Becker, L., Karam, M.-C., Dicko, A., 2016. Effect of particle size on antioxidant activity and catechin content of green tea powders. *J. Food Sci. Technol.* 53, 2025-2032.

<https://doi.org/10.1007/s13197-016-2201-4>.

Zhu, F.-M., Du, B., Li, J., 2014. Effect of ultrafine grinding on physicochemical and antioxidant properties of dietary fiber from wine grape pomace. *Food Sci. Technol. Int.* 20, 55-62.

<https://doi.org/10.1177/1082013212469619>.



## Appendix

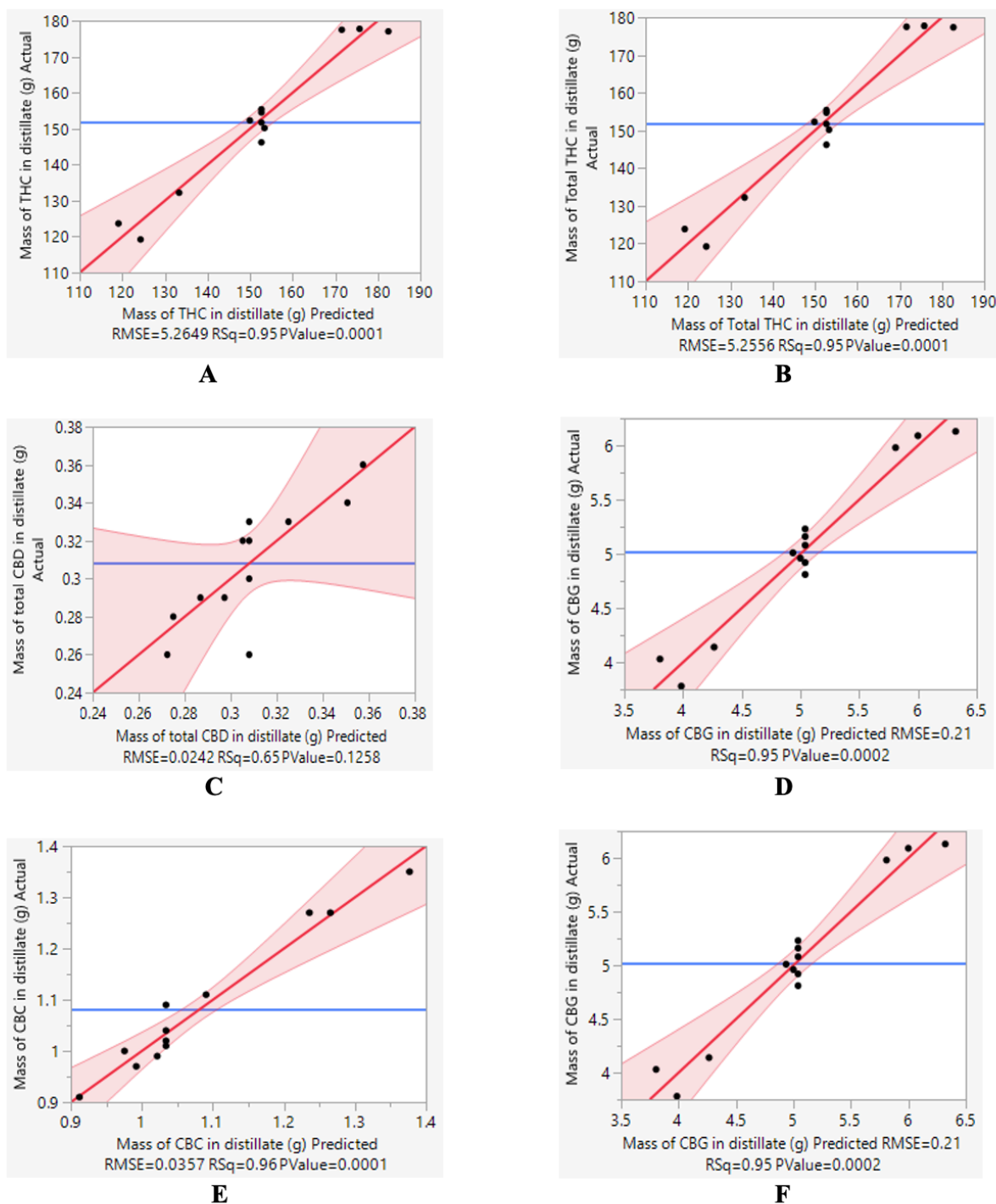
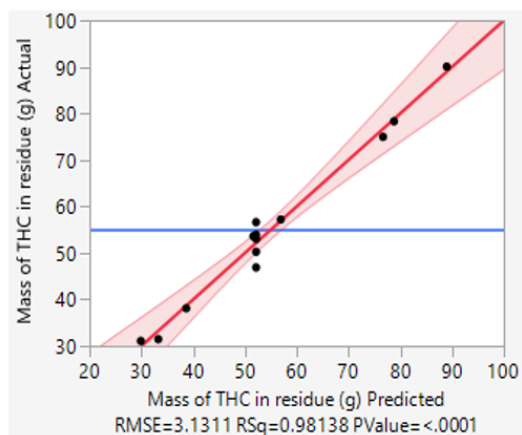
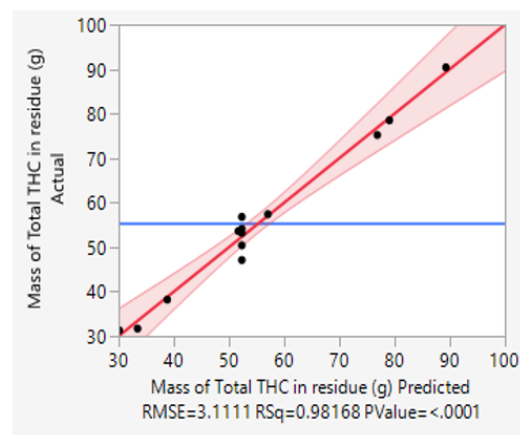


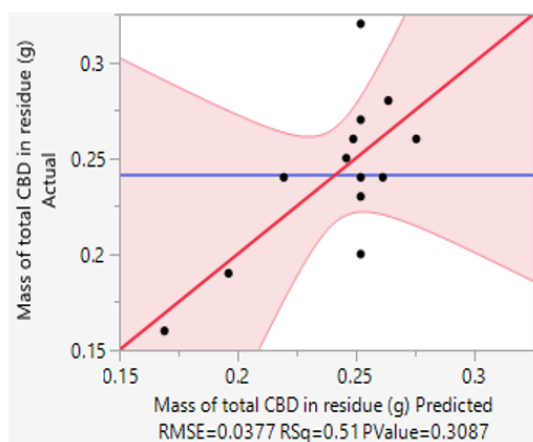
Figure A.1. Plots comparing the actual and predicted RSM values for the mass (g) of (A) THC, (B) Total THC, (C) Total CBD, (D) CBG, (E) CBC, and (F) CBN in the distillate.



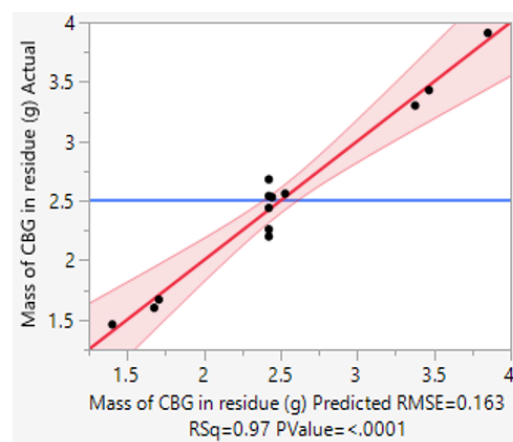
**A**



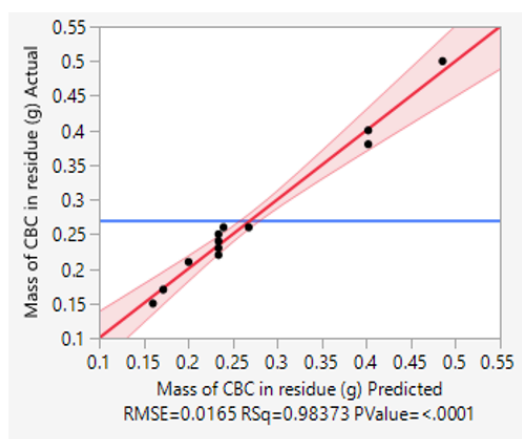
**B**



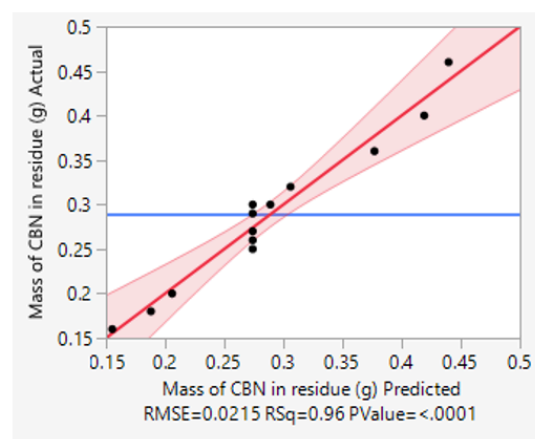
**C**



**D**



**E**



**F**

Figure A.2. Plots comparing the actual and predicted RSM values from RSM for the mass (g) of (A) THC, (B) Total THC, (C) Total CBD, (D) CBG, (E) CBC, (F) CBN in the residue.

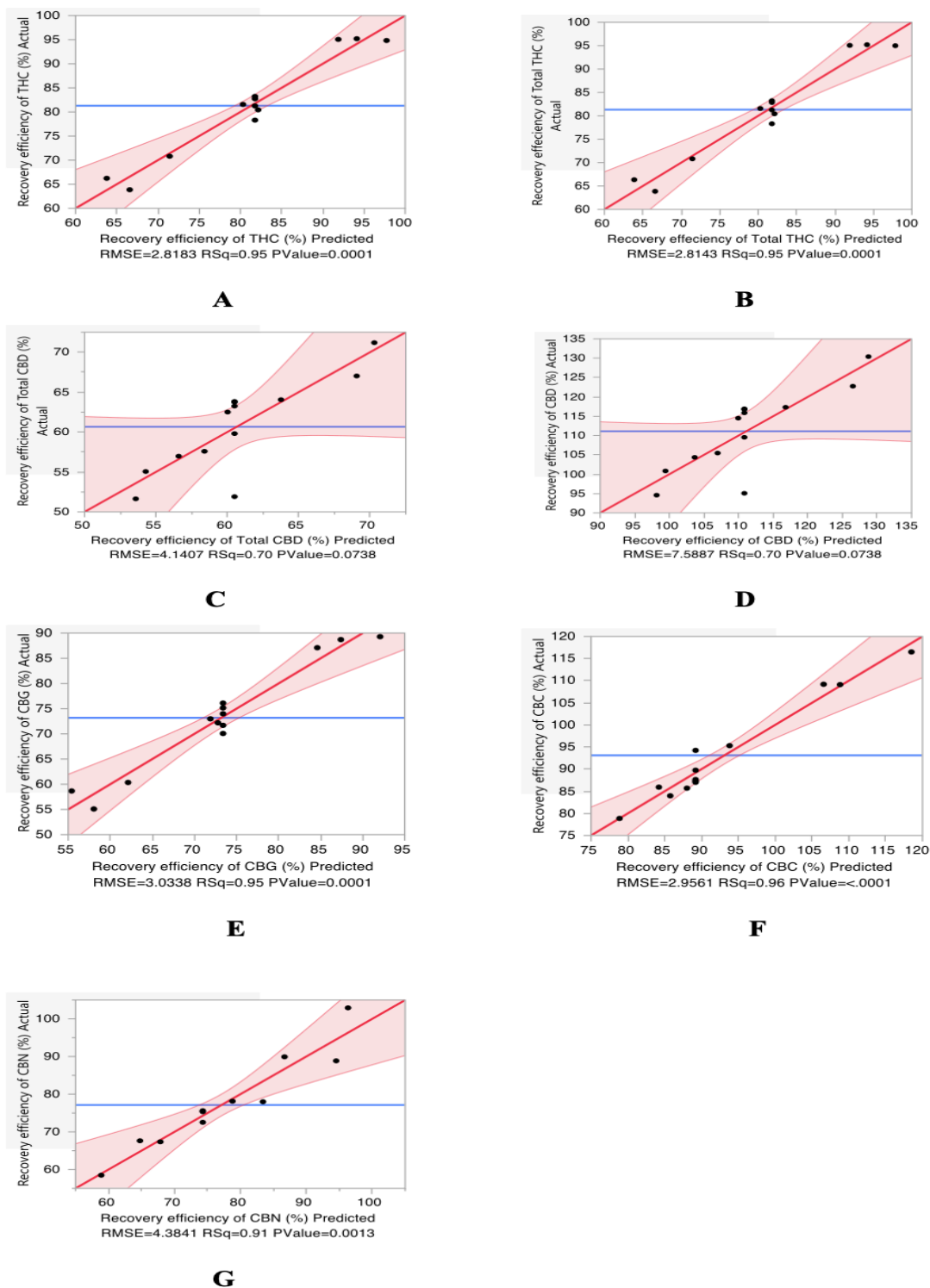


Figure A.3. Plots comparing the actual and predicted RSM values for recovery efficiency (%) of (A) THC, (B) Total THC, (C) Total CBD, (D) CBD, (E) CBG, (F) CBC, (G) CBN in the distillate.

Table A.1. Regression equation coefficients for different experimental conditions.

Response variables		Regression model effect parameters					
		Intercept	Linear		Quadratic		Interaction
		$\beta_0$	$\beta_1$	$\beta_2$	$\beta_{11}$	$\beta_{22}$	$\beta_{12}$
Mass of cannabinoids in the distillate							
THC	Coefficient	152.68	-22.41	-1.21	-0.94	-0.5	-3.31
	<i>p</i> value	<0.0001*	<0.0001*	0.53	0.65	0.81	0.25
Total THC	Coefficient	152.72	-22.43	-1.22	-0.87	-0.55	-3.31
	<i>p</i> value	<0.0001*	<0.0001*	0.53	0.68	0.79	0.25
CBD	Coefficient	0.31	-0.03	0	0	0	-0.01
	<i>p</i> value	<0.0001*	0.0113*	0.75	0.67	0.72	0.43
Total CBD	Coefficient	0.31	-0.03	0	0	0	-0.01
	<i>p</i> value	<0.0001*	0.0113*	0.75	0.67	0.72	0.43
CBG	Coefficient	5.04	-0.89	-0.02	0.01	-0.04	-0.12
	<i>p</i> value	<0.0001*	<0.0001*	0.77	0.89	0.66	0.3
CBC	Coefficient	1.03	-0.14	-0.03	0.07	0	-0.02
	<i>p</i> value	<0.0001*	<0.0001*	0.03*	0.01*	0.8	0.3
CBN	Coefficient	0.62	-0.11	0.01	0.01	0.03	-0.02
	<i>p</i> value	<0.0001*	<0.0001*	0.34	0.45	0.05	0.19
Mass of cannabinoids in the residue							
THC	Coefficient	52.15	20.89	1.89	3.64	1.06	-0.82
	<i>p</i> value	<0.0001*	<0.0001*	0.13	0.02*	0.4	0.62
Total THC	Coefficient	52.32	20.90	1.9	3.7	1.02	-0.8

	<i>p</i> value	<0.0001*	<0.0001*	0.13	0.02*	0.41	0.62
CBDA	Coefficient	0.29	0.02	-0.02	-0.02	0	0.03
	<i>p</i> value	<0.0001*	0.14	0.15	0.32	0.7	0.13
Total CBD	Coefficient	0.25	0.02	-0.02	-0.01	0	0.02
	<i>p</i> value	<0.0001*	0.2	0.2	0.34	0.88	0.19
CBG	Coefficient	2.42	0.86	0.03	0.1	0.03	0.01
	<i>p</i> value	<0.0001*	<0.0001*	0.61	0.14	0.62	0.86
CBC	Coefficient	0.23	0.11	0.01	0.05	0.01	-0.01
	<i>p</i> value	<0.0001*	<0.0001*	0.13	<0.0001*	0.16	0.26
CBN	Coefficient	0.27	0.1	0.01	0.01	0.01	0.01
	<i>p</i> value	<0.0001*	<0.0001*	0.45	0.19	0.19	0.2

---

Recovery efficiency of cannabinoids in the distillate

---

THC	Coefficient	81.77	-12	-0.65	-0.5	-0.27	-1.77
	<i>p</i> value	<0.0001*	<0.0001*	0.53	0.65	0.81	0.25
Total THC	Coefficient	81.79	-12.01	-0.65	-0.46	-0.29	-1.77
	<i>p</i> value	<0.0001*	<0.0001*	0.53	0.68	0.79	0.25
CBD	Coefficient	110.84	-10.37	1.05	1.63	-1.19	-3.8
	<i>p</i> value	<0.0001*	0.01*	0.71	0.59	0.69	0.35
Total CBD	Coefficient	60.5	-5.66	0.57	0.89	-0.64	-2.08
	<i>p</i> value	<0.0001*	0.01*	0.71	0.59	0.69	0.35
CBG	Coefficient	73.4	-12.96	-0.32	0.17	-0.53	-1.72
	<i>p</i> value	<0.0001*	<0.0001*	0.77	0.89	0.66	0.29
CBC	Coefficient	89.19	-12.13	-2.85	6.08	0.29	-1.73

	<i>p</i> value	<0.0001*	<0.0001*	0.03*	0.01*	0.8	0.03*
CBN	Coefficient	74.3	-12.6	1.63	1.21	3.41	-3.18
	<i>p</i> value	<0.0001*	<0.0001*	0.33	0.49	0.08	0.19

---

Effects are statistically significant if *p* value \* < 0.05. The coefficients of the polynomial model include the model intercept ( $\beta_0$ ), linear terms ( $\beta_1$  and  $\beta_2$ ), interaction terms ( $\beta_{11}$  and  $\beta_{22}$ ), and quadratic term ( $\beta_{12}$ ).